ROLES OF PROTEIN SEQUENCE AND CELL ENVIRONMENT IN CROSS-SPECIES PRION TRANSMISSION AND AMYLOID INTERFERENCE

A Dissertation
Presented to
The Academic Faculty

By

Kathryn L. Bruce

In Partial Fulfillment
of the Requirements for the Degree
Doctor of Philosophy in Biology

Georgia Institute of Technology
August, 2014

ROLES OF PROTEIN SEQUENCE AND CELL ENVIRONMENT IN CROSS-SPECIES PRION TRANSMISSION AND AMYLOID INTERFERENCE

Approved by:

Dr. Yury Chernoff, Advisor
School of Biology
Georgia Institute of Technology

Dr. Kirill Lobachev
School of Biology
Georgia Institute of Technology

Dr. Andreas Bommarius
School of Chemical & Biomolecular Engineering
Georgia Institute of Technology

Dr. Michael Gleason
School of Biology
Georgia College

Dr. Francesca Storici
School of Biology
Georgia Institute of Technology

Date Approved: 05/13/2014

ACKNOWLEDGEMENTS:

I wish to thank my advisor Dr. Yury Chernoff and my committee members Dr. Kirill Lobachev, Dr. Andreas Bommarius, Dr. Michael Gleason, and Dr. Francesca Storici for their instruction and helpful comments and suggestions for this work. I wish to thank Mr. Gary Newnam for mentoring me and for providing useful suggestions. Many thanks to all past and present lab members for their contributions to my project. Lastly, I am grateful to our undergraduate students Ankita Tippur, David Deng, Kudo Jang, Ilenne Del Valle, and our high school volunteer Rohit Konda for their help and for the privilege of teaching them.

TABLE OF CONTENTS

LIST OF TABLES

Page

LIST OF FIGURES:

Page

LIST OF SYMBOLS OR ABBREVIATIONS

- α-aa – α-aminoadipic acid
- 5-FOA – 5-Fluoroorotic Acid
- GuHCl – guanidine hydrochloride
- CuSO4 – copper sulfate
- $Sup35_{Sc}$ – Sup35 from *S. cerevisiae*
- $Sup35_{Sp}$ – Sup35 from *S. paradoxus*
- $Sup35_{Sb}$ – Sup35 from *S. bayanus*
- PrD – prion domain
- EDTA – (ethylenediaminetetraacetic acid)
- SDS – (sodium dodecyl sulphate)
- aa – amino acid
- SDD-AGE – semi-denaturing detergent agarose gel electrophoresis
- OR's – region of oligopeptide repeats
- QN – QN-rich stretch
- PrP – prion protein
- Prion – proteinaceous infectious particles
- $ade1\text{-}14_{Sc}$ –ade1-14 originated from *S. cerevisiae*
- Sc – *S. cerevisiae*
- Sp – *S. paradoxus*
- Sb – *S. bayanus*
- Amp – ampicillin
- Cm – chloramphenicol
- LB – Luria Bertani broth
- SDS-PAGE sodium dodecyl sulfate polyacrylamide gel electrophoresis

SUMMARY

Proteinaceous infectious particles, termed "prions" are self-perpetuating protein isoforms that transmit neurodegenerative diseases in mammals and phenotypic traits in yeast. Each conformational variant of a prion protein is faithfully propagated to a homologous protein in the same cell environment. However, a reduction in the efficiency of prion transmission between different species is often observed and is termed "species barrier." Prion transmission to a heterologous protein may, in some cases, permanently change the structure of the prion variant, and divergent proteins may interfere with prion propagation in a species-specific manner. To identify the importance of both protein sequence and the cell environment on prion interference and cross-species transmission, we employed heterologous Sup35 proteins from three *Saccharomyces sensu stricto* species: *Saccharomyces cerevisiae* (Sc), *Saccharomyces paradoxus* (Sp), and *Saccharomyces bayanus* (Sb). We performed our experiments in two different cell environments (Sc and Sp). Our data show that Sup35 from one species can form a prion in another, and we employed a transfection procedure to perform cross-species transfer of the prion. Using a shuffle procedure, we demonstrate that the specificity of prion transmission is determined by the protein itself rather than by the cell environment. Interestingly, we noted that variant-specific prion patterns can be altered irreversibly during cross-species transmission through *S. bayanus* module II. We further show that prion interference does not always correlate with cross-species prion transmission, and the identity of particular regions or even a specific amino acid, rather than the overall level of PrD homology is crucial for determining cross-species transmission and

interference. Lastly we provide evidence to suggest that prion interference is specific to the cell environment.

CHAPTER 1 INTRODUCTION: BACKGROUND AND SIGNIFICANCE

This chapter includes data published in *Seminars in Cell and Developmental Biology*. [Bruce KL, Chernoff YO. (2011) Sequence specificity and fidelity of prion transmission in yeast. *Semin Cell Dev Biol* **22**(5): 444-451]

1.1 AN INTRODUCTION TO AMYLOIDS AND PRIONS

Amyloid is a fibrous highly ordered cross-β protein aggregate that is highly resistant to degradation [1]. Many proteins form amyloids *in vitro*. Amyloid disorders include more than 30 diseases, among them such widespread conditions as Alzheimer's and Parkinson's diseases and type-II diabetes [1]. Amyloid may also play a variety of positive biological roles [2, 3]. In addition, many proteins have been found to form amyloids *in vitro* [4].

Amyloid-based prions (proteinaceous infectious particles) can be transmitted to other cells or organisms [3]. Once induced, the prion state propagates through immobilization of endogenous monomeric protein to the ends of existing prion "seeds" (Fig. 1). Fragmentation of polymers initiates new rounds of prion propagation. Mammalian and human prion diseases or spongiform encephalopathies, including "mad cow" disease and scrapie, are fatal and incurable. Recent studies show that other amyloid disorders may also be transmissible, at least in experimental conditions or at a cellular level [5-7]. This hastens the need for novel therapies aimed at slowing or preventing amyloid progression or transmission.

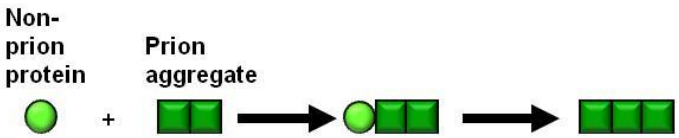

Figure 1: Model for prion propagation: The prion model proposes that a prion aggregate or "seed" comes in contact with a monomeric protein having the exact or similar sequence. The monomer then joins onto the ends of the aggregate, using the aggregate as a structural template for its own incorporation as part of the aggregate.

Remarkably, prions exist as distinct "strains" that have the same primary sequence but differ in the structural organization of their amyloid core [8,9]. Particular strains of mammalian prion protein PrP correspond to distinct disease phenotypes and can be distinguished by characteristics such as differences in disease incubation periods, overall disease severity, proteinase K restriction patterns, and amyloid core length [10-12].

Prion transmission between heterologous proteins, originated from different organisms, is typically less efficient or not observed and is strongly influenced by the degree of sequence divergence [13]. This phenomenon is known as a "species" or "transmission" barrier (Fig 2). Uncovering the mechanisms underlying the sequence-dependence of prion transmission will ultimately allow predictions of interspecies prion transmission.

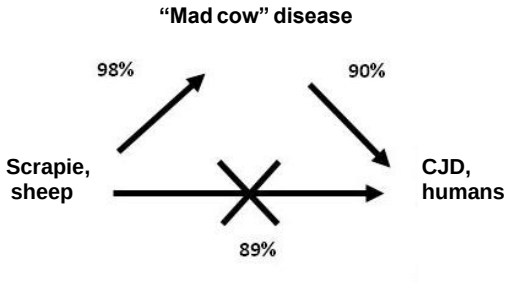

Figure 2: Example of a species barrier for cross-species transmission: PrP is known to adopt a prion fold and can propagate as a prion in different mammalian species. PrP homologues are found in sheep, cows, and humans, and the % given indicates the PrP sequence similarity between them. Despite the high level of sequence similarity, species-specific differences in protein sequence or cell environment may prevent cross-species prion transmission, thus generating a "species barrier" (Arrows indicate successful prion transmission; "X" represents a species barrier)

A variety of amyloid-based prions have been identified in fungi, especially in yeast. Yeast prions serve as a convenient model for investigations of amyloid and prion formation in general, and for elucidation of the sequence determinants of the species barrier. To date, at least eight different proteins have been proven to form a prion in *S. cerevisiae* yeast [14-22], and 18 others showed the ability to promote prion characteristics in *Saccharomyces cerevisiae* when fused to a reporter protein [23]. These proteins possess prion domains (PrDs) that convey prion-forming ability and are located at the terminal ends of proteins. Yeast PrDs are generally unrelated to the major cellular function of a protein and typically contain a QN-rich sequence (Fig. 3). Some PrDs also contain a region of oligopeptide repeats. Some well-characterized yeast prion-forming proteins (for review, see [3, 24]) include: 1) the translational termination factor Sup35 (eRF3) whose prion form is termed [PSI^+], 2) a protein of unknown function, Rnq1 whose prion form is termed [PIN^+], and 3) a regulatory protein in the nitrogen

metabolism pathway, Ure2, whose prion form is termed [URE3]. Sup35 and other yeast proteins can form prions *de novo*, albeit the presence of [PIN^+] greatly speeds up prion nucleation. Rnq1, first adopts a prion aggregation state known as "[PIN^+]" [85]. [PIN^+] is then thought to cross-seed aggregation of other proteins, such as Sup35, by serving as a structural template for their assembly and nucleation into a prion form [81, 31, 15, 87].

It is debated whether yeast prions play biologically positive regulatory roles [3, 23, 25, 26] or whether they are detrimental to their host, Regardless, prion formation can be classified as an epigenetic change analogous to a gene mutation but occurring at the protein level [30].

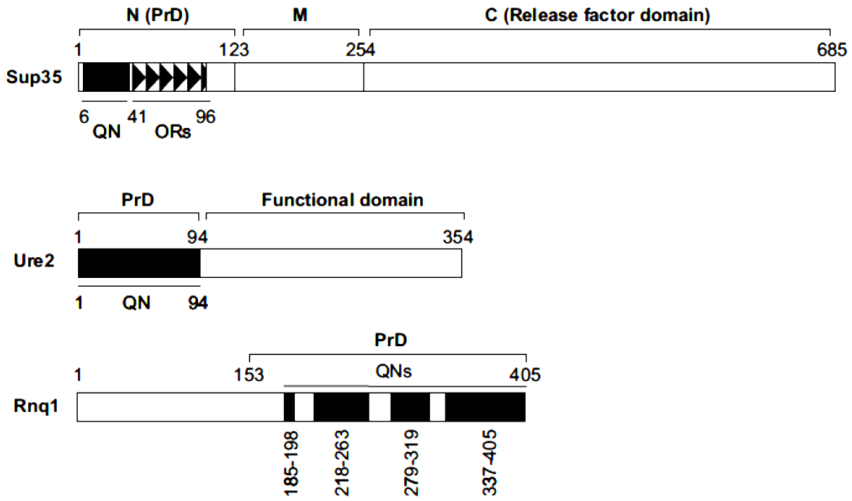

Figure 3: Structural and functional organization of yeast prion proteins Sup35, Ure2, and Rnq1. PrD refers to the prion domain. "QN" denotes the glutamine/asparagine-rich regions (shaded in figure). "Ors" refers to the region of oligopeptide repeats. "N," "M," and "C" mark the Sup35N-terminal (prion) domain, middle domain, and C-proximal domain, respectively. "Functional domain" refers to the region essential for cellular function of the protein. Numbers correspond to amino acid positions.

1.2. PRION VARIANTS IN YEAST

As in the case of mammalian prions, yeast prions with the same primary sequence, also exist as distinct strains, more typically termed "variants," whose

characteristics are controlled by the prion protein itself. Note that the term variant is used to avoid confusion with yeast strains that differ genotypically. Prion variants have been well documented to occur in well studied yeast prions including [*PSI*$^{+}$], [URE3] and [*PIN*$^{+}$] [31-33]. Not only are distinct phenotypes observed for their corresponding prion strains, but these differences are faithfully perpetuated as the prion is propagated both *in vitro* and *in vivo*. Prion variants were further shown to be maintained by a purified prion protein as they are reproduced through various cycles of propagation *in vitro* [8,9].

Impairment of Sup35 function in translation (Fig 4) is more severe in the strong variants when compared to the weak variants [31]. At a phenotypic level, "strong" [*PSI*$^{+}$] variants were shown to exhibit close to 100% mitotic stability (that is homologous transmission in cell divisions) while weak variants can lose the prion state in mitotic division with a detectable frequency (Fig 5). Prion variants also differ in sensitivity to molecular chaperones that control prion fragmentation in yeast [31, 34].

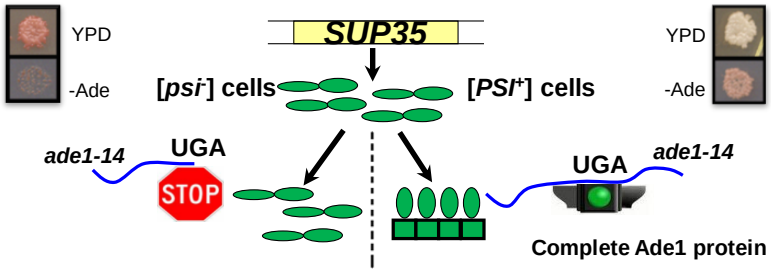

Figure 4: *ade1-14* supression assay for [*PSI*$^{+}$] detection. Detection of the Sup35 prion ([*PSI*$^{+}$]) by nonsense suppression. (Left of figure) The *ade1-14* allele contains a premature UGA stop codon, allowing Sup35 to help termination before the complete Ade1 protein is made, so cells cannot live on media lacking adenine. When Sup35 is misfolded to form [*PSI*$^{+}$], translation termination is less efficient, allowing readthrough of the stop codon to produce the complete Ade1 protein, so cells can live on media lacking adenine. [*psi*$^{-}$] cells are red in color due to the accumulation of an intermediate in the adenine pathway.

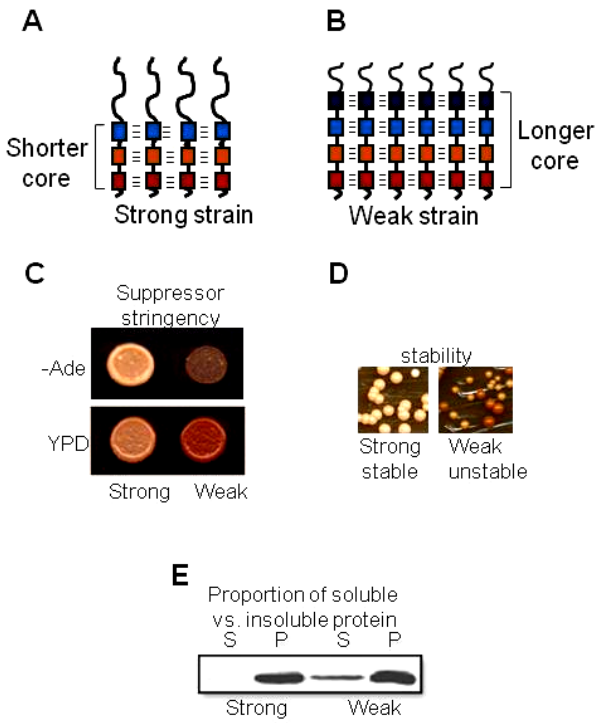

Figure 5: Phenotypic differences in [*PSI*$^+$] variants: [*PSI*$^+$] strength inversely correlates with prion core length **A**—Strong variant having less of the PrD composing the prion core as compared to **B**—having a larger core but a weak phenotype. (boxes - β-strands, dashes - H-bonds). **C**—Prion variant strength can be measured by color on YPD or by suppression on media lacking adenine. **D**—Strong [*PSI*$^+$] variants exhibit stable propagation after many mitotic divisions, but weak variants lose the prion with higher frequencies. **E**—after ultracentrifugation, strong [*PSI*$^+$] variants exhibit most of the Sup35 in the pellet fraction; weaker variants contain a significant fraction in both the supernatant and pellet.

Various biochemical and biophysical methods can be employed to distinguish between different [*PSI*$^+$] strains. Zhou *et al*. [35] showed that "weak" prion variants contain more protein remaining in the soluble fraction after centrifugation while "strong" prions showed almost all Sup35 protein in the pellet. This explains more severe impairment of translation termination in strong prion variants. Strong prions are more readily fragmented, and this facilitates more efficient propagation of a prion [36]. A smaller average size of SDS-insoluble prion polymers, uncovered by agarose electrophoresis, generally correlated with a stronger prion phenotype [37]. Smaller

polymer size possibly results from more efficient fragmentation by the Hsp104 chaperone *in vivo*, and this explains a greater efficiency of prion propagation. Protection from H-D exchange revealed a shorter amyloid core in a strong variant of Sup35 prion as compared to a weak variant [38]. Derdowski *et al.* [39] observed that smaller prion polymers are more readily transmitted to daughter cells. That may explain higher transmissibility of strong prion variants.

While phenotypic manifestation of the variant-specific patterns is achieved via interactions between the prion protein and cellular machinery, the molecular differences underlying these patterns are controlled by the prion protein itself. It was demonstrated that propagation of a purified *S. cerevisiae* Sup35NM amyloid was able to maintain a particular prion pattern in *vitro* and was then able to transfer the prion state to yeast cells upon transfection, providing strong support for a mechanism of protein-only templating [8,9].

1.3. PRION SPECIES BARRIER IN YEAST

1.3.1. "Long distance" transmission barriers

Prion species barriers between heterologous proteins are well documented in yeast. Examples of "long-distance" species barriers include those between *Saccharomyces cerevisiae* and highly divergent yeast species *Pichia methanolica* and *Candida albicans* (Fig. 6). The PrD of Sup35 evolves much faster than the C-proximal release factor domain [3], so that only 30-40% amino acid similarity is retained between PrDs of *S. cerevisiae*, on one side, and *Pichia* or *Candida*, on the other side [40]. It appears that such a low level of sequence similarity is insufficient to promote co-aggregation of divergent proteins under normal cellular conditions [27, 40, 41]. As a

result, a strong species barrier that is controlled by the QN-rich stretch is detected. A chimeric Sup35 PrD with fused portions of the *S. cerevisiae* and *C. albicans* QN-rich stretch exhibited a "promiscuous" prion behavior allowing transmission of prion conformation from both *S. cerevisiae* and *C. albicans* PrDs [42].

Heterologous coaggregation with the *S. cerevisiae* Sup35 protein was observed for its orthologs from less divergent species, *Kluyveromyces lactis* and *Yarrowia lipolytica* [28]. Although these proteins aggregate, it is unclear whether or not stable transmission of a prion state occurs between proteins from these species.

Despite a profound barrier normally observed between *S. cerevisiae* and Pichia or Candida, rare instances of cross-species transmission were detected. In such cases, generation of multiple prion variants, rather than faithful reproduction of the initial prion variant, was observed [43]. Thus, cross-species prion transmission between highly divergent PrDs is reminiscent of promotion of prion nucleation by a non-homologous aggregated protein [16, 44]. Heterologous nucleation is covered in more detail by Nelson and Ross [45].

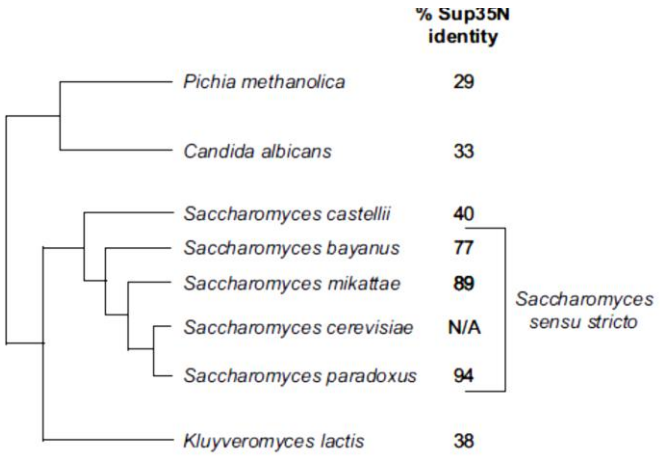

Figure 6: Yeast species used in the prion species barrier studies. The phylogenetic tree is not drawn to scale. The percentage of amino acid sequence identity between the Sup35N domain of each species and the Sup35N domain of *S. cerevisiae* is shown.

1.3.2. "Short distance" transmission barriers

The level of sequence divergence between PrDs of proteins from the different yeast genera is much higher that the level of divergence between the mammalian PrP proteins, for which the species barrier was initially described. Protein of closely related yeast species of the *Saccharomyces* genera, therefore, represent a more appropriate model for studying the general mechanisms of the species barrier that are applicable to mammalian systems [46]. Our lab has obtained detailed information about transmission of the prion state between the Sup35 protein originated from the species of the *Saccharomyces sensu stricto* group, namely *S. cerevisiae*, *S. paradoxus*, and *S. bayanus* (Fig 7). The level of identity between the PrDs of these proteins varies from 94% (*S. cerevisiae* to *S. paradoxus*) to 77% (*S. cerevisiae* to *S. bayanus*) [46]; that is similar to the range of identity among mammalian PrPs [47] (Fig. 2).

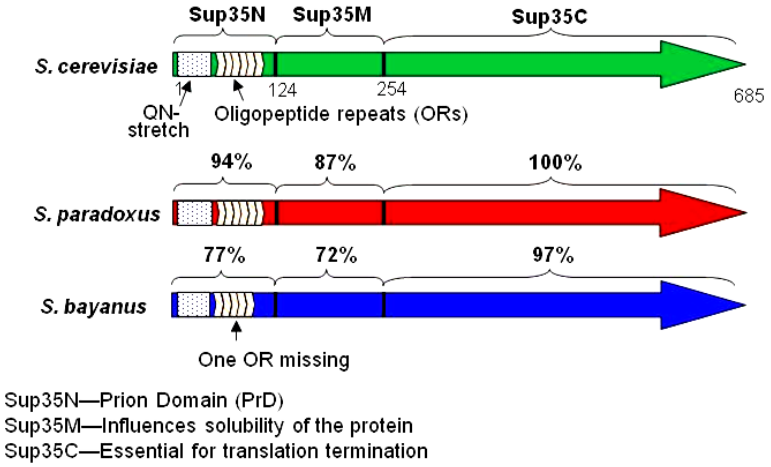

Figure 7: *Saccharomyces* Sup35 proteins. Sup35 proteins are shown from three closely related *Saccharomyces* species. Sup35 has 3 domains: Sup35N or the "prion domain" (PrD), Sup35M which is highly charged and influences the solubility of the protein, and Sup35C which is essential for the protein's role of translation termination. Designations "QN-stretch"

and "OR" refer to a region of QN-rich residues in the Sup35N sequence, and oligopeptide repeats, respectively. Numbers correspond to amino acid positions. Percentages indicate the sequence similarity between the domain of a particular species and that of *Saccharomyces cerevisiae*.

Our lab has previously shown that Sup35 proteins of *S. paradoxus* and *S. bayanus* are found to co-aggregate with endogenous Sup35 prion in *S. cerevisiae* cells [46]. However, a prion transmission barrier was detected in at least some combinations, despite coaggregation [46]. Our latest results show that cross-species transmission depends on both sequence divergence and the prion variant. We also show that the short distance barrier is not necessarily controlled by differences in the QN-rich stretch and is not directly proportional to the overall percentage of sequence divergence. These results will be discussed in Chapter 3. Interestingly, our data resemble results obtained for mammalian PrP [13] and support the hypothesis that the identity of relatively short key stretches, rather than overall sequence identity of PrDs controls is crucial for cross-species prion transmission.

"Short distance" transmission barriers were also observed for Ure2 proteins originated from different *Saccharomyces* species [49-52]. The strength of the barriers varied widely for different species combinations and did not directly correlate with the overall percentage of sequence divergence. Ure2 from *S. paradoxus* and *S. castellii* were unable to adopt a prion form despite conservation of the PrD sequence [50]. Like in case of Sup35, particular prion variant was shown to determine the extent to which the species barrier can be crossed. For one specific [URE3] variant produced in a *S. bayanus* protein, the prion could be readily transmitted to other Ure2 proteins from different species. However, for different [URE3] variants produced in a *S. bayanus* protein, a strong preference for prion transmission to the *S. bayanus* Ure2 protein was observed [50].

Transmission barriers were also recorded for artificially prepared Rnq1 constructs that contained no aa mismatches but did contain various deletions in one or more of the protein's four QN-rich regions [53]. Data were consistent with the model suggesting that multiple prion determinants work in tandem to produce a particular conformation. For all three proteins, Sup35 ([46, 48]; see Fig. 3B), Ure2 [50] and Rnq1 [53], transmission barriers in some combinations were asymmetric, resembling the observations made in mammalian systems [54].

1.4. AMYLOID INTERFERENCE

Another possible consequence of interactions between non-identical amyloidogenic proteins is amyloid interference, sometimes called "poisoning." It occurs when a heterologous protein, its fragment (or altered derivative) of the homologous protein is co-expressed in the presence of a pre-existing amyloid. For the [URE3] prion, amyloid interference was detected as prion curing by truncated versions of Ure2 or by GFP-tagged Ure2 [49, 55]. In a perhaps related process, [*PSI*$^+$] propagation from wild-type Sup35 to Sup35 having a single amino acid mutation was diminished, and was further inhibited by higher Hsp104 dosage. [102]. An interference component may also be involved in interactions between prions such as [*PIN*$^+$], [*PSI*$^+$], and [URE3] that can, in some combinations, interfere with propagation of each other [56]. Interestingly, for [*PIN*$^+$] and [*PSI*$^+$], such incompatibility was shown to be variant-specific [57]. Furthermore, our lab previously found that overexpression of Sup35 or its PrD caused loss of [*PSI*$^+$] *in vivo* [58], although it was not clear in that study if such curing occurred via interference heterologous interference was detected for the *S. sensu stricto* Sup35NM

amyloids *in vitro*: in some combinations, introduction of the previously polymerized protein delayed rather than "seeded" polymerization of a heterologous soluble substrate [46]. In this work we provide evidence that heterologous interference also occurs *in vivo* and is attributed to heterologous interaction rather than sequestration of cofactors mechanisms or was due to sequestration of cofactors. Previously, our lab also observed that (K. Bruce, A. Romanyuk, and Y. Chernoff, unpublished). We show these results in chapter 6.

1.5 FIDELITY AND AMBIGUITY OF CROSS-SPECIES PRION TRANSMISSION

Amyloid transmission is characterized by a high level of conformational fidelity. Prion propagation faithfully reproduces patterns of the original variant or "strain." However, fidelity of prion transmission is not absolute. Phenotypic changes to the prion state were observed after a prion crosses a transmission barrier [12, 60, 61]. It is worth noting note that Sup35N regions of different lengths were found to be necessary for faithful maintenance of particular strong and weak [*PSI*$^+$] prion variants in yeast [62, 63]. In this work, we show that for the yeast "short-distance" cross-species transmission, two types of variant changes were detected. The first type is a transient change in the phenotypic manifestation of prion variant patterns. The second type is an irreversible variant switch. Our results are presented in chapters 3 and 5 of this work. Kadnar *et al.* [53] also observed variant alterations occurring during transmission of the [*PIN*$^+$] prion across the barriers created by deletions in the Rnq1 protein. In the case of the [URE3]

prion, variant type originating from *S. cerevisiae* also exhibited a high degree of fidelity as it was passaged across other *Saccharomyces* species [50].

1.6. STRUCTURAL BASIS OF AMYLOID SPECIFICITY AND FIDELITY

1.6.1. Structural models for yeast prions

Unfortunately, the inability to crystallize prion material has prevented researchers from solving the prion structure to the level of atomic resolution, although [Het-s] provides an exception. Regions of prion-forming proteins (called the "prion domain" or "PrD") are thought to aggregate in a cross β-sheet rich amyloid fold, making up the fiber's axis (or "core" region), and portions of the protein may remain soluble (Fig 8). This explains how prions or amyloids may retain cellular function, even while a portion of the protein is aggregated. However, there is debate about the mechanisms of amyloid formation by yeast prion proteins, and *in vitro* evidence is interpreted in support of two distinct models. A parallel in-register β-sheet fold is suggested by NMR analysis of Sup35NM, Rnq1, and Ure2 amyloids formed *in vitro* [64, 1]. This model proposes that cross-β stretches are separated by regions of unpaired loops, facilitating a superpleated arrangement of β-sheets, although the precise boundaries of the β-strands are not known. This is referred to as a "β-archade" structure and may be a feature common to stable pathogenic amyloids produced in *vivo*. [100, 101]. An alternative β-helix model was proposed based on cross-linking studies performed on Sup35NM amyloids generated *in vitro* and suggests "head-to-head" and "tail-to-tail" cross-β intermolecular interactions between short stretches (Figure 8). Unfortunately, the β-helix model cannot currently explain the mechanism for the faithful propagation of specific prion variants.

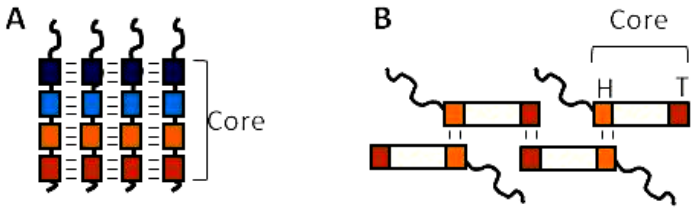

Figure 8 .Structural model of Sup35 amyloids. Only a portion of the protein (the prion domain, or "PrD," shown as boxes) may adopt the compact β-rich conformation, leaving the rest of the protein without an amyloid fold. A – parallel in-register β-sheet. Boxes indicate β-strands. B – β-helix. Colored boxes indicate sites of intermolecular contact (H – head, T – tail). Dashes indicate hydrogen bonds. The core and the rest of the protein are not drawn in scale.

1.6.2. The role of short sequences

Overall, the identity of specific short sequence regions or even individual residues was found to be crucial for faithfully maintaining propagation of specific prion variants. The roles these sequences or residues play is still under investigation, but direct correlation between the overall PrD sequence divergence and the success of cross-species prion transmission was not observed. Interestingly, experiments with small sequence changes such as single substitutions in mammalian PrP [69] or to the interspecies Sup35 chimera [42] produced transmission barriers

Accumulated evidence also indicates that regions which are significantly shorter than the whole PrD are required for the maintenance of variant-specific prion patterns. Moreover, strong variants of [*PSI*$^{+}$] require shorter regions of PrD for their faithful reproduction, compared to weak variants [63, 70, 71]. The 40-50 amino acid fragment was sufficient to faithfully propagate strong prion through *in vitro* stage [70]. Mutagenesis studies of Sup35 PrD were used to define specific regions that control a protein's ability to acquire the prion state from different variants. It turned out that

identity of only a 15 amino acid stretch was required for susceptibility to the strong prion [70].

Peptide arrays that were composed of overlapping 20-mer peptides, together covering the whole Sup35 PrD sequence were employed to identify the primary sites of interaction between Sup35 molecules potentially involved in amyloidogenesis. For proteins derived from either *S. cerevisiae* or *C. albicans*, interacting peptides were located at species-specific positions. Chimeric protein, capable of acquiring a prion state from both parental proteins, also interacted with both sets of peptides. Changes in temperature, altering the species specificity of a chimeric protein, also altered the efficiency of interaction with the respective peptide set, suggesting a role for the short amino acid stretches in determining the host-specific and variant-specific properties of a prion [72, 73].

Remarkably, the interacting region defined by peptide arrays is also included in the above mentioned stretch required for the faithful reproduction of a strong prion, and overlaps the so-called "amyloid stretch" consensus located at positions 9-14 (Fig. 22, Fig. 23). Hexapeptides conforming to this vague consensus are found in essentially all proteins capable of efficient amyloid formation and propagation *in vitro* [74]. The *S. cerevisiae* Sup35 PrD contains two more hexapeptides conforming to an amyloid stretch consensus, at positions 45-50 and 102-107 (Fig. 22, Fig. 23). Amino acid substitutions breaking the amyloid stretch consensus were found in *S. paradoxus* at position 12, and in *S. bayanus* at position 49 (here and further, *S. cerevisiae* numbering is used for simplicity). In this work, we present results obtained by using mutagenesis to restore the amyloid stretch consensus in both *S. paradoxus* and *S. bayanus* sequences, as well as

single substitutions to generate respective changes in the *S. cerevisiae* sequence. These results are shown in chapter 3 and 5. Overall, our data implicate the amyloid stretch consensus in the control of transmission specificity and fidelity, but also indicate that other sequence elements influence these processes as well. An additional indication in the same direction is that while a majority of yeast PrDs (see ref. [3]), including the artificially made "scrambled" versions of Sup35 PrD [1], contain the amyloid stretch hexapeptide(s) according to our analysis, Ure2 PrD does not appear to contain them (see ref. [48]).

1.7 OBJECTIVES

The overall objectives of this work were to document the effects of both 1) protein sequence and 2) the cell environment on cross-species [*PSI*$^{+}$] transmission and interference. Before this work was begun, the *Saccharomyces* model for species barrier was in use by our lab, but much was unknown about the role of protein sequence on these processes. Our objective was to determine conclusively whether overall sequence divergence or divergence in key sequence regions of the protein is most important for these processes, and we sought to map the sequence elements responsible for transmission barriers. Our hypothesis now states that such sequence elements may be crucial for initial interactions between aggregates and soluble protein and may determine the type of variants formed. Another objective was to determine variant-specific differences in cross-species infectivity. Such knowledge is useful for dissecting the mechanisms governing prion propagation, and for providing insight into predicting cross-species prion transmission and control of amyloid aggregation kinetics. We further sought to compare aspects of [*PSI*$^{+}$] propagation in different cell environments by

introducing the same [*PSI*$^{+}$] state used for previous *S. cerevisiae* experiments into the *S. paradoxus* species and then performing the same experiments in the new cell environment. A related goal was to document the effect of heterologous Sup35 co-expression on [*PSI*$^{+}$] propagation and to pinpoint key sequence elements responsible for interference with [*PSI*$^{+}$] propagation. Furthermore, we wanted to determine whether [*PSI*$^{+}$] propagation is possible in *S. bayanus*. Finally, we removed our studies of prion species barriers and [*PSI*$^{+}$] interference from the dependence of cellular influences *in vivo* to ascertain the roles attributed by the sequence alone. Overall, accomplishing these goals has provided new information about how prions propagate, and uncovered factors and processes that can inhibit their propagation. Ultimately, our continuing goal is to contribute to a thorough understanding of protein misfolding, allowing the process to be thoroughly controlled for applications in amyloid disease treatments and for advances in biotechnology

1.8: CHAPTER 1 ACKNOWLEDGEMENTS

We thank G. P. Newnam for help with figure design, A. V. Romanyuk for providing unpublished data, E.D. Ross and A.G.C. Nelson for coordination of the review contents.

CHAPTER 2: MATERIALS AND METHODS

2.1 MATERIALS

2.1.1 Yeast strains

The genotypes for all yeast and bacterial strains used for this work are provided on Table 1 (Appendix).

S. cerevisiae strains

The GT81 strain [27], served as the parent strain for all *S. cerevisiae* strains used in this work, with the exception of cytoduction strains. GT81 has the following genotype: *MAT***a** (or *MATα*) *ade1-14$_{SC}$ his3 leu2 lys2 trp1 ura3*. Some specified strains contained the *sup35*Δ*::HIS3* chromosomal replacement and were maintained by different *SUP35* versions expressed from plasmids (for plasmid descriptions, see [27, 77]). A plasmid shuffle procedure (Described in Figure 11 [77]) was used to exchange different Sup35 versions. *S. cerevisiae* strains GT256-23C (strong [*PSI*$^+$]) and GT988-1A (weak [*PSI*$^+$]), as well as the control [*psi*$^-$] strain GT255-2A, were haploid derivatives of GT81 with the following genotype: *MATα ade1-14* (UGA) *his3 leu2 lys2 trp1 ura3* (see [46] and references therein). They contained the *sup35*Δ*::HIS3* transplacement on the chromosome (constructed as described previously, see [27], and were maintained alive by the *S. cerevisiae – E. coli* shuttle plasmids bearing the *SUP35* gene. *S. cerevisiae* stains having strong [*PSI*$^+$] (GT256-23C) and weak [*PSI*$^+$] (GT988-1A) were used as the source of donor [*PSI*$^+$] for transfection into *S. paradoxus* and *S. bayanus*.

The 1B-D910 strain (a gift from Dr. A. Galkin; St. Petersburg University, Russia) served as the parent for all *S. cerevisiae* cytoduction recipient strains used in this work. 1B-D910 had the following genotype: *MAT***a** *ade1-14$_{SC}$ his3 leu2 trp1 ura3 cyh^R kar1-1*

[*rho*$^-$ *psi*$^-$ *pin*$^-$] and had the *sup35*Δ*::HIS3* chromosomal replacement. The strains were maintained by different *SUP35* versions expressed from plasmids (for plasmid descriptions, see [27, 77]) A plasmid shuffle procedure (Described in Figure 11 [77]) was used to exchange different Sup35 versions.

S. paradoxus strains

The diploid GT749-1B strain (engineered by Mr. G. Newnam in the Chernoff lab) served as the parent strain for all *S. paradoxus* strains used in this work. GT749-1B has the following genotype: *MATα/MATa lys2/lys2 ura3-P2/ura3-P2.*

The *S. paradoxus* strain GT1320-5B was a haploid derivative of SP7-1D (kindly provided by Dr. G. Naumov, State Institute for Genetics and Selection of Industrial Microorganisms, Moscow, Russia) with the following genotype: *S. paradoxus MATα ura3-P2 lys2 Δho::KanMX6 ade1SP::ade1-14*$_{Sc}$ *[LYS2 SUP35S*$_X$*]*. This strain contained the *sup35*Δ*::natNT2* transplacement on the chromosome (constructed as described in Chapter 4), and was maintained alive by *S. cerevisiae – E. coli* shuttle plasmids bearing the *SUP35* gene originating from either *S. cerevisiae*, *S. paradoxus*, or *S. bayanus*. Strong or weak [*PSI*$^+$] was induced in Sup35Sc by transfection from *S. cerevisiae* strains GT256-23C (strong variant) or GT988-1A (weak variant).

S. bayanus strains

The haploid Su1A and Su1B strains (kindly provided by Dr. N. Talarkek) [78] served as the parent strains for all *S. bayanus* strains used in this work. Sul1A and Sul1B have the following genotype(s): *MAT***a** (or *MATα*), *ura3-1*, *ho::KANMX4.*

2.1.2 Plasmids

Table 2 (Appendix) provides a list of all plasmids constructed or used for this work together with their descriptions. Plasmids used for a particular chapter are listed in that chapter's material and methods.

The *SUP35*$_{Sp}$ gene used for this work was obtained from the SP7-1D *S. paradoxus* strain (a gift from Dr. G. Naumov; State Institute for Genetics and Selection of Industrial Microorganisms, Moscow, Russia.) The *SUP35*$_{Sb}$ gene used for this work was obtained from the FM361 *S. bayanus* strain (a gift from Dr. M. Johnston; Washington University, St. Louis, MO). Descriptions of these strains are listed with their descriptions on Table 1 (Appendix).

2.1.3 Primers

Table 3 (Appendix) provides a list of all primers used for this work with their sequences and descriptions.

2.1.4 Antibodies

The Sup35C antibody was kindly provided by Dr. D. Bedwell (University of Alabama; Birmingham, AL). The Sup35M antibody was a gift from Dr. I. Vorberg (German Center for Neurodegenerative Diseases; Bonn, Germany). Ssb antibody was provided by E. Craig (University of Wisconsin; Madison, WI). Hsp104 antibody was a gift from Dr. Susan Lindquist (Massachusetts Institute of Technology, MA). The Ade2 antibody was provided by V. Alenin (St. Petersburg State University; St Petersburg,

Russia). The Sup35NM antibody was produced and purchased from Cocalico Biologicals, Inc. (Reamstown, PA).

2.1.5 Gammabodies

Three different gammabodies, each having different Sup35 residues (either residues 7-17, 7-26, or 12-21) grafted into a variable domain were provide by Dr. Pete Tessier (Rensselaer Polytechnnic Institute)

2.2 GENETIC AND MICROBIOLOGICAL TECHNIQUES

2.2.1 Standard yeast media and growth conditions

S. cerevisiae yeast cultures were grown at 30°C, and *S. paradoxus* and *S. bayanus* were grown at 25°C, unless otherwise indicated. Liquid yeast cultures were grown with at least a 1:5 culture: flask volume ratio in a shaking incubator (New Brunswick Scientific series 25D incubator/shaker (30°C), New Brunswick Scientific G24 incubator/shaker (37°C) or New Brunswick Scientific Innova 4080 (25°C) for 200-250 rpm. Standard procedures for yeast cultivation, phenotypic and genetic analysis, sporulation and dissection were used **[79]**. Synthetic media lacking an amino acid such as uracil, trypophan, leucine, lysine, adenine, or histidine were labeled as "–Ura", "-Trp", "-Leu", "-Lys", "-Ade", or "–His," respectively. Synthetic media lacking a combination of amino acids such as uracil and leucine was labeled as "–Ura-Leu". Unless otherwise specified, 2% glucose was used as a carbon source for all yeast media. To induce expression of the *GAL* promoter (P_{GAL}), 2% galactose was used as a carbon source rather than 2% glucose. To induce expression from the P_{CUP} promoter, copper sulfate ($CuSO_4$) was added at the indicated concentration up to a maximum of 150 μM $CuSO_4$. To select for hygromycin

resistant colonies, hygromycin B was added to YPD at a concentration of 0.3 mg/ml. To select for nourseothricin resistant colonies, nourseothricin was added to YPD at a concentration of 0.1 mg/ml. A Singer MSM System 300 micromanipulator was used for tetrad dissection of sporulating cultures.

2.2.2 Bacterial transformation procedure

Chemicals competent DH5α *E. coli* were transformed using standard laboratory protocols [80].

2.2.3 Yeast transformation procedure

A single yeast colony was inoculated into 5mls YPD and cultured at 30°C with shaking to OD_{600} = 1.0-5.0. The culture was diluted with 5 ml of YPD and allowed to grow for 2-4 hours as described. Cells were collected using centrifugation at 4000 x *g* for 5 minute and were resuspended in 10 mls of Lithium Acetate-TE solution (LiAc-TE) (100 mM lithium acetate, 10 mM Tris-HCl, 1 mM EDTA, pH 8.0) and were grown for 1 hour at 30° C with shaking. Cells were collected and resuspended in 0.5-1 ml LiAc-TE. 100 µl of cells was added to a microcentrifuge tube together with 20 µg carrier DNA and 1-10 µg of plasmid DNA. Tubes were placed on a rotator at room temperature for 30 minutes. 700 µl PEG-LiAc-TE (40% PEG 4000, 100 mM lithium acetate, 10 mM Tris-HCl, pH 7.5, 1 mM EDTA) was added, and cells were rotated at room temperature for 1 hour. The sample was heat-shocked for 5 minutes in a 42° C waterbath and was centrifuged at 3000 x *g* for 5 minutes to pellet the cells. Cells were resuspended in 150 µl water and plated on media selective for the plasmid. This transformation procedure was based on one from Ito *et al*, [82].

2.2.4 Yeast transfection procedure

Sonicated *in vitro*-generated amyloids or prion-containing yeast cellular extracts was transfected into yeast using our modified version of a protocol described by [16] (Fig 9). Our modifications differed from the published protocol as follows; 1) 1 M dithiothreitol was added separately to the SCE buffer (1 M sorbitol, 100 mM sodium citrate, 10 mM EDTA, pH 5.8) to a final concentration of 10 mM; 2) PEG buffer was prepared with 44% (w/v) PEG 3350; and 3) the top agar concentration was 0.8%, and it was incubated at 42°C to prevent solidification. An empty plasmid containing a *URA3* marker was transformed together with the transfected protein as a marker for protein uptake, and cells were plated on media lacking uracil to identify transformants (having plasmid uptake and therefore, potential protein uptake as well). Colonies that grew on media lacking uracil were replica plated onto YPD and –Ade for phenotypical characterization of the strains.

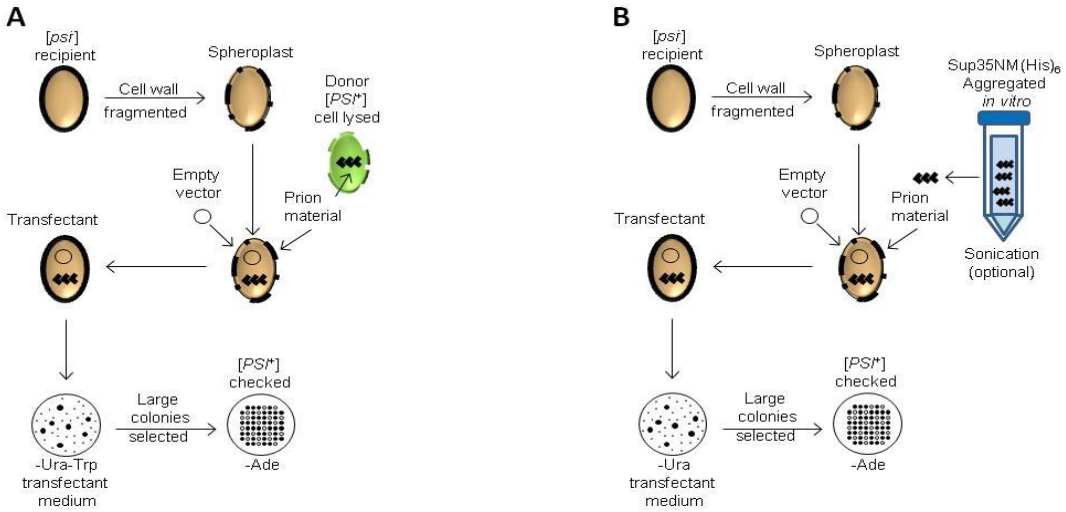

Figure 9: Transfection scheme. The cell wall of a [*psi*$^-$] recipient cell is fragmented with zymolase, generating a spheroplast with an intact cell membrane. **A—**Cell extract (including prion material) is isolated from a [*PSI*$^+$] strain and is chemically transfected across the recipient cell membrane. An empty *URA3* vector is simultaneously transformed into the

recipient as an indicator that material has passed across the cell membrane. The cells are plated on –Ura-Trp to select for recipient colonies (donor strain is trp^-) successfully transformed with the *URA3* plasmid. Both small and large colonies are observed on –Ura-Trp. Only large colonies contain the *–URA3* plasmid, smaller colonies (without the plasmid) are present due to a low concentration of YPD in the transfectant selection medium. The large Ura^+ colonies are tested on –Ade medium to check for [PSI^+]. **B—**protein aggregated *in vitro* is sonicated (optional) and chemically transfected across the cell membrane. Transfection medium contains Trp because no selection against a donor strain is needed. Other steps are the same as described in panel A.

The effect of sonication on transfection efficiency of *in vitro* generated amyloid

Sup35NM$(His)_6$ was purified from *E. coli* and aggregated *in vitro*. Because the *in vitro* aggregation mix lacks disaggregation factors such as Hsp104, aggregates may grow too large to be efficiently transfected across the cell membrane. Thus, sonication at low setting for 20 seconds, was used prior to transfection to break up the aggregates. The influence of sonication on transfection efficiency was tested for two different yeast strains.

Here, Sup35NM$(His)_6$ aggregates generated *in vitro* at either 4° or 37°C were transfected with or without sonication for comparison. It was observed that aggregates produced at 4° were more efficiently transfected without sonication. However, aggregates produced at 37°C were more efficiently transfected with sonication. See Figure 10 and Table 4.

This may be explained by findings that aggregates prepared at 4° tend to have a stronger [PSI^+] phenotype than those generated at 37°C [9]. It has been shown that a stronger [PSI^+] phenotype is correlated with a shorter prion core [38]. Therefore, sonication of smaller aggregates (produced at 4°) may fragment them to monomers;

whereas, sonication would be beneficial to break down larger aggregates (produced at 37°C) for more efficient transfection.

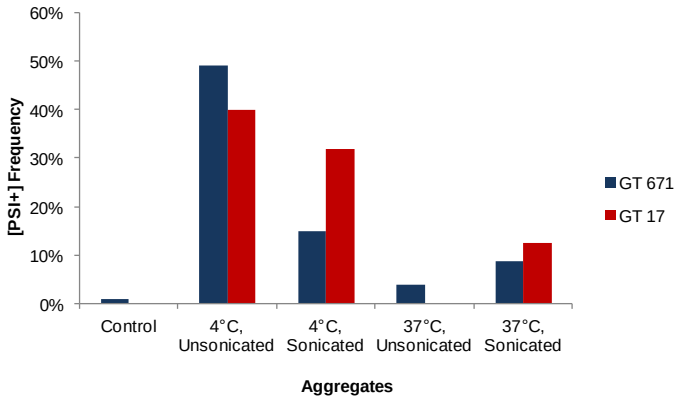

Figure 10 The effects of sonication on transfection efficiency of *in vitro* generated aggregates. Sup35NM$(His)_6$ protein originated from *S. cerevisiae* was purified from *E. coli* and aggregated at either 4° or 37° C. The protein was transfected into two yeast strains, either with prior sonication (S) or without (NS) sonication. The numbers of transfectants obtained were recorded with percentages of [PSI^+] shown. Yeast having no protein transfected was also included as a negative control. The yeast strain GT17 carried a chromosomal copy of *SUP35*, while GT671 was chromosomally deleted for *SUP35* but carried a copy on a plasmid. Data shown in this graphs is presented in Table 4.

2.2.5 *E. coli* HMS174 [pLysS] expression system

Sup35NM$(His)_6$ was isolated from the *E. coli* strain HMS174 [pLysS] (Novagen) by binding of the protein's $(His)_6$ tag to nickel resin. This strain is a lysogen of bacteriophage λDE3. HMS174 [pLysS] was transformed with a pET20b expression plasmid having the desired Sup35NM version. IPTG (isopropyl-ß-thiogalactopyranoside) was used to turn on expression of a target gene by inducing expression of a T7 RNA polymerase gene that is under control of a *lacUV5* promoter. The strain also contains a plysS plasmid (to prohibit basal expression from the pET20b vector before IPTG is added.) this plasmid was transformed by inoculating 5 ml LB + 75 µg/ml

chloramphenicol (Cm) with bacteria and was cultured overnight with shaking at 37°C. 100 µL of the culture was added to 5 ml of fresh LB + 75 µg/ml chloramphenicol and was grown for three hours under the same conditions. Cells were obtained by centrifugation at 3000 x *g* for 5 minutes and were resuspended in 2.5 ml cold (4°C) 50 mM $CaCl_2$ and placed on ice for 40 minutes. The sample was centrifuged again, and cells were resuspended in 0.5 ml of cold (4°C) 50 mM $CaCl_2$. 100 µl of cells was added to 1-10 µg of plasmid DNA in a microcentrifuge tube and was mixed well and placed on ice for 30 minutes. The sample was heat shocked at 42°C for 2 minutes and immediately placed on ice for 2 minutes. 0.5 mL SOC media (0.5% yeast extract, 2% tryptone, 10 mM NaCl, 2.5 mM KCl, 10 mM MgCl2, 10 mM MgSO4, 20 mM glucose) was added, and the culture was incubated for 1.5 hours at 37°C with shaking. Cells were pelleted using centrifugation at 3000 x *g* for 5 minutes and were resuspended in 150 µl water and plated on LB + 50 µg/ml ampicillin (Amp) to select for the plasmid.

2.2.6 Plasmid shuffle

To perform the plasmid shuffle (Fig. 11) [77, 46, 48], a *S. cerevisiae* [PSI^+] *sup35*Δ strain with the *S. cerevisiae SUP35* gene on a *LEU2* (or *LYS2)* plasmid was transformed by a *URA3* plasmid bearing a homologous, heterologous, chimeric or mutated *SUP35* construct. Transformants were obtained on medium lacking uracil and leucine (−Ura, Leu) that is selective for both plasmids, and checked for suppression of the *ade1-14* reporter on both medium lacking only adenine (−Ade) and medium lacking uracil, leucine and adenine (−Ura, Leu, Ade). The former medium enabled us to identify and exclude from further analysis colonies that have lost [PSI^+] prior to or in the process

of transformation, while the latter medium was used to determine whether newly introduced Sup35 protein is converted into a non-functional form or remains functional. Transformation-associated [*PSI*$^+$] loss was almost negligible for strong [*PSI*$^+$] but significant for weak [*PSI*$^+$]. In parallel, transformants were streaked out on −Ura medium and velveteened to −Leu medium, in order to identify the Ura$^+$ Leu$^-$ colonies that have lost the original *LEU2* plasmid. Only one Ura$^+$ Leu$^-$ colony was analysed from each individual [*PSI*$^+$] transformant, to ensure independence of all colonies from each other. Reverse shuffle was performed in a similar way, except that medium with 5-fluoroorotic acid (5-FOA) was used to cure transformants of the *URA3* plasmid.

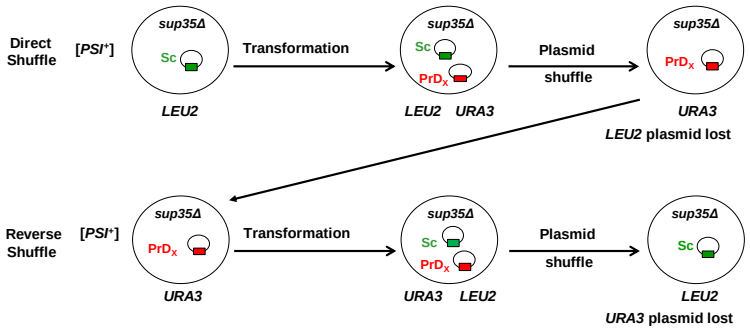

Figure 11: Plasmid shuffle scheme: Scheme of direct and reverse plasmid shuffle. "Sc" refers to *SUP35* from *S. cerevisiae*. "PrD$_X$" refers to *SUP35* genes of various origins, or chimeric constructs.

2.2.7 Prion interference assay

Prion interference is phenotypically detected in a procedure similar to plasmid shuffle. The difference in these procedures is that for interference, the newly transformed *URA3* plasmid (rather than the original plasmid) is lost after a period of co-existence. Following loss of the newly added plasmid, the original [*PSI*$^+$] phenotype is analyzed to look for changes caused by co-existence of the interfering protein. A modification to this procedure is described in detail in Chapter 6, Fig. 54.

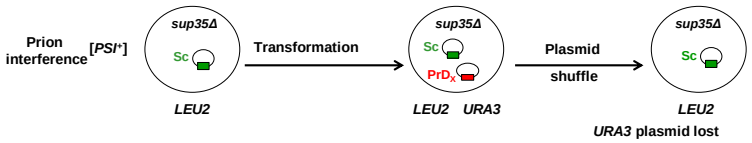

Figure 12: Interference scheme: Scheme of prion interference using a plasmid shuffle technique. "Sc" refers to *SUP35* from *S. cerevisiae*."PrD_X" refers to *SUP35* genes of various origins, or chimeric constructs.

2.2.8 Cytoduction

Cytoduction experiments (Fig. 13) were performed as described previously [46]. Donor strains were mated to the respective derivatives of the strain 1B-D910 by mixing them on YPD medium. After overnight incubation, mixtures were streaked onto selective synthetic medium with 5 µg ml^{-1} cycloheximide, containing 2% ethanol and 2% glycerol instead of glucose. This medium is selective for cytoductants getting the cytoplasm with mitochondrial DNA from the donor. Selected colonies were tested on the medium lacking adenine, and for the transfer of the donor plasmid on −Ura medium. Rare colonies getting *URA3* plasmid from the donor were excluded.

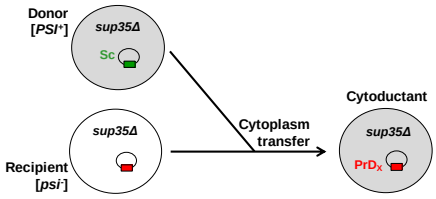

Figure 13: Cytoduction scheme: Donor strains were mated to the respective derivatives of the *S. cerevisiae* strain 1B-D910 by mixing them on YPD medium. After overnight incubation, the mixtures were streaked onto selective medium having 5 µg ml^{-1} cycloheximide and containing 2% ethanol and 2% glycerol instead of glucose. This medium is selective for cytoductants getting the cytoplasm with mitochondrial DNA from the donor.

2.3 DNA ANALYSIS AND CONSTRUCTIONS

2.3.1 *E. coli* small-scale DNA isolation protocols

Two methods were used for quick isolation of small amounts of plasmid DNA from *E. coli.*

Boiling-prep method

E. coli was patched onto LB plates containing antibiotics selective for the target plasmid. Wooden toothpicks were used to collect cells that were resuspended in 180 µl STET buffer (5% Triton X-100, 8% sucrose, 20 mM ethylenediaminetetraacetic acid (EDTA), 50 mM Tris-HCl, pH 8.0) with lysozyme added to a final concentration of 1 mg/ml. Samples were boiled for 3 minutes and were centrifuged at 16000 x *g* for 15 minutes. The pellet was removed using a sterile toothpick and discarded. One volume of isopropanol was used to precipitate the DNA at -20 for 30 minutes. DNA was precipitated by centrifugation at 16000 x *g* for 10 minutes, was washed once with 70% ethanol, dried, and resuspended in TE + RNase (10mM Tris-HCl, 1 mM EDTA, 0.1 mg/ml RNase, pH 7.4.) The sample was incubated at 37° for 30 minutes for RNA removal [80].

Alkaline lysis method

The alkaline lysis method yielded cleaner DNA than that obtained from the boiling prep method. *E. coli* was patched onto LB plates containing antibiotics selective for a target plasmid. Wooden toothpicks were used to collect cells that were then resuspended in 100 µl of Solution I (25 mM Tris-HCl, 10 mM EDTA, 50 mM glucose, pH 8.0). 200 ul of Solution II (0.2 M NaOH, 1% sodium dodecyl sulfate (SDS)) was added and mixed by inversion, and the samples were kept on ice. 150 µl of Alkaline

Lysis Solution III (5 M potassium acetate, pH 5.0) was added and mixed by inversion. The sample was then incubated on ice for 3-5 minutes and centrifuged at 16,000 x *g* for 5 minutes at 4°C to pellet the cell debris. The supernatant was collected in a new tube, and 2 volumes of 95% ethanol was added, followed by vortexing to mix, and incubated at room temperature for 5 minutes. The sample was centrifuged at 16000 x *g* (4°C) for 5 minutes, and the supernatant was discarded. The pellet was washed with 70% ethanol and vortexed briefly. The sample was centrifuged again at 16000 x *g* (4°C) for 5 minutes, and the supernatant was discarded. The DNA pellet was dried thoroughly and resuspended in 50ul of TE (or water) containing 10ug/ml RNase A. The sample was incubated at 37° for 30 minutes for RNA removal.

2.3.2 *E. coli* large-scale DNA isolation protocol

For large-scale preparation of plasmid DNA from *E. coli* DH5α, 250 mLs of Luria-Bertani broth (LB) + antibiotic selective for the plasmid was inoculated with bacteria and was incubated to OD_{550}=0.8 (New Brunswick Series G24 Environmental Incubator/Shaker). Cells were collected by centrifugation at 7000 rpm for 5 minutes and were washed with 10 mLs of Solution I (50 mM glucose, 10 mM EDTA, 25 mM Tris-HCl pH 8.0) and were collected again using centrifugation. The cell pellet was resuspended in 4.5 mLs of Solution I, and 0.5 mLs of 20 mg/mL lysozyme was added. The sample was incubated at room temperature first for 10 minutes and then 20 minutes on ice. 10 mLs of freshly prepared Solution II (0.2 N NaOH, 1% SDS) was added, and the sample was placed on ice for 15 minutes. 7.5 mLs of 3 M sodium acetate pH 5.0 was added, and the sample was placed on ice for 1 hour and then centrifuged at 14,000 rpm at

4°C for 20 minutes. The supernatant was collected, and DNA was precipitated by addition of 20 mLs isopropanol (20 minute at room temperature). The DNA was collected by centrifugation at 12,000 rpm for 15 minutes and was washed once with 70% ethanol and dried. The pellet was resuspended in 4 mLs of Tris-EDTA buffer, pH 8.0 (TE) and was combined with 4 mLs of 9M Lithium Chloride and placed at -20°C for 20 minutes. The sample was centrifuged at 12,000 rpm for 20 minutes. DNA was precipitated by the addition of 16 mLs ethanol (1 hour incubation on ice) and was collected by centrifugation at 12,000 for 15 minutes. The pellet was washed with 70% ethanol, dried thoroughly, and resuspended in TE buffer to the desired concentration.

2.3.3 Yeast DNA isolation

Modifications to a standard protocol [79] were used to isolate genomic DNA from yeast. 10 mLs of YPD was inoculated with one yeast colony and was cultured overnight at 30° C with shaking. Cells were collected by centrifugation at 2000 rpm for 5 minutes and were resuspended in 0.5mL of 1 M sorbitol, 0.1 M Na EDTA (pH7.5). 20 μL of 4 mg/mL lyticase (or zymolase 100,000) was added, and the sample was incubated at 37° C for 60-90 minutes and then centrifuged at high speed for 1 minute. The cell pellet was resuspended in 0.5 mL of 50 mM Tris-Cl (pH7.4), 20 mM Na EDTA on a rotator or by pipetting. 55 μL of 10% SDS was added; the sample was mixed well; and was incubated at 65° C for 30 minutes. 0.2 mL of 5 M potassium acetate was added, and the sample was mixed and incubated on ice for 1 hour followed by centrifugation at high speed for 5 minutes. DNA was precipitated by combining the supernatant with 0.75 mL of isopropanol at room temperature and was collected using centrifugation for 5 minutes at

12,000 x g. The DNA pellet was washed with 70% ethanol, dried briefly, and resuspended in 0.4 mL of TE buffer (pH 7.4) on a rotator. 22 μL of a 1 mg/mL solution of RNase A was added and followed by incubation at 37° C for 30 minutes. If desired, plasmid DNA was ethanol precipitated to yield cleaner DNA.

2.3.4 IsoPure gel extraction protocol

DNA fragments generated from restriction digestion were run on a 1% TBE agarose gel stained with ethidium bromide (100V). Bands were visualized using a UV transilluminator (UVP Gel Doc-it 300 Imaging system.) Target fragments were excised with a scalpel and were purified using an IsoPure DNA Purification Prep Kit (Denville).

2.3.5 DNA sequencing

DNA was purified for sequencing using an IsoPure DNA Purification Prep Kit (Denville) and was eluted in water. DNA sequencing was performed by Eurofins MWG Operon Sequencing (Huntsville, AL).

2.4 PROTEIN ANALYSIS

2.4.1 Yeast protein isolation

Previously described methods [81] were used to isolate protein from yeast. Yeast cultures were grown to the desired OD_{600}. Samples were centrifuged at 5000 x *g* (4°C) for 5 minutes to collect a cell pellet. The cells were washed with water, collected again, and resuspended in 300 μl of chilled lysis buffer (25 mM Tris HCl pH7.5, 100 mM NaCl, 10 mM EDTA, 2mM PMSF, 1 mM NEM, and 1X Roche complete protease inhibitor

cocktail). Next, the samples were combined with an equal volume of acid-washed glass beads (Sigma) and were lysed at 4°C using a Vortex Genie 2 (USA Scientific) at 4°C for 6 minutes. To remove cell debris, the samples were centrifuged at 3000 x *g* (4°C) for 2 minutes. Protein was analyzed immediately or stored at -80°C.

2.4.2 Protein ultracentrifugation

Ultracentrifugation is used to separate polymerized vs. monomeric Sup35 from crude cell extracts. Polymerized Sup35 is precipitated in the pellet, while the soluble Sup35 remained in the supernatant [81]. The strength of a [PSI^+] variant is positively correlated with the amount of Sup35 precipitated in the pellet, whereas [psi^-] yeast contains most Sup35 in the supernatant. Yeast strains were grown to an OD_{600} of 2.0 and lysed to obtain total protein (as described above). Cell lysate was centrifuged at 39 000 x *g* at 4° in an Optima TXL tabletop ultracentrifuge (Beckman Coulter) for 30 minutes. The pellet was dissolved in the original volume of protein lysis buffer, and equal amounts of dissolved pellet and supernatant were run side by side on a polyacrylamide gel for either gel entry assay or boiled gel analysis.

2.4.3 SDS-PAGE/ western blot

Proteins were isolated from yeast as described and were centrifuged at 3000 x *g* for 2 minutes to precipitate cell debris. Protein samples were combined in a 1:3 ratio with 4X Loading Buffer (240 mM Tris-Cl, pH 6.8, 8% SDS,40% glycerol, 12% 2-mercaptoethanol, and 0.002% bromophenol blue), were boiled for 15 minutes (if soluble protein was desired) and were loaded on a 10% SDS-polyacrylamide gel having a 4% stacking gel. Electrophoresis was performed at approximately 100 V in Tris-glycine-SDS

running buffer (25 mM Tris, 192 mM glycine, 0.1% SDS, pH 8.3). Protein was transferred to Hybond-ECL nitrocellulose membrane (Amersham) using a Trans-Blot® SD Semi-Dry Electrophoretic Transfer Cell (BIO-RAD), and the membrane was blocked in 5% milk. The membrane was then incubated with the desired antibodies.

2.4.4 Boiled-gel procedure

The 'Boiled gel' procedure was performed as described [76] (see Fig. 14). In brief, protein samples containing 2% SDS were loaded onto a SDS-PAGE gel and run halfway. Electrophoresis was interrupted, and the wells were sealed with the addition of acrylamide. Once the newly added polyacrylamide was solidified, the gel was placed in a water-tight bag, and the entire gel was boiled for 15 min and cooled. Electrophoresis was resumed. SDS-resistant polymers initially trapped in the wells became solubilized by boiling and could enter the gel when electrophoresis was resumed.

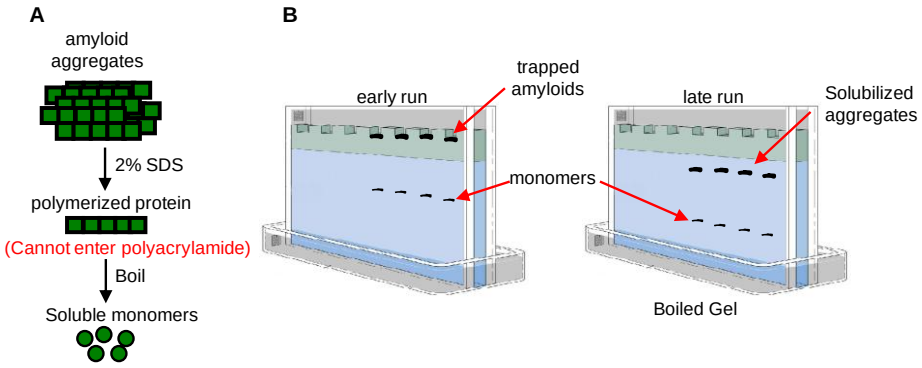

Figure 14 The boiled gel assay. A — Amyloid aggregates are too large and cumbersome to enter polyacrylamide gel. Boiling for 15 minutes in Sample buffer (see methods) containing 2% SDS sufficiently solubilizes the protein into monomers that can enter the gel. **B—**A boiling gel procedure [76] is used to measure the percentage of protein in the soluble (monomeric) vs. polymerized (amyloid) form. Protein samples are combined in a 1:3 ratio with Sample Buffer and are loaded onto a standard 10% polyacrylamide gel. The gel is run halfway at 100V, allowing the soluble protein to enter the gel, but polymerized protein is trapped in the

wells. Electrophoresis is stopped, and the wells are sealed with polyacrylamide to prevent escape of aggregates while boiling. The entire gel is then sealed in a bag and boiled for 15 minutes to solubilize the trapped aggregates. Electrophoresis is resumed, and the newly solubilized protein in the wells can now also enter polyacrylamide.

2.4.5 Gel-entry procedure

To perform the gel-entry procedure, the protein sample to be tested is mixed with 4X loading buffer containing 2% SDS and then divided into two aliquots. One aliquot is boiled for 15 minutes to solubilize any aggregates. Both samples are then run side-by-side on a standard 10% polyacrylamide gel. Aggregated protein (present in the sample that is not boiled) cannot enter the gel, allowing only the soluble protein to enter. The amount present on the gel can then be compared to the boiled control in the neighboring lane to determine the percentage of aggregated protein. The protein is then transferred to a nitrocellulose membrane, blocked, and incubated with the appropriate antibodies as previously described.

2.4.6 SDD-AGE

Aggregates were separated according to size using the semi-denaturing detergent agarose gel electrophoresis procedure (SDD-AGE) [37]. Protein isolated from yeast (previously described) was combined in a 1:3 ratio with 4X loading buffer (240 mM Tris-Cl, pH 6.8, 8% SDS, 40% glycerol, 12% 2-mercaptoethanol, and 0.002% bromophenol blue). This was run loaded on a 1.8% Tris-acetate-EDTA (TAE)-based agarose gel and was run in 1X TAE buffer containing 0.1% SDS was used. The proteins were transferred to a nitrocellulose Protran membrane (Whatman) using a capillary blotting procedure. 5% milk was used to block the membrane, and the membrane was incubated with the desired antibody.

2.4.7 Sup35NM(His)$_6$ purification from *E. coli* using Ni-NTA His-bind® resin

Several fresh bacterial colonies were inoculated into 100 mL of LB media containing 75 μg/ml Cm and 50 μg/ml Amp and were grown overnight at 37° C with shaking. An aliquot was added to flasks containing a combined total of 1.7L of LB+75 μg/ml Cm and 50 μg/ml Amp and was grown at 37° C with shaking for several hours to an OD_{550} of 0.5. 1M IPTG was added to a final concentration of 1 mM, and cultures were incubated for 4 hours at 37° C with shaking to induce the expression of Sup35NM. Samples were centrifuged at 2000 x g for 10 minutes at 4° C to collect the cells for either immediate protein purification or short-term storage at -80° C.

Either a guanidine hydrochloride or a urea-based method was used to purify Sup35NM(His)$_6$. The guanidine-based method allowed for all purification steps to be performed at 4°C (the urea-based method required room temperature purification due to urea precipitation from the buffer) but was not ideal for electrophoresis. The urea-based method worked well for electrophoresis but was hypothesized to yield modified protein that was not preferred for hydrogen/deuterium exchange.

To purify Sup35NM using the guanidine hydrochloride-based method, cells were mechanically disrupted in the presence of 16g of guanidine hydrochloride and 16 ml of guanidine buffer (6 M guanidine hydrochloride, 40 mM Tris-HCl, 300 mM NaCl, 3 mM imidazole). The slurry was centrifuged at 18,000 rpm at 4° C for 25 minutes. The supernatant was combined with Ni-NTA His-Bind® resin (Novagen) prewashed with guanidine buffer and incubated for several hours on a rotator at 4° C to allow protein binding to the resin. The beads were collected and washed once with guanidine buffer.

The beads were added to the column and washed with guanidine buffer to an OD 280 <0.02. The column was clamped to prevent flow-through, and 10 ml of elution buffer (6 M guanidine hydrochloride, 40 mM Tris-HCl, 300 mM NaCl, 200 mM imidazole) was added. After 30 minutes, the protein was collected and combined with methanol and placed at -20 overnight (ratio of 1:5 protein to methanol.) Protein was either stored at -80° C in methanol or used immediately for experiments. To collect the protein, samples were centrifuged at 4000 rpm for 10 minutes and dried to remove methanol. Protein was resuspended in a small volume of either 6M guanidine hydrochloride or 8M urea.

To purify Sup35NM using the urea-based method, cells were mechanically disrupted in the presence of 16g of urea and 16 ml of urea buffer (8 M urea, 40 mM Tris-HCl, 300 mM NaCl, and 3mM imidazole). The slurry was centrifuged at 18,000 rpm at 25° C for 25 minutes. The supernatant was combined with Ni-NTA His-Bind® resin (Novagen) prewashed with urea buffer and incubated for several hours on a rotator at 25° C to allow protein binding to the resin. The beads were collected and washed once with urea buffer. The beads were added to the column and washed with urea buffer to an OD 280 <0.02. The column was clamped to prevent flow-through, and 10 ml of elution buffer (8 M urea, 40 mM Tris-HCl, 300 mM NaCl, 200 mM imidazole) was added. After 30 minutes, the protein was collected and combined with methanol and placed at -20 overnight (ratio of 1:5 protein to methanol.) Protein was either stored at -80° C in methanol or used immediately for experiments. To collect the protein, samples were centrifuged at 4000 rpm for 10 minutes and dried to remove methanol. Protein was resuspended in a small volume of either 6M guanidine hydrochloride or 8M urea.

2.4.8 Preparation of *in vitro* aggregated Sup35NM(His)$_6$ seed

Sup35NM(His)$_6$ seed was prepared using protein purified from *E. coli* (sections 2.2.5, 2.4.7). Sup35NM(His)$_6$ was first boiled for 15 minutes to solubilize potential aggregates and was then added with aggregation buffer (5 mM KPO_4, 150 mM NaCl, pH 7.4) to an eppendorf tube at the 150μg/ml concentration and was placed on a rotator at either 4°C, room temperature (approximately 25°C) or 37°C until the sample was aggregated (confirmed by gel entry assay (section 2.4.5)).

2.4.9 *In vitro* protein polymerization and cross-seeding

Aggregation with rotation

Sup35NM(His)^6 was boiled for 15 minutes as a precaution to solubilize potential aggregates and was added with aggregation buffer (see 2.4.8). Pre-formed seed was added if desired using a 1:20 seed to protein ratio. The sample was placed on a rotator at either 4°C, room temperature (approximately 25°C) or 37°C, and aliquots were removed at time=0 and at subsequent timepoints. Each aliquots was combined with 4X loading buffer and was frozen at -80°C for boiling gel analysis followed by coomassie staining.

Quiescent aggregation

Sup35NM(His)^6 was boiled for 15 minutes as a precaution to solubilize potential aggregates and was added with aggregation buffer (see 2.4.8). Pre-formed seed was added if desired using a 1:20 seed to protein ratio. The sample was mixed by pipetting 20X and placed without rotation at either 4°C, room temperature (approximately 25°C) or 37°C, and aliquots were removed at time=0 and at subsequent timepoints. Samples were mixed by pipetting up and down 20X before each sample was removed to ensure accurate

protein concentrations (It was assumed that large aggregates might precipitate). Each aliquots was combined with 4X loading buffer and was frozen at -80°C for boiling gel analysis followed by coomassie staining.

2.4.10 Gammabody isolation and use

Gammabodies (see Chapter 8) were prepared by transforming bacterial strain BL21(DE3)pLysS (Stratagene) with the desired gammabody plasmids. The strain was inoculated into 150 ml of autoinduction media [98] with 75 μg/ml chloramphenicol and 50 μg/ml ampicillin to select for both the gammabody plasmid and the LysS plasmid. The cells were grown at 30° for 2 days with shaking. Supernatant was collected by centrifugation at 3500 x *g* for 10 minutes at 4°C and was incubated overnight on a rotator with Ni-NTA His-bind® resin. The resin was collected and washed with PBS buffer, pH 7.0 and packed into a column and washed again with the same buffer. Gammabody was eluted using PBS, pH 3.0 and then neutralized to a pH of 7.0.

Aggregates were detected using the following protocol: Approximately 10 μl aliquots of *in vitro* aggregated protein or total cell lysate was spotted onto a dry Hybond-ECL nitrocellulose membrane (Amersham) and was allowed to dry for approximately 10 minutes. The membrane was blocked 3X for a combined time of about 12 hours in a 10% powdered milk solution at 4°C without shaking. (Milk was changed to dilute excess protein that did not bind to the membrane). The membrane was then incubated in a PBS (pH 7.0) solution containing gammabody and 1% powdered milk. After 3, 10 minute washes, anti-FLAG antibody was used with 1% milk and was followed by anti-mouse-HPR antibody. The gammabody was detected using a standard chemiluminescence procedure.

CHAPTER 3: CROSS-SPECIES TRANSMISSION AND VARIANT SWITCH IN *S. CEREVISIAE*

This chapter includes data published in *Mol Microbiol*. [Chen B, Bruce KB, Newnam GP, Gyoneva S, Romanyuk AV , and Chernoff YO. (2010) Genetic and Epigenetic Control of the Efficiency and Fidelity of Cross-species Prion Transmission. *Mol Microbiol* 76(6): 1483-1499.

3.1 CHAPTER SUMMARY

Our lab previously confirmed the existence of a species barrier for [PSI^+] transmission from the *S. cerevisiae* Sup35 to Sup35 from *S. paradoxus* or *S. bayanus*, and implicated the PrD as the major determinant of the barrier [46]. Here, we employ the same experimental strategy to further decipher the role of various PrD modules and prion variants in cross-species prion transmission. The studies we present in this chapter demonstrate that differences between yeast prion variants influence 1) the efficiency of cross-species transmission, and 2) the ability to faithfully reproduce variant-specific patterns via a heterologous protein in the *S. cerevisiae* cell environment. Our data also identify potential amino acid stretches and single residues within the Sup35 PrD that are involved in the control of species specificity in prion transmission.

3.2 MATERIALS

3.2.1 Plasmids

All plasmids used in this chapter were centromeric (low-copy) vectors with either *URA3* or *LEU2* markers. Plasmids containing complete *SUP35* genes from *S. cerevisiae*

(SUP35$_{Sc}$), S. paradoxus (SUP35$_{Sp}$) or *S. bayanus (SUP35$_{Sb}$)* under control of the endogenous *S. cerevisiae SUP35* (P_{SUP35}) promoter were described previously (see [46] and references therein). Major plasmids constructed in this work and primers used for plasmid construction and mutagenesis are listed in the Appendix in Table 2 and Table 3, respectively).

For construction of *SUP35* genes with chimeric *SUP35N* domains, we employed recognition sites for restriction endonucleases *Hin*dIII (located between modules I and II) and *Pfl*MI (located between modules II and III) that are conserved among the three *Saccharomyces* species in this work. The *Pfl*MI site is unique while another *Hin*dIII site is present in *SUP35M*, close to the N/M boundary. The construction strategy is explained in detail in Figure 35 (Appendix). Due to the construction procedure, all chimeric proteins contained the insertion of two additional aa residues at Sup35N/M boundary. To make sure that this insertion does not influence prion transmission, the *S. cerevisiae SUP35* gene with the same insertion was constructed and used as a control in all experiments; no differences from intact *SUP35* were observed. The mutagenesis strategy for constructs with alterations within amyloid stretches is described in Mutagenesis strategy in Figure 36 (Appendix) and Figure 37 (Appendix). All chimeric *SUP35N* domains constructed as described here and further were verified with sequencing by Nevada Genomics Center and Eurofins MWG Operon. The various *SUP35* constructs were introduced and exchanged by transformation and plasmid shuffle (Fig.11)

3.2.2 Strains

S. cerevisiae strains used for cross-species transmission studies, cytoduction studies and biochemical analysis are described in Chapter 2.

3.3 RESULTS AND DISCUSSION

3.3.1 The effect of prion variants on cross-species conversion

To see whether differences in prion variants affected the efficiency of cross-species transmission, we compared transmission of the strong and weak *S. cerevisiae* prion variants from the *S. cerevisiae* Sup35 protein to chimeric proteins, bearing the PrDs of *S. paradoxus*, *S. bayanus*, or *S. cerevisiae* at the phenotypic level by using plasmid shuffle, (Fig. 11) and cytoduction (Fig. 13). The strong *S. cerevisiae* [PSI^+] variant showed only a slight decrease in transmission to the *S. paradoxus* PrD but exhibited a clear transmission barrier with the *S. bayanus* PrD (Fig. 15 and Table 5 (Appendix) and Table 6 (Appendix)).

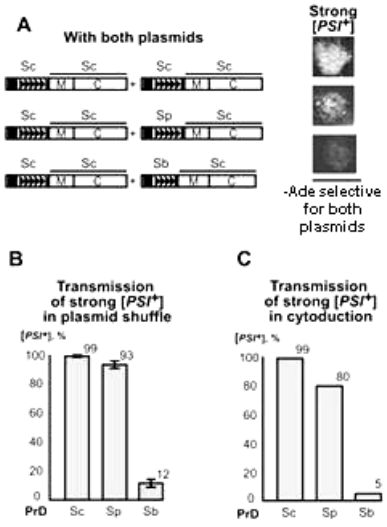

Figure 15: Transmission of a strong *S. cerevisiae* [PSI^+] variant to Sup35 proteins with different PrDs. "Sc", "Sp", and "Sb" refer to *S.*

cerevisiae, *S. paradoxus*, and *S. bayanus*, respectively. "PrD" refers to the Sup35 prion domain. **A—**Growth of transformants containing both the original and the newly introduced plasmid on –Ade medium selective for both plasmids. **B—**The results of direct plasmid shuffle performed in a strong [*PSI*$^{+}$] variant as shown on Plasmid shuffle scheme Fig. 11. Here, standardized errors are indicated. For exact numbers, see Table 5 C (Appendix)— Results of cytoduction experiments performed in a strong [*PSI*$^{+}$] variant as shown on Cytoduction scheme Fig. 13. For exact numbers, see Table 6 (Appendix). Errors were not calculated for cytoduction experiments, as our procedure does not guarantee that all cytoductants, obtained for a given construct, were independent of each other.

In contrast, the weak *S. cerevisiae* [*PSI*$^{+}$] variant exhibited a transmission barrier with the *S. paradoxus* PrD in both versions of the experiment, but showed a clear barrier with the *S. bayanus* PrD only in plasmid shuffle (Fig. 16 and Tables 7 (Appendix) and Table 8 (Appendix)). Even in this case, the barrier was not as severe as for strong [*PSI*$^{+}$]. Relatively efficient transmission of the strong [*PSI*$^{+}$] variant to the chimeric construct having the *S. paradoxus* PrD contrasted with the previously detected barrier in the transmission of this prion variant to intact *S. paradoxus* Sup35 [46]. This agrees with our lab's observation that the strong *S. cerevisiae* [*PSI*$^{+}$] variant efficiently converts all of the chimeric construct but not all of the intact *S. paradoxus* protein into the SDS-insoluble polymers (Andrey Romanyuk,[48]).

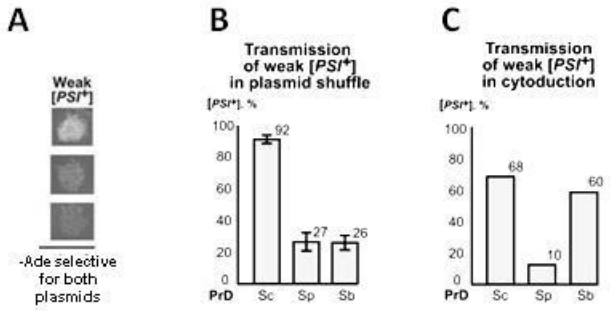

Figure 16 Transmission of a weak *S. cerevisiae* [*PSI*$^+$] variant to Sup35 proteins with different PrDs. Designations are as on Fig. 15. **A—**Growth of transformants containing both the original and newly introduced plasmids on –Ade medium selective for both plasmids. **B—**Results of direct plasmid shuffle performed in a weak [*PSI*$^+$] variant as shown on Plasmid shuffle scheme (Fig. 11). Here, standardized errors are indicated. For exact numbers, see Table 7 (Appendix). C—Results of cytoduction experiments performed in a weak [*PSI*$^+$] variant as shown on Cytoduction scheme (Fig. 13). For exact numbers, see Table 8 (Appendix). Errors were not calculated for cytoduction experiments, as our procedure does not guarantee that all cytoductants, obtained for a given construct, were independent of each other.

3.3.2 Asymmetry and infidelity of cross-species prion conversion

Even when the parental *S. cerevisiae* [*PSI*$^+$] variant was strong, prion isolates resulting from cross-species transmission to proteins with *S. paradoxus* or *S. bayanus* PrDs were phenotypically weak (Fig. 17). This was similar to both our previous observations for complete *S. paradoxus* and *S. bayanus* proteins [46] and some previous reports on cross-species transmission of mammalian prions [12].

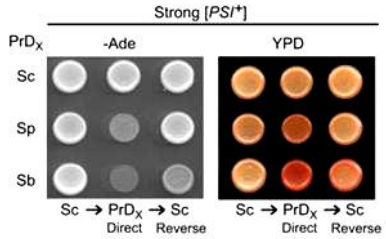

Figure 17: Reproduction and switch of prion variants during cross-species transmission. Designations are as on Fig. 15. Patterns of [*PSI*$^+$] isolates obtained from a strong *S. cerevisiae* prion variant via direct

shuffle to the control *S. cerevisiae* Sup35 protein or to chimeric proteins having either *S. paradoxus* or *S. bayanus* PrDs. This was followed by reverse shuffle back to *S. cerevisiae* Sup35 (Fig. 11). "PrD_X" refers to PrDs of various origins as indicated. The –Ade plate was photographed after 6 days. The YPD plate was photographed after 3 days of incubation followed by 4 days in the refrigerator.

To determine whether such an alteration of the variant-specific patterns is reversible, we performed a "reverse shuffle" (Fig. 11), thus transmitting the prion state back to the *S. cerevisiae* Sup35 protein. In agreement with our previous observations for intact proteins [46], the prion state was efficiently transmitted from protein with the *S. paradoxus* PrD to the *S. cerevisiae* protein, confirming asymmetry of cross-species prion transmission in this combination (Fig. 18 and Tables 9 (Appendix) and Table 10 (Appendix)).

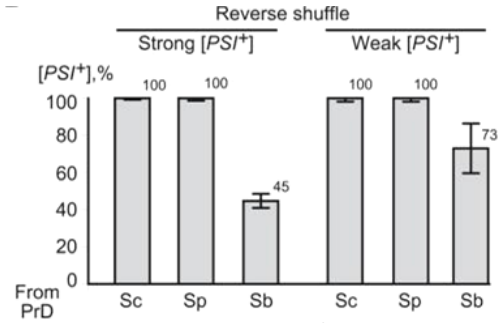

Figure 18: Frequencies of reverse [*PSI*$^+$] transmission in a strong and weak *S. cerevisiae* [*PSI*$^+$] variant. Species designations are as on Fig. 15. For exact numbers, see Tables 9 (Appendix) and Table 10 (Appendix).

In the case of the *S. bayanus* PrD, asymmetry of cross-species prion transmission was also observed, but it was less pronounced for strong *S. cerevisiae* prion variant. Alteration of phenotypic patterns of the strong prion variant propagated via the *S. paradoxus* PrD was reversible, as strong [*PSI*$^+$], phenotypically indistinguishable from the parental *S. cerevisiae* variant, was recovered after the reverse shuffle to *S. cerevisiae*

Sup35 protein (Fig. 17). In contrast, [*PSI*$^+$] isolates produced by the reverse shuffle from the protein with *S. bayanus* PrD to the *S. cerevisiae* protein were weaker (Fig. 17) and produced more protein in the soluble state (Fig. 19), compared to the strong *S. cerevisiae* [*PSI*$^+$] variant that has not been propagated through the heterologous PrD. These isolates were confirmed by plasmid isolations and subsequent DNA analysis to contain the unaltered *S. cerevisiae SUP35* gene (data not shown), thus excluding the possibility that they might originate from any recombination events during the period of coexistence of the *S. cerevisiae* and *S. bayanus* genes within the same cell. Therefore, our data demonstrate that variant-specific prion patterns could be altered irreversibly during cross-species transmission involving *S. bayanus* PrD, so that the resulting prion may keep a "memory" of being transiently propagated via a heterologous PrD.

Figure 19: **Centrifugation analysis of Sup35 aggregation.** Ultracentrifugation was performed for cell lysate from two different isolates obtained via shuffle from the strong *S. cerevisiae* [*PSI*$^+$] strain to the chimeric protein with *S. bayanus* PrD, followed by a reverse shuffle to the *S. cerevisiae* protein as shown on Figure 17. Extract of the strong *S. cerevisiae* strain that has not been propagated through a heterologous protein ("Strong Sc") is shown as a control. Protein extracts were fractionated by centrifugation at 39 000 x *g*. Supernatant (S) and pellet (P) fractions were boiled in 2% SDS, run on a SDS-PAGE gel, and analyzed by western blotting with the Sup35C antibody. The prion isolates obtained from reverse shuffle contain more Sup35 protein in the supernatant, as compared to the control strong prion strain. This confirms irreversible change in the prion variant patterns during propagation through a heterologous stage.

Moreover, various [*PSI*$^{+}$] isolates obtained from reverse shuffle exhibited different levels of suppression, even though none of them could match the original strong *S. cerevisiae* [*PSI*$^{+}$] variant in suppression efficiency (Fig. 20). This indicates that heterologous conversion could be imprecise and generate multiple variants of a prion.

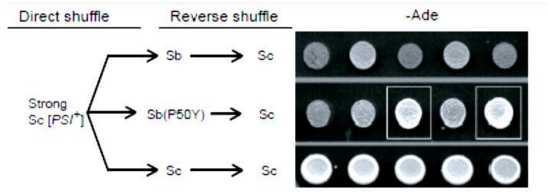

Figure 20: Variability in [*PSI*$^{+}$] stringency after propagation through a protein with the *S. bayanus* PrD. The shuffle was performed starting from the strong *S. cerevisiae* [*PSI*$^{+}$] strain GT256-23C, as shown on Figure 11 and Figure 17. Designations "Sc" and "Sb" refer to *S. cerevisiae* protein and protein with the *S. bayanus* PrD, respectively. "P50Y" refers to a mutation at amino acid position 50 of the *S. bayanus* Sup35 sequence. All colonies shown on the figure originate from reverse shuffle and contain only *S. cerevisiae* Sup35 protein. Prion derivatives that come from reverse shuffle via the *S. bayanus* PrD show variable stringencies of suppression (as measured by intensity of growth on –Ade medium), in contrast to the control isolates propagated only through the *S. cerevisiae* protein that are always homogenous. Remarkably, some prion variants originated from reverse shuffle through the Sb (P50Y) protein (denoted by squares) match the *S. cerevisiae* strong [*PSI*$^{+}$] by stringency, while prion variants originated from reverse shuffle through the Sb protein never do.

Such an infidelity in prion transmission was not detected with the weak *S. cerevisiae* [*PSI*$^{+}$] variant, which produced even weaker prion isolates while propagated via a heterologous protein but was restored after the reverse shuffle (Fig. 21). Therefore, the *S. bayanus* PrD can faithfully propagate weak *S. cerevisiae* prion despite a temporary change in its phenotypic expression, but irreversibly alters patterns of the strong *S. cerevisiae* prion.

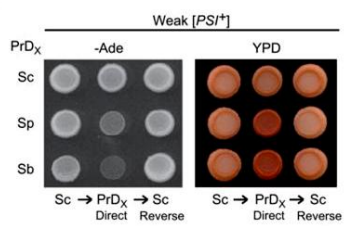

Figure 21: **Reproduction of prion variants during cross-species transmission** Patterns of [*PSI*$^{+}$] isolates obtained from a weak *S. cerevisiae* prion variant via direct shuffle to the control *S. cerevisiae* Sup35 protein and chimeric proteins with either *S. paradoxus* or *S. bayanus* PrDs, followed by reverse shuffle back to *S. cerevisiae* Sup35 (Fig. 11). "PrD_X" refers to PrDs of various origins as indicated. The –Ade plate was photographed after 7 days; The YPD plate was photographed after 3 days of incubation followed by 4 days in the refrigerator.

3.3.3 Construction of Sup35 proteins with the chimeric prion domains

To determine which specific region of Sup35N is responsible for the species barrier, we constructed a set of chimeric *SUP35* genes as described in chimeric genes diagram (Fig. 35). The convenient location of conserved restriction sites enabled us to divide the Sup35N-coding region of the *SUP35* gene into 3 exchangeable modules, designated as modules I, II and III (Fig. 22). Module I includes most of the QN region up to (and including) position 33, encompassing the whole fragment 8-27 with the maximal percentage of QN residues, which is primarily responsible for the species barrier in the *Saccharomyces-Candida* combination [41]. Module II includes the very end of the QN region and the whole ORs region, while module III includes the remaining portion of Sup35N. There is no difference in aa sequence between *S. cerevisiae* and *S. bayanus* within the "tail" of the QN region that falls into module II (positions 34 to 40), and there is only one aa substitution within this region in *S. paradoxus* (Fig. 23).

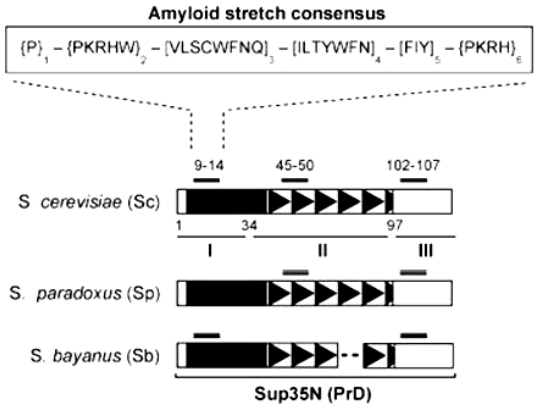

Figure 22: Modules of Sup35 PrDs from three closely related *Saccharomyces* species. Designations "PrD" "QN," and "ORs" refer to prion domain, QN-rich region, and region of oligopeptide repeats, respectively. Roman numerals represent exchangeable modules of Sup35 PrD used in our experiments. Numbers correspond to amino acid positions. The "Tail" (position 34-40) of the QN region in module II is identical in *S. cerevisiae* and *S. bayanus* and shows one amino acid change in *S. paradoxus*. Dashed lines mark a missing oligopeptide repeat in *S. bayanus*. Short, bold lines denote amyloid stretches, according to a hexapeptide consensus from ref. **[74],** as shown. Residues forbidden or permitted at a given position (indicated by number) are placed within { } or [ ], respectively.

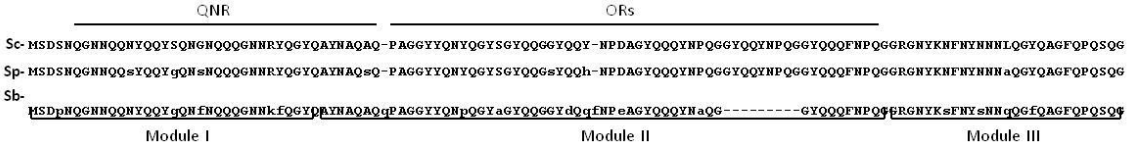

Figure 23: Divergence of Sup35 prion domains in *Saccharomyces sensu stricto* yeast. "Sc", "Sp,"and "Sb" refer to *S. cerevisiae*, *S. paradoxus*, and *S. bayanus*, respectively. QNR and ORs refer to QN-rich stretch and the oligopeptide repeats, respectively. Locations of the exchangeable modules are indicated.

We generated a set of *SUP35* genes with chimeric *SUP35N* domains, combining modules I, II and III of *S. cerevisiae*, *S. paradoxus* or *S. bayanus* in various combinations (Fig. 24). Chimeric PrDs were fused in frame to the *SUP35MC* region from *S. cerevisiae* and placed under control of the endogenous *S. cerevisiae SUP35* promoter (P_{SUP35}), located on a low-copy (centromeric, or *CEN*) plasmid with the *URA3* selectable marker.

All constructs were proven to maintain viability of *S. cerevisiae* in the absence of endogenous Sup35, and remained completely functional in translation termination, as confirmed by inability of the [*psi*$^-$] *sup35Δ* strain, bearing each of these constructs, to grow on –Ade medium, that is, to read through the *ade1-14* reporter. Each chimeric construct tested was expressed at the same level as *S. cerevisiae* Sup35 when placed on a plasmid of the same structure (Fig. 38). For most chimeric proteins, we also show that the protein can be induced into a prion ([*PSI*$^+$]) state by transient overproduction of the same chimeric construct and/or at least one of the parental *SUP35* genes. All the constructs could generate both strong and weak prion strains, with the exception of constructs containing module II of *S. bayanus* that produced preferentially weak variants (data not shown).

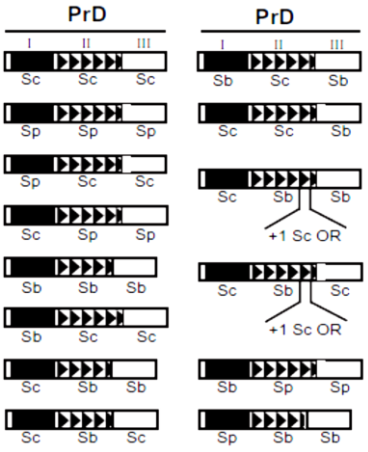

Figure 24: Chimeric PrDs constructed in this study. Exchangeable modules are designated by Roman numerals. Designations "PrD" "ORs" refer to prion domain and region of oligopeptide repeats, respectively. "Sc", "Sp", and "Sb" refer to *S. cerevisiae*, *S. paradoxus*, and *S. bayanus*, respectively.

3.3.4 Identification of PrD modules responsible for the species barrier

In order to determine which module of Sup35N controls the species specificity of prion conversion from *S. cerevisiae* Sup35 to the other *S. sensu stricto* Sup35 proteins, we performed the plasmid shuffle experiments (Fig. 11) with each of the chimeric *SUP35* constructs. Our results unambiguously demonstrated that module I of *S. paradoxus* is responsible for the transient decrease in [*PSI*$^+$] phenotypic stringency (data not shown) and for the species barrier in prion transmission (Fig. 25 A and B, and Tables 5 (Appendix) and Table 7 (Appendix)), while the region encompassing modules II and III of *S. paradoxus* exhibits little or no effect. In contrast, module II of *S. bayanus* was responsible for the species barrier, while modules I and III of *S. bayanus* exhibited little or no affect Fig. 25 A and B and Tables 5 (Appendix) and 7 (Appendix)). Even in this case, the barrier was not as severe as for strong [*PSI*$^+$].

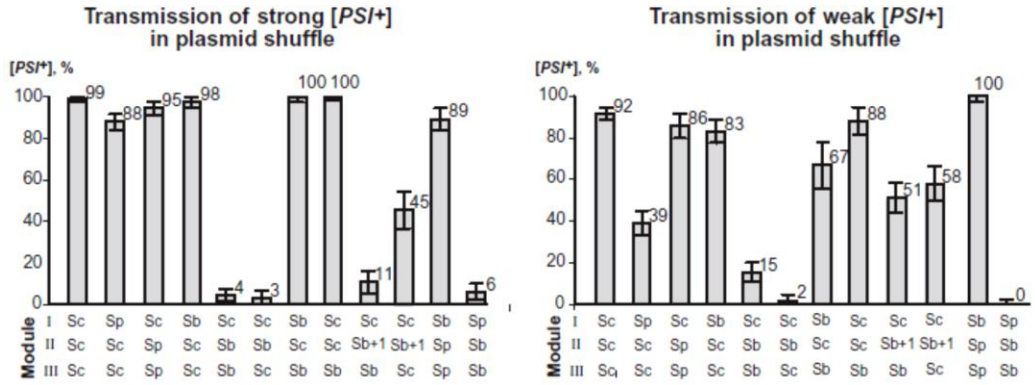

Figure 25: Frequency of transmission of strong and weak [*PSI*$^+$] to Sup35 proteins with chimeric PrDs by plasmid shuffle. Direct plasmid shuffle was performed beginning with either a strong (panel A) or weak (panel B) [*PSI*$^+$] variant as shown on the plasmid shuffle scheme Figure 11. Data for the control *S. cerevisiae* construct reproduce those shown on Fig. 15(B) and 16 (B). For exact numbers, see Tables 5 (Appendix) and Table 7 (Appendix).

These results were generally confirmed by cytoduction experiments Fig. 26 A and B and Tables 6 (Appendix) and 8 (Appendix)).

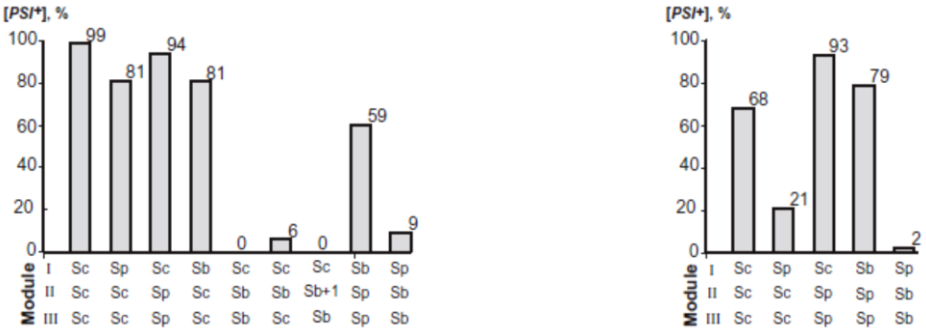

Figure 26: Frequency of cytoduction transmission of strong and weak [*PSI*$^+$] to Sup35 proteins with chimeric PrDs. Cytoduction was performed beginning with either a strong (left panel) or weak (right panel) [*PSI*$^+$] variant as shown on Cytoduction scheme Fig. 13. Data for the control *S. cerevisiae* construct reproduce those shown on Fig. 15 (C) and 16 (C).

Notably, the insertion of an additional OR unit of *S. cerevisiae* origin into the *S. bayanus* module II somewhat increased cross-species prion conversion but did not completely eliminate the barrier in plasmid shuffle (Fig. 25, A and B) and did not show any effect on the barrier in cytoduction (Fig. 26, A). This indicates that while the size of module II plays a certain role in cross-species prion transmission, its specific sequence features are also important. Importantly, module II of *S. bayanus* was both required and sufficient for switching the strong [*PSI*$^+$] variant to the weaker variant as detected in reverse shuffle (Fig. 27).This demonstrates that in addition to controlling the frequency of cross-species prion conversion in the *S. cerevisiae* / *S. bayanus* combination, module II also controls fidelity of reproduction of the variant-specific prion patterns via a heterologous stage. Based on the observed differential effects of PrD modules, we predicted that artificial PrD composed of module I of *S. bayanus* and modules II and III

of *S. paradoxus* would show "promiscuous" behavior, while the reciprocal artificial PrD, composed of *S. paradoxus* module I and *S. bayanus* modules II and III would exhibit a very stringent species barrier in all combinations. Indeed, our data confirmed this prediction (Fig. 25 and Fig. 26).

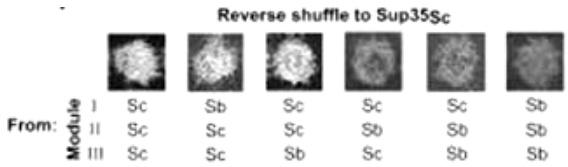

Figure 27: Changes in phenotypic patterns after reverse shuffle. Phenotypic patterns of strong prion variant are switched in the chimeric constructs bearing module II of *S. bayanus*, as detected after reverse shuffle to the *S. cerevisiae* Sup35 protein, performed as shown on Plasmid shuffle scheme Fig. 11. –Ade plates were photographed after 6 days.

3.3.5 The role of amyloid stretches in cross-species prion conversion

Within module I, more amino acid substitutions are found between *S. cerevisiae* and *S. bayanus* (5 out of 33 positions) than between *S. cerevisiae* and *S. paradoxus* (only 3, see Fig. 23). This seems to disagree with our observation that module I of *S. paradoxus* is sufficient for the species barrier while module I of *S. bayanus* is not (see above, Fig. 25 and Fig 26). However, all three aa substitutions in the *S. paradoxus* sequence are located between positions 12 and 20, while *S. bayanus* has only 2 substitutions within this fragment (Fig. 23). It therefore appears that identity of the fragment 12-20 rather than that of the whole module I is crucial for prion transmission and stringency. Moreover, 2 out of 3 variable positions within this region are changed in both *S. paradoxus* and *S. bayanus*, so that only asparagine (N) to serine (S) substitution at position 12 is specific to *S. paradoxus*. We changed the codon for S12 into a codon for N in the *S. paradoxus* sequence, and found that such a substitution significantly increased both cross species

transmission of weak *S. cerevisiae* [*PSI*$^{+}$] from either complete *S. paradoxus* PrD or chimeric PrD containing *S. paradoxus* module I (Fig. 28), and phenotypic stringency of the strong prion variant in a heterologous protein background (Fig. 29).

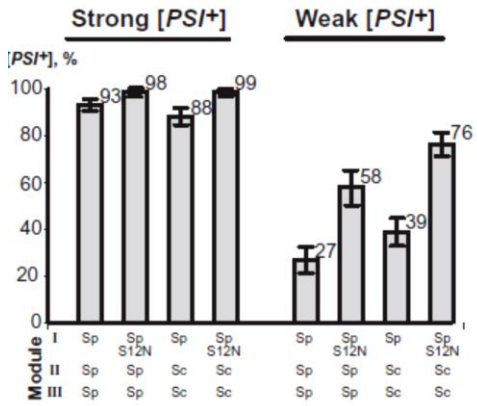

Figure 28: The effects of the S12N mutation at position 12 on cross-species [*PSI*$^{+}$] transmission. Frequencies of the *S. cerevisiae* prion transmission in direct shuffle from either a strong (panel A) or weak (panel B) variant to derivatives containing *S. paradoxus* module I with the S12N mutation at residue 12.

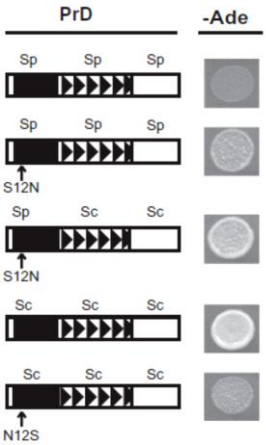

Figure 29: The effects of position 12 exchange on phenotype. Residue 12 controls phenotypic expression of the strong *S. cerevisiae* prion in the *S. cerevisiae* / *S. paradoxus* combination, as seen on –Ade plates photographed after 6 ds.

Next, we mutated the codon for N12 (*S. cerevisiae* version) into a codon for S (*S. paradoxus* version) in the otherwise intact *S. cerevisiae SUP35* gene, and demonstrated that transmission of weak *S. cerevisiae* prion to the mutant protein is decreased, even though not to such an extent as in the case of the substitution of the whole module I by its *S. paradoxus* counterpart (Fig.30). In the case of the strong prion variant, N12S substitution impaired prion transmission more severely than did the whole module I of *S. paradoxus* (Fig.28) and decreased the phenotypic stringency of the prion maintained by a heterologous protein (Fig. 29). This was not due to inability of the mutant protein to maintain a phenotypically strong prion variant in principle, as it could be induced into a strong prion variant *de novo* by overproduction of the *S. cerevisiae* Sup35N fragment (data not shown).Taken together, our results show that a single aa substitution at position 12 of the Sup35 protein plays an important role in both specificity of prion transmission and stringency of the prion isolates obtained from cross-species conversion, even though it is not solely responsible for the specificity.

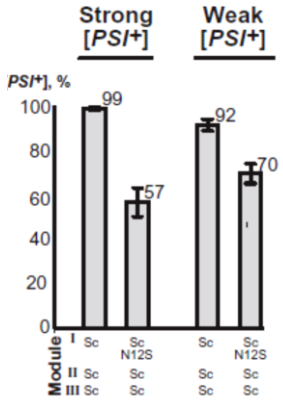

Figure 30: Frequencies of the *S. cerevisiae* prion transmission in direct shuffle to the *S. cerevisiae* protein with N12S mutation at residue 12. Frequencies of the *S. cerevisiae* prion transmission in direct shuffle from either a strong (panel A) or weak (panel B) variant to derivatives containing *S. cerevisiae* module I with mutated residue 12.

The location of residue 12 is quite remarkable, as it falls within the only sequence found in module I (see above, Fig. 23) that satisfies requirements for the "amyloid stretch" (Fig. 22), a consensus hexapeptide detected in most proteins efficiently forming amyloids *in vitro* [92, 74]. Moreover, the N12S substitution breaks this consensus (Fig. 22). Despite a relatively high level of flexibility allowed at some positions of the amyloid stretch (Fig. 22), the *S. cerevisiae* Sup35N region contains only two more hexapeptides satisfying the consensus requirements, at positions 45-50 within module II, and 102-107 within module III (see above, Fig. 22). Both stretches are conserved in *S. paradoxus*; however, they contain respectively one and two aa substitutions in *S. bayanus.* Substitutions within module III do not break the amyloid stretch consensus, but substitution of tyrosine (Y) to proline (P) at position 49 (*S. bayanus* position 50) within module II does (Fig. 22). We mutated P50 into Y in the *S. bayanus* sequence and found that this substitution significantly increased cross-species transmission of both strong and weak *S. cerevisiae* prions to the mutated protein (Fig. 31).

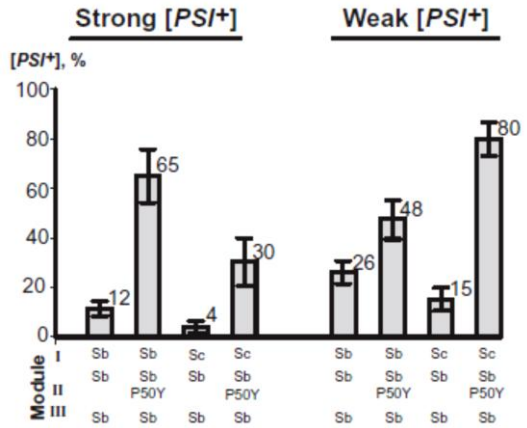

Figure 31: Frequencies of the *S. cerevisiae* prion transmission in direct shuffle to the *S. bayanus* PrD derivatives with the P50Y mutation at position 50. Data for the control Sb-Sb-Sb construct reproduces that shown on Fig. 15 (B) and 16 (B). Data for the Sc-Sb-Sb construct reproduces that shown on Fig. 25. Species designations are as on previous

figures. Shuffle was performed as shown on Plasmid shuffle scheme Fig. 11. Exact numbers are shown in Tables 5 (Appendix) and Table 7 (Appendix). Species designations are as on previous figures.

In the case of weak [*PSI*$^{+}$], the species barrier was essentially eliminated when mutated module II of *S. bayanus* was combined with module I of *S. cerevisiae* origin. Although P50Y substitution did not restore the phenotypic stringency of a heterologous prion (Fig. 32), and did not completely restore the fidelity of reproduction of the variant-specific prion patterns during reverse shuffle in case of strong [*PSI*$^{+}$] (Fig. 20), it altered the spectrum of the prion variants obtained after reverse transmission to the *S. cerevisiae* Sup35 protein, so that at least some isolates now matched the original strong *S. cerevisiae* prion in suppression efficiency.

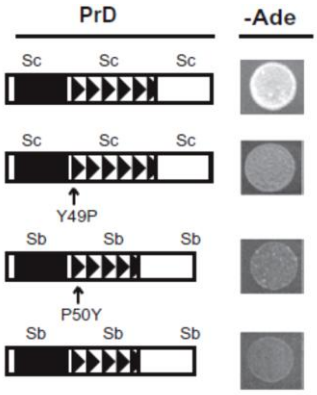

Figure 32: Effect of the Y49P and P50Y substitutions on the phenotypic expression of strong [*PSI*$^{+}$] in direct shuffle.

Reciprocal substitution Y49P within the *S. cerevisiae* Sup35N domain moderately decreased transmission of the strong *S. cerevisiae* prion but had no detectable effect on transmission of the weak *S. cerevisiae* prion to a mutated protein, indicating that disruption of the amyloid stretch II consensus by itself is not sufficient for the species barrier (Fig. 33)

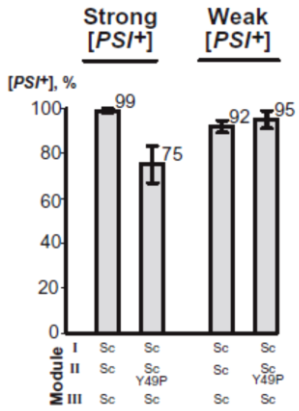

Figure 33: Frequencies of the *S. cerevisiae* prion transmission in direct shuffle to the *S. cerevisiae* protein with altered position 49. Data for the control Sc-Sc-Sc reproduces that shown on Fig. 15 (B) and Fig. 16 (B). Species designations are as on previous figures. Shuffle was performed as shown on Plasmid shuffle scheme Fig 11. Exact numbers are shown in Tables 5 (Appendix) and Table 7 (Appendix). Species designations are as on previous figures. Shuffle was performed as shown on Fig. 1E. Exact numbers are shown in Tables 5 (Appendix) and Table 7 (Appendix).

Notably, this mutation decreased phenotypic stringency of the strong prion (Fig. 32), although this was not sufficient for the irreversible switch of a prion variant, as stringency was restored after the reverse shuffle to the non-mutant *S. cerevisiae* protein (data not shown). Taken together, our data point to the important even though not exclusive role of amyloid stretches in control of the species specificity and fidelity of cross species prion transmission.

3.4 DISCUSSION

3.4.1 Relationship between coaggregation, polymerization and prion transmission

Interestingly, the efficiency of prion conversion of the heterologous Sup35 protein does not appear to be entirely determined by its PrD. Transmission of the strong *S. cerevisiae* prion variant to the intact *S. paradoxus* Sup35 protein is inefficient at the phenotypic level [46], While a chimeric protein bearing only the PrD of *S. paradoxus*

shows only a weak barrier in prion transmission (Fig. 15). This result somewhat contradicts our previous observation of a strict species barrier in transmission of strong *S. cerevisiae* [*PSI*$^+$] to the chimeric protein with *S. paradoxus* PrD made for a small sample of colonies [46]. It is possible that we have either dealt with a statistical fluctuation previously, or more likely, overlooked the [*PSI*$^+$] colonies appearing after heterologous transmission, as Sup35 PrD from *S. paradoxus* significantly decreases suppression efficiency of [*PSI*$^+$] generated by transmission from *S. cerevisiae* protein, thus requiring longer time for detection of [*PSI*$^+$] by suppression (for example, see Fig. 29). In any case, our new data unequivocally confirm that while the PrD of *S. paradoxus* is sufficient to generate a strong transmission barrier for the weak [*PSI*$^+$], it causes only a slight decrease in transmission of strong [*PSI*$^+$]. However, it should be stressed that PrD of Sup35 remains the major region responsible for the species barrier between *S. cerevisiae* and *S. bayanus*, and at least in case of weak [*PSI*$^+$], between *S. cerevisiae* and *S. paradoxus*.

As Sup35C domains of *S. paradoxus* and *S. cerevisiae* are 100% identical to each other, the differences in behavior of complete *S. paradoxus* protein and chimeric protein with *S. paradoxus* PrD must be due to Sup35M. Indeed, we previously observed that the Sup35M region of *S. paradoxus* is partly responsible for extreme mitotic instability of prions generated by intact *S. paradoxus* Sup35 in the *S. cerevisiae* cell [46]. The non-PrD region of *S. bayanus* Sup35 also influences some patterns of cross-species interactions, as introduction of the chimeric protein with *S. bayanus* PrD into the strong *S. cerevisiae* [*PSI*$^+$] strain results in a larger fraction of protein remaining in the supernatant and a larger proportion of non-polymerized protein associated with aggregates if compared to complete *S. bayanus* Sup35 (Result by A. Romanyuk [48]).

Interestingly, the non-PrD region of *S. bayanus* acts "in favor" rather than "against" prionization. One possibility is that interactions with the host-specific cellular factor, such as chaperone Hsp104 [88, 89], partly modulated by Sup35M [90], might influence physical stability of heteroaggregates and/or a freshly generated heterologous prion (see future discussion in Chapter 6, Model Fig. 58). If so, this may point to an additional level at which specificity of cross-species prion transmission could be controlled. However it should be noted that, in general, correlation between the mitotic instability (observable after 20-40 generations for weak prions in general and some heterologous prions in particular, see Table 11 (Appendix)) and species barrier has not been observed, as some constructs exhibiting instability (e.g. Sb-Sp-Sp) did not show a strong barrier.

3.4.2 Prion variants and species barrier

Our results confirm previous findings in mammalian and yeast systems showing that variant-specific patterns of a prion affect cross-species prion transmission. In addition, we also demonstrate that different prion variants of Sup35 may influence prion transmission at a different level. The stringency of the prion variant influenced cross-species prion transmission to different orthologous proteins in different ways, so that a strong prion variant was transmitted to *S. paradoxus* PrD more efficiently than a weak variant, while for *S. bayanus* PrD, the ratio was the opposite (Fig. 15 (B) and 16 (B). Interestingly, the *S. bayanus* PrD usually drives a weak prion phenotype in *S. cerevisiae* [46], and this pattern is, at least in part, controlled by its module II region including the ORs (see above).

The weak *S. cerevisiae* [PSI^+] prion variants possess a larger portion of the PrD that is "protected" from hydrogen exchange and is, therefore, likely to be included in the β-structured region [38]. Weak variants also require a larger PrD region for the faithful propagation of variant-specific patterns [70, 71, 63], as compared to the strong prion variants. It is possible that prions formed by *S. bayanus* PrD are weak because shorter β-structured regions are insufficient for keeping this protein in the amyloid-proficient state. Therefore, more efficient transmission of the weak *S. cerevisiae* prion variant to *S. bayanus* PrD could be due to a larger size of the β-structured region involved in such a conversion, while a shorter region generated in the case of a strong prion cannot be stably maintained by the *S. bayanus* PrD sequence.

3.4.3 The fidelity of cross-species prion conversion

While transmission of the prion state from the *S. cerevisiae* protein to a protein with the *S. paradoxus* PrD, or transmission of the weak *S. cerevisiae* prion to a protein with the *S. bayanus* PrD resulted in phenotypically weakened prion variants, the patterns of the original *S. cerevisiae* prion were restored after reverse transmission back to *S. cerevisiae* protein (Fig. 17 and Fig. 21). Possibly in these cases, sequence divergence led to the alteration of growth and/or fragmentation kinetics of prion polymers; however, the structural characteristics of prion units remained faithfully reproducible and were restored upon return back to the original sequence. In contrast, the variant patterns were switched irreversibly when strong *S. cerevisiae* prion was transmitted to the protein with *S. bayanus* PrD and then back to *S. cerevisiae* protein (Fig. 17 and Fig 19). Perhaps the prion state can be transmitted from the strong *S. cerevisiae* prion by the *S. bayanus* PrD

only in exceptional situations when an extended β-structured region is occasionally formed in the heteroaggregate. Resulting *S. bayanus* prion represents a new (weaker) variant which in turn, generates weaker variants of the *S. cerevisiae* prion in the reverse shuffle. Appearance of the multiple prion variants reflects imprecise interactions between the divergent PrD regions. Such a mechanism could fit into the "conformational selection" model **[12],** with a clarification that formation of the new conformational variant is stimulated within a heteroaggregate when accurate transmission of the properties of a pre-existing conformer is impaired due to differences in the sequence. It is unlikely that new conformers pre-exist in the strong prion "population," as intraspecies transmission of the strong prion does not produce weak variants at a detectable level. The variant switch apparently does not occur in the case of transmission of the weak *S. cerevisiae* prion variant via *S. bayanus* PrD (Fig. 21) as the weak variant already contains a large β-structured region. Generation of multiple prion variants was previously reported in the case of promotion of prion formation by a highly divergent Sup35 protein [43]; however, this occurred with a much lower frequency than in the *S. bayanus* / *S. cerevisiae* reverse shuffle. Prion transmission between some artificially modified derivatives of Rnq1 protein with altered combinations of prionogenic regions also generated multiple prion variants [53].

3.4.4 Identity determinants of prion proteins

Previous work with highly divergent Sup35 proteins implicated the N-proximal QN-rich region of the PrD, encompassing the first 40 aa residues, as a major determinant of the sequence-specificity in prion transmission [42, 91, 41]. However, our data (Figures

25, 26 and 27) surprisingly show that in the *S. cerevisiae* / *S. bayanus* combination, specificity of transmission is primarily determined by module II of PrD encompassing residues 34-96. As the "tail" of the QN region located within module II (positions 34-40) is identical in both species, it is obvious that sequence elements located within the region of ORs contribute to transmission specificity. Indeed, mutational alteration at position 50 (Fig. 31 and/or addition of the missing OR unit to *S. bayanus* PrD significantly increased cross-species prion conversion (Fig. 25 and Fig 26).

Moreover, even in the *S. cerevisiae* / *S. paradoxus* combination where the QN region is the primary determinant of the species barrier, it is not the overall sequence divergence of this region that is most important. Indeed, the QN region of *S. paradoxus*, which is responsible for the barrier in transmission of a weak prion from *S. cerevisiae*, is less divergent from *S. cerevisiae* than is the QN region of *S. bayanus* which does not show a barrier (Fig. 23 and Fig 25, (B). A combination of the QN region of *S. bayanus* with the rest of the PrD sequence from *S. paradoxus* generates an artificial PrD that is highly susceptible to transmission of prion state from *S. cerevisiae* (Figures 25, 26 and 27), despite retaining only about 93% of sequence identity. This is less than in case of the complete *S. paradoxus* PrD (94%) which does not exhibit such promiscuity, at least for the weak prion variant. In contrast, the reciprocal chimeric combination (Sp-Sb-Sb) possesses a slightly higher identity to the *S. cerevisiae* PrD than does the complete *S. bayanus* PrD but exhibits an even stronger barrier. The only plausible explanation for these phenomena is that identity of the relatively short aa stretches located at different positions within the PrD is more important for determining conversion specificity than is overall conservation of PrD sequences. Indeed, if prion specificity is controlled by at

least two short stretches, one of which is located within the QN region and is identical between *S. cerevisiae* and *S. bayanus* but different in *S. paradoxus*, while another stretch is located within ORs region and is identical for *S. cerevisiae* and *S. paradoxus* but different in *S. bayanus*, we would get the observed results. This model also agrees with the recent observations for Rnq1 prion, where multiple prion determinants control transmission specificity [53].

Remarkably, our search for the altered prion identity determinant located within module I (QN region) of *S. paradoxus* led to the base substitution at position 12, that disrupts the only hexapeptide in module I satisfying the requirements for the amyloid stretch (Fig. 22), a consensus sequence detected in most proteins that efficiently form amyloids *in vitro* [92, 74]. Even though position 12 is not solely responsible for the barrier, its alteration has a drastic effect on the efficiency of cross-species prion transmission (Fig. 28 and Fig. 30). Notably, single aa substitutions with an anti-prion effect were previously generated in the region between positions 8 and 26 that surrounds and includes amyloid stretch I [59]. Amyloid stretch I also overlaps with the Sup35N peptide (7-13) shown to form amyloid-like microcrystals *in vitro* [93], and is included in the region between positions 9 and 20, present in all peptides capable of efficiently immobilizing Sup35NM on the peptide array *in vitro* and promoting its conversion into an amyloid [72].

There are two more amyloid stretches in the *S. cerevisiae* Sup35 PrD, that are located within modules II (ORs region) and III, respectively (Fig. 22 and Fig. 23). Consensus of stretch II is broken by an aa substitution at position 50 in *S. bayanus* (Fig. 22). As mentioned above, we have proven that this substitution has a drastic effect on the

cross-species prion transmission (Fig. 31). Interestingly, substitutions within amyloid stretch I or II weaken the phenotypic patterns of the *S. cerevisiae* prion (Fig. 29 and Fig. 32). However, none of these substitutions alone is sufficient for the irreversible variant switch. Stretch III, located at positions 102-107, is conserved in *S. paradoxus* and conforms to consensus requirements despite two aa substitutions in *S. bayanus* (Fig. 22). Interestingly, this stretch is located within the second (less stringent) region of intermolecular interactions uncovered by the peptide array analysis [72]. It remains to be seen if alterations within this region contribute to the species specificity of prion transmission.

In addition to specific sequences, the size of a PrD is apparently playing a role in the species barrier, as it could be seen in the case of addition of a missing OR unit to *S. bayanus* PrD (Figures 24, 25, 26 and 27) Possibly, PrD size is important for the proper formation of the β-structured amyloid core and/or for correct alignment of the interacting sequences in different amyloid units. Experiments with Rnq1 protein also indicate that alterations of PrD size via removing certain prionogenic regions influence efficiency of prion transmission between the normal and altered protein [53].

The specific mechanism of the action of amyloid stretches remains unclear, as structural models of Sup35 amyloids, based on different experimental approaches, disagree with each other (for example, see [68, 65, 66]. It does not seem likely that amyloid stretches, deduced from *in vitro* experiments, are required for the prion formation in yeast *per se*, as some yeast PrDs (e. g. Ure2) do not appear to contain them (data not shown). Attempts were made recently to define compositional determinants of prion formation in yeast by approaches that are independent of amyloid stretch consensus

[94]. However, it is possible that amyloid stretches mark some (although not necessarily all) regions of intermolecular interactions determining the specificity of transmission of the amyloid state to a newly immobilized protein molecule, rather than the initial amyloid formation. Due to a significant level of flexibility allowed by consensus requirements for an amyloid stretch, it can potentially be formed in various sequences of similar aa composition. Indeed, each of the "reshuffled" Sup35 PrDs retaining prion-forming properties [96, 97] contains one or more amyloid stretches, however of different sequences and locations (data not shown), which may explain the generation of prion transmission barriers between these proteins. Previous data for both chimeric Candida-*Saccharomyces* prion [42] and mammalian prions [95, 69] demonstrated that even single aa substitutions may generate transmission barriers, suggesting that short stretches rather than large regions are involved in control of prion specificity in these cases as well. Further experiments are needed to completely decipher the *in vivo* code of amyloid recognition.

3.5. MODEL FOR SPECIFICITY AND FIDELITY OF PRION TRANSMISSION

We propose that the specificity and fidelity of amyloid transmission is primarily determined by the identity of short amino acid sequences, termed "specificity stretches" (Fig. 34) These sequences initiate intermolecular interactions, immobilizing new molecules into an amyloid. Association of heterologous molecules at only one specificity stretch is insufficient for prion conversion. Specificity stretches also control the variant-specific prion patterns via determining the location and size of the cross-β region. Formation of the intermolecular "zippers" by at least two stretches initiates generation of the cross-β region, flanked by them, in a newly joining molecule. (It is possible that

interactions may include more than two stretches and multiple cross-β regions can be formed, but existing data are insufficient to state this with certainty.)

If at least one of the stretches in a newly joining molecule is altered, heterologous association may still occur, but conversion of the new molecule into a prion could be impaired, thus generating a barrier. In the case of a reversible change in the variant-specific patterns (as in the *S. cerevisiae* / *S. paradoxus* combination), the interaction between the altered stretches still occurs, but it is weakened. However, the size of the cross-β core remains intact after cross-species transmission, and only the stringency of intermolecular interactions is changed, leading to alteration of either the rate of polymer growth or efficiency of its fragmentation by Hsp104, thus altering the phenotypic manifestation of the variant patterns. Restoration of sequence identity restores the original prion variant.

In the case of a variant switch (as in *S. cerevisiae / S. bayanus* combination), the interaction between altered sequences within one of the pairs of specificity stretches is too weak to initiate the cross-β structure. However, the occasional use of secondary specificity stretch(es), located outside of the typical core region, may overcome the barrier (Fig. 34). In this case, a new prion variant can be generated, with a cross-β region of a different location and/or size. As alternative stretches located at different positions could be employed, multiple variants with the cross-β core of different locations and /or sizes can be formed. A weak prion does not show a variant switch in the same combination, as its core region is longer and is initiated by other (possibly unaltered or less dramatically altered) stretch(es).

In the parallel in-register ß-sheet model [1, 48, 49], specificity stretches would be located on the flanks of the cross-β region and would be responsible for initiation of its formation (Fig. 34). In another proposed β-helical model [50] (not shown), specificity stretches may coincide or overlap with "recognition elements" that are responsible for the "head-to-head, tail-to-tail" intermolecular interactions, holding the units of the amyloid fiber together. However, it should be noted that the ß-helical model does not currently suggest a mechanism for continued propagation of distinct variants formed by protein of the same sequence.

Recent experiments with mammalian PrP [57] suggest that, in reality, at least some prion variants ("strains") represent a mixture of the sub-variants ("substrains") from which different predominant variants could be selected in specific conditions. Within the framework of our model, this could be explained by limited range of fluctuations in size of the cross-region. Sub-variant selection may provide an additional mechanism for the reversible change in prion phenotypic manifestations, as different sequences may provide an advantage to different subvariants. Formation of multiple variants as a result of a variant switch could reflect fixation of different subvariants as new variants after crossing the transmission barrier.

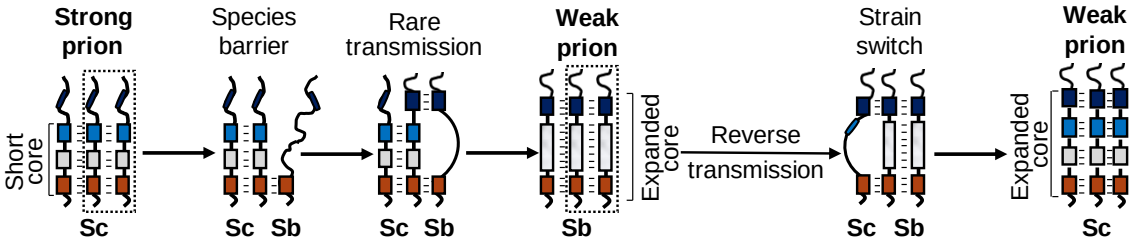

Figure 34: Model for strain adaptation. "Sc" and "Sb" refer to *S. cerevisiae* and *S. bayanus*, respectively. Box regions depict areas of the prion core (having a cross-β fold) and may be separated by looped regions. Lines depict

the soluble portion of the protein. A prion may make efficient interactions with key sequence stretches (shown as red and cerulean) in a homologous monomer and readily transmit the prion state to the same protein. Regions of sequence divergence in these stretches between heterologous proteins may prevent or inhibit typical points of interaction, causing a species barrier. In rare cases, atypical interactions at different sequence stretches (shown as navy) may facilitate transmission to a heterologous protein. This could change the borders of the prion core, expanding it and altering the variant. This new variant may then be transmitted back to the original protein, resulting in a permanent variant switch through propagation in a heterologous protein.

3.6 CHAPTER 3 CONCLUSIONS:

- The efficiency of cross-species conversion is influenced by the prion variant
- Variant-specific prion patterns can be altered irreversibly during cross-species transmission.
- Heterologous conversion can be imprecise and generate multiple variants of a prion.
- Module I of *S. paradoxus* is responsible for the transient decrease in [PSI^{+}] phenotypic stringency and for the species barrier. The region encompassing modules II and III of *S. paradoxus* exhibits little or no effect.
- Module II of *S. bayanus* was responsible for the species barrier, while modules I and III of *S. bayanus* exhibited little or no effect.
- In addition to controlling the frequency of cross-species prion conversion in the *S. cerevisiae* / *S. bayanus* combination, module II also controls the fidelity of reproduction of the variant-specific prion patterns via a heterologous stage.
- The size of module II plays a role in cross-species prion transmission together with its specific sequence features.

- A single amino acid substitution at position 12 of the Sup35 protein plays an important role in both specificity of prion transmission and stringency of the prion isolates obtained from cross-species conversion, but is not solely responsible for the specificity.
- A single amino acid substitution at position P50 in the Sup35 protein significantly affected cross-species transmission of both strong and weak *S. cerevisiae* prions to the mutated protein.
- Our data suggest the important of amyloid stretches, rather than overall sequence identity in control of the species specificity and fidelity of cross species prion transmission.

CHAPTER 4: DEVELOPMENT OF A NON-*S. CEREVISIAE* SYSTEM FOR [*PSI*$^+$] ANALYSIS

4.1 CHAPTER SUMMARY

Initial investigations of sequence-dependent effects on species barrier and prion interference were performed in the *S. cerevisiae* cell environment. Interestingly, both transitory and permanent phenotype changes to [*PSI*$^+$] were observed when the prion was transmitted through proteins from different species and back to the original $Sup35_{Sc}$ protein. Presumably, the transitory phenotype changes may be due to differential interactions with *S. cerevisiae* cellular factors such as chaperones that fragment [*PSI*$^+$] aggregates. However, the extent of the influence of protein sequence vs. cell environment was unknown. It was hypothesized that performing the same experiments in related species would facilitate identification of species-specific cellular factors contributing to these processes. The closely related *S. paradoxus* and *S. bayanus* members of the *Sacccharomyces sensu stricto* group were selected for these comparisons, thus necessitating the genetic strain modifications described in this chapter. In addition, we show that strong and weak [*PSI*$^+$] used for experiments in *S. cerevisiae* (see Chapter 3) were transfected to the modified *S. paradoxus* and *S. bayanus* strains in attempts to generate the same starting variants.

4.2 MATERIALS

4.2.1 Plasmids

Plasmids PFA6a-kanMX6 [83], pBluescript-URA3 I plasmid (constructed by J. Kumar), pRS303N [84], and pRS303H [84] were used in PCR to amplify genes used for genetic markers. Plasmid pRS317 was used in the *S. paradoxus ade1-14*$_{Sc}$ construction (as described) to increase transformation efficiency of the PCR product.

4.2.2 Strains

Descriptions and genotypes of all *S. paradoxus*, *S. bayanus, and S. cerevisiae* strains used or constructed in this study are described in Chapter 2 and are listed in Table 1 (Appendix).

4.3 RESULTS AND DISCUSSION

4.3.1 *S. paradoxus* and *S. bayanus* strain modifications: auxotropic mutations

Generation of *lys2* and *ura3-P2* mutations

Both the *lys2* and *ura3-P2* auxotrophic mutations were present in all *S. paradoxus* and *S. bayanus* strains used for this work. Gary Newnam (Chernoff lab) introduced both mutations in *S. paradoxus* and the *lys2* mutation in *S. bayanus* by subjecting the strains to UV light for 15-45 seconds to induce each mutation (Fig. 39). For *S. paradoxus*, haploid versions containing each mutation were independently obtained and mated to generate diploids having both the *lys2* and *ura3* genotype. Diploids were sporulated, dissected and plated on –Ura and –Lys medium to verify the diploid contained both mutations. For *S. bayanus*, the *lys2* mutation was generated in a beginning *ura3* haploid strain.

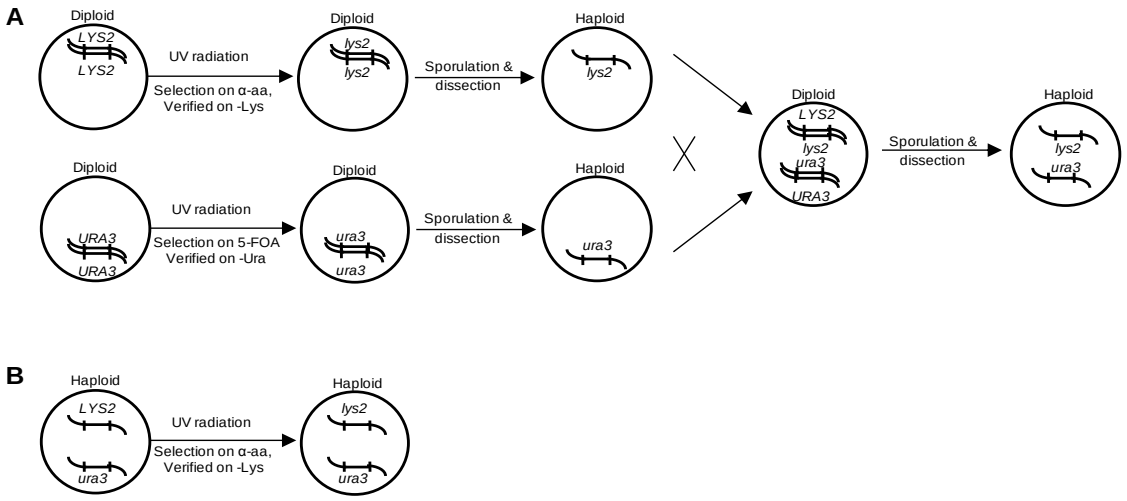

Figure 39: Generation of *lys2* and *ura3-P2* mutants in *S. paradoxus* and *S. bayanus.* A—A diploid *S. paradoxus* strain was irradiated with UV light for 15-45 seconds and was plated on α-aa medium to select for *lys2* mutants and also independently on 5-FOA medium to independently select for *ura3* mutants. Haploid versions of strains containing a mutation were mated to generate diploids and were sporulated and dissected, and selected for the inability to grow on both –Ura and on –Lys media. **B—**A haploid *S. bayanus* strain already containing the *ura3* mutation was irradiated with UV light for 15-45 seconds and was plated on α-aa medium to select for *lys2* mutants.

4.3.2 *S. paradoxus* strain constructions

***HO* disruption** (Fig. 40, A)

Haploid yeast can switch between two distinct mating types (a and α), frequently producing undesirable diploid strains from haploid strains. A gene coding for the homothallic switching endonuclease (*HO)* initiates mating-type conversion by engineering a double-stranded DNA break, facilitating homologous recombination to replace the particular *MAT* allele. *S. paradoxus* mating-types were stabilized by *HO* replacement with the bacterial *KANMX6* gene. (See Figure 4.X).

To prevent a mating type switch, *KANMX6* (highlighted in gray) was amplified from plasmid PFA6a-kanMX6 [83] using PCR. The primers had 50 bp extensions with

homology to flanking regions of the *S. paradoxus HO* gene on both sides. The PCR fragment was used to transform the GT749-1B *S. paradoxus* diploid strain (homozygous for the wildtype *HO* gene), and the fragment was incorporated by homologous recombination. Replacement of *HO* by *KANMX6* conveyed G418 resistance in yeast, and PCR was used to verify the gene disruption. A haploid strain having the desired *ho::KANMX6* genotype was obtained by sporulation and dissection. (*HO* replacement was performed by B. Chen)

Generation of the *ade1-14$_{Sc}$* mutation in *S. paradoxus* (Fig 40, B-C)

In *S. paradoxus*, replacement of the wildtype *ADE1* allele with the *ade1-14$_{Sc}$* mutant allele was desired to facilitate [*PSI*$^{+}$] detection by read-through suppression (see Figure 4). Specifically, *ade1-14* originating from *S. cerevisiae* ("*ade1-14*$_{Sc}$") was desired for comparison of [*PSI*$^{+}$] between different *Saccharomyces* species. The replacement was performed in two steps. 1) Disruption of *ADE1* by *URA3$_{Sc}$* followed by 2) *URA3*$_{Sc}$ replacement with *ade1-14*$_{Sc}$. To disrupt *ADE1* in *S. paradoxus* with *URA3* from *S. cerevisiae (URA3*$_{Sc}$*), URA3*$_{Sc}$ was PCR amplified from the pBluescript-URA3 I plasmid (constructed by J. Kumar) using primers with 40 bp 5' extensions having homology on both sides to *ADE1*. The PCR fragment was used to transform a *S. paradoxus* haploid strain having a wildtype copy of *ADE1* and was incorporated by homologous recombination. Target *ade1Δ::URA3$_{Sc}$* transformants diplayed an Ade^{-}Ura^{+} phenotype and were selected on synthetic "drop-out" media.

Both *ade1-14*$_{Sc}$ and *ura3* mutations were desired in *S. paradoxus* for [*PSI*$^{+}$] detection and for auxotropic selection, respectively. To create these, *ade1-14$_{Sc}$* (highlighted in gray) from a *S. cerevisiae* strain was PCR amplified using primers with 60

bp 5’ extensions homologous to flanking regions of *URA3*$_{SC.}$ To further increase the length of the homologous regions for more efficient homologous recombination, a second round of PCR was performed. The product from the first round was used as a template to add additional 80 bp 5’ extensions homologous to flanking *S. paradoxus* sequences located further upstream and further downstream, respectively. The final PCR product contained 140 bp 5’ extensions and was transformed together with the pRS317 *LYS2* plasmid (to increase transformation efficiency) into a haploid *ade1Δ::URA3*$_{SC}$ *S. paradoxus strain.* Homologous recombination produced target *ade1-14, ura3* transformants that were selected on 5-FOA media and were subsequently tested on –Ade and –Ura media. These were further verified by PCR and sequencing. A strain containing *ADE1* from *S. cerevisiae* (rather than *ade1-14*) was also created using the same steps described here. (*ade1-14*$_{Sc}$ *was* incorporated by B. Chen)

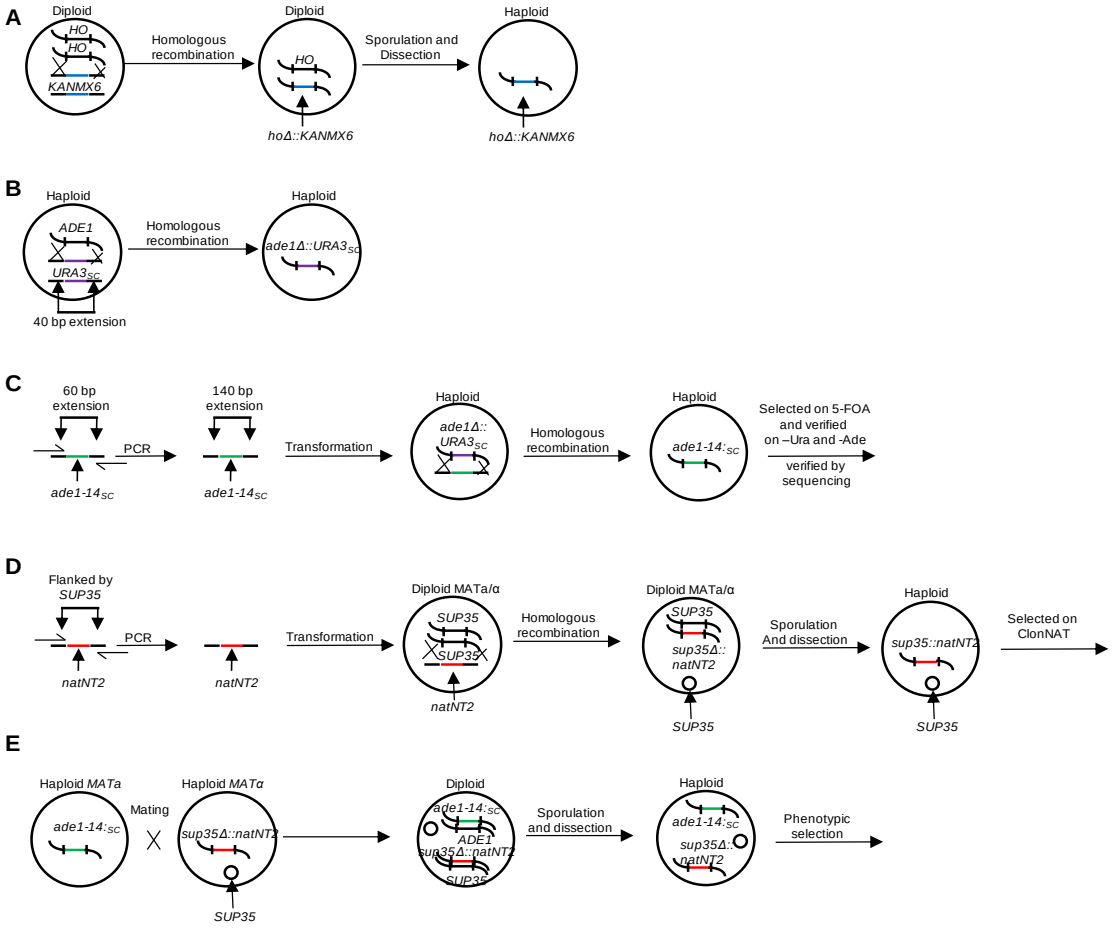

Figure 40 *S. paradoxus* strain construction steps. A—The *HO* gene was disrupted by replacement with the bacterial *KANMX6* gene as described in section 4.3.2. **B—** The *ADE1* gene in *S. paradoxus* was disrupted by the *URA3* gene from *S. cerevisiae* ($URA3_{Sc}$) as described in section 4.3.2. **C—** *ade1-14* and *ura3* mutations were engineered by replacing $URA3_{SC}$ (previously inserted to disrupt *ADE1*) with $ade1\text{-}14_{Sc}$ as described in section 4.3.2. **D—** The *SUP35* gene in a *S. paradoxus* chromosome was replaced by *natNT2* (conveying resistance to nourseothricin) as described in section 4.3.2. **E—** A *S. paradoxus* strain having both the *ade1-14* and *sup35Δ::natNT2* genotype, was obtained by crossing two *S. paradoxus* yeast strains (one containing *ade1-14* and another containing *sup35Δ::natNT2* and a wildtype copy of *SUP35* on a plasmid) of opposite mating type. This was followed by sporulation and dissection.

Generation of *sup35Δ::natNT2* in *S. paradoxus* (Fig 40, D)

In *S. paradoxus*, deletion of the chromosomal *SUP35* gene was desired for study of complete or chimeric *SUP35* versions (on a centromeric plasmid) originating from different species. The *SUP35* gene on a *S. paradoxus* chromosome was replaced by *natNT2* (conveying nourseothricin resistance). PCR was used to amplify *NatNT2* (highlighted in gray) from plasmid pRS303N [84]. The primers had 40 bp 5' extensions with homology to flanking regions of the *S. paradoxus SUP35* gene on both sides. The PCR fragment was used to transform a diploid *S. paradoxus* strain homozygous for wildtype *SUP35* and was incorporated by homologous recombination. An essential *SUP35* copy was provided on a plasmid. This was followed by sporulation and dissection, and *sup35Δ::natNT2* recombinants were selected on YPD with added nourseothricin. The *sup35Δ::natNT2* replacement was performed by B. Chen

Generation of a *S. paradoxus* strain having both *ade1-14$_{Sc}$* and *sup35Δ::natNT2*

(Fig 40, E)

To obtain a *S. paradoxus* strain having both the *ade1-14* and *sup35Δ::natNT2* genotype, two *S. paradoxus* yeast strains (one containing *ade1-14* and another containing *sup35Δ::natNT2* with a wildtype copy of *SUP35* on a plasmid) of opposite mating type were crossed and followed by sporulation and dissection. Synthetic "drop out" media and YPD containing nourseothricin were used to screen for the desired phenotype. The strain having both *ade1-14$_{Sc}$* and *sup35Δ::natNT2* was obtained by K. Bruce

Generation of *hsp104Δ::HYG* in *S. paradoxus*

A *hsp104Δ S. paradoxus* strain was required for mating interference experiments, so *HYG* was amplified from the pRS303H plasmid with primers each having a 20 bp homology to *HYG* and a 40 bp flanking region complementary to *HSP104* from *S. paradoxus*. The PCR product was transformed into the desired *S. paradoxus* strain and was incorporated by homologous recombination. YPD containing hygromycin was used to select for colonies with the *hsp104Δ::HYG* genotype. The strain having *ade1-14*$_{Sc}$, *sup35Δ::natNT2* and *hsp104Δ::HYG* was obtained by K. Bruce

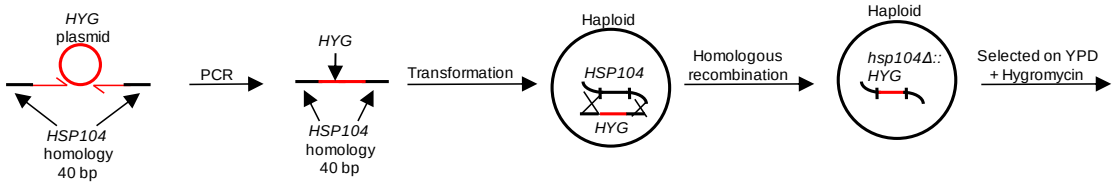

Figure 41 *S. paradoxus hsp104Δ* strain construction steps. *HYG* Was amplified from plasmid pRS303H using primers with homology to *HYG* and flanking regions homologous to *HSP104*$_{Sp}$. The PCR product was transformed into a *S. paradoxus* strain and was incorporated by homologous recombination. Target colonies having *hsp104Δ* were selected on YPD medium containing hygromycin.

4.3.3 S. bayanus strain constructions (by B. Chen)

HO disruption

The *S. bayanus* strains obtained from N. Talarek already had the *HO* replacement with the bacterial *KANMX6* gene (*ho::KANMX6)*, as described for *S. paradoxus*.

Generation of the *ade1-14$_{Sc}$* mutation in *S. bayanus* (Fig 42, A-B)

In *S. bayanus,* replacement of the wildtype *ADE1* gene with the *ade1-14* mutant allele was desired to facilitate [*PSI*$^+$] detection by read-through suppression (see Figure 4). Specifically, *ade1-14* originating from *S. cerevisiae* ("*ade1-14*$_{Sc}$", used in previous *S. cerevisiae* experiments) was employed for comparison of [*PSI*$^+$] between different *Saccharomyces* species. This replacement was performed in two steps. 1) Disruption of *ADE1* by *URA3$_{Sc}$*, followed by 2) replacement of *URA3*$_{Sc}$ with *ade1-14*$_{Sc}$. To disrupt the *ADE1* gene in *S. bayanus* with the *URA3* gene from *S. cerevisiae (URA3*$_{Sc}$*), URA3* $_{Sc}$ was PCR amplified from the pBluescript-URA3 I plasmid (constructed by J. Kumar) using primers with 40 bp 5' extensions having homology on both sides to *ADE1*. The PCR fragment was used to transform a *S. bayanus* haploid strain having a wildtype copy of *ADE1* and was incorporated by homologous recombination. Target *ade1Δ::URA3$_{Sc}$* transformants diplayed an Ade$^-$Ura$^+$ phenotype and were selected on synthetic "drop-out" media. Both *ade1-14*$_{Sc}$ and *ura3* mutations were desired in *S. bayanus* for [*PSI*$^+$] detection and for auxotropic selection, respectively. To create these, *ade1-14* (highlighted in gray) from a *S. cerevisiae* strain was PCR amplified using primers with 60 bp 5' extensions homologous to flanking regions of the *URA3*$_{Sc}$ on the *S. bayanus* chromosome. The final PCR product was transformed into a haploid *ade1Δ::URA3$_{SC}$ S. bayanus strain.* Homologous recombination produced target *ade1-14, ura3* transformants, displaying an Ade$^-$Ura$^-$ phenotype. These were selected on 5-FOA media and were subsequently tested on –Ade and –Ura media. These were further verified by sequencing. A *S. bayanus* strain containing *ADE1* from *S. cerevisiae* (rather than *ade1-14*) was also created using the same steps described here.

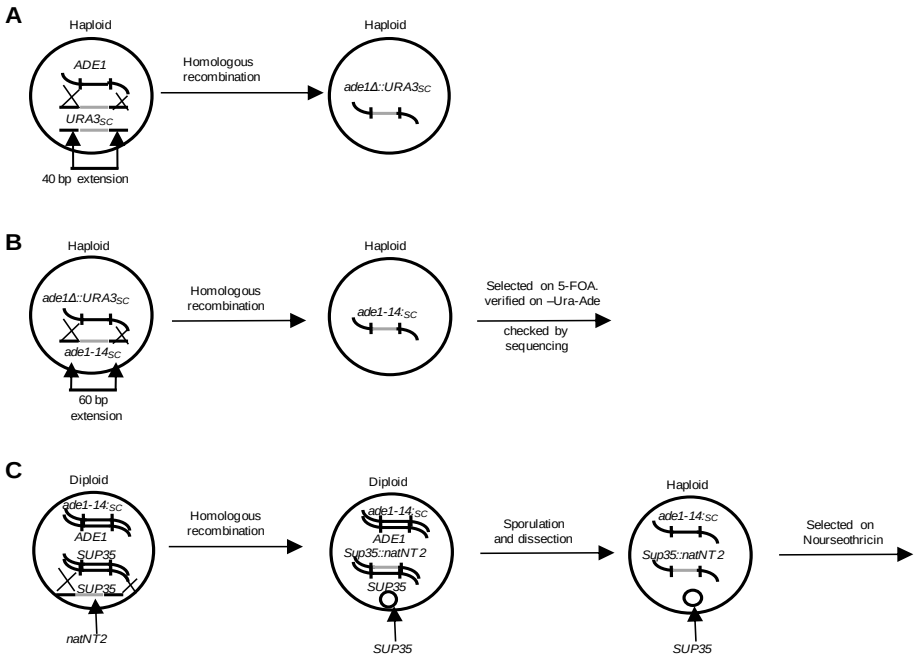

Figure 42 *S. bayanus* strain construction steps. A— The *ADE1* gene in *S. bayanus* was disrupted by the *URA3* gene from *S. cerevisiae* (*URA3*$_{SC}$) as described in section 4.3.3. **B—** *ade1-14* and *ura3* mutations were engineered by replacing *URA3*$_{Sc}$ (previously inserted to disrupt *ADE1*) with *ade1-14*$_{Sc}$ as described in section 4.3.2. **C—**The *SUP35* gene in a *S. bayanus* chromosome was replaced by *natNT2* as was described in section 4.3.3.

Generation of *sup35Δ::natNT2* in *S. bayanus* (Fig 42, C)

In *S. bayanus*, deletion of the chromosomal *SUP35* gene was desired for study of various complete or chimeric *SUP35* versions (on a centromeric plasmid) originating from different species. The *SUP35* gene on a *S. bayanus* chromosome was replaced by *natNT2* (conveying resistance to nourseothricin). PCR was used to amplify *natNT2* (highlighted in gray) from plasmid pRS303N [84]. The primers had 40 bp 5' extensions with homology to flanking regions of the *S. bayanus SUP35* gene on both sides. The PCR fragment was used to transform a diploid *S. bayanus* strain (*ADE1/ade1Δ::ade1-14SC* and *LYS2/lys2* but homozygous for wildtype *SUP35*) and was incorporated by

homologous recombination. An essential copy of *SUP35* was provided on a centromeric plasmid. This was followed by sporulation and dissection, and *sup35Δ::natNT2, ade1-14SC, lys2* were selected by screening with YPD containing nourseothricin.

4.4 CROSS-SPECIES [*PSI*$^+$] TRANSFECTION

In addition to *de novo* [*PSI*$^+$] induction, [*PSI*$^+$] can be transferred across the cell membrane of a [*psi*$^-$] strain to induce prion infection (Section 2.2.4, Fig. 9). The "transfection" process differs from *de novo* [*PSI*$^+$] formation by introduction of a pre-formed aggregate, reflecting characteristic of unique conditions of its induction environment. Typically, in the same species, the phenotype of a particular [*PSI*$^+$] donor variant is expected to be faithfully perpetuated in a recipient protein of the same sequence. However, transfection of prion material into a new species may cause the transfected prion to exhibit a phenotype unlike *de novo* [*PSI*$^+$] formed in the same cell environment. This may occur even though the recipient strain expresses the same protein. Transfection, thus, becomes a valuable tool, giving us the ability to examine one and the same prion variant in different cellular backgrounds, providing insight into the effects of the cell environment on [*PSI*$^+$] maintenance.

In addition, we show it is possible to transfect a donor prion formed in one *Saccharomyces* species into a different *Saccharomyces* species and observed that at least some properties of prion variants are maintained by the same protein in the cells of a different species (Fig 43). For example, cellular extract transfected from the GT256-23C strong [*PSI*$^+$] *S. cerevisiae* strain generated strong [*PSI*$^+$] in both *S. paradoxus* and *S. bayanus* [*psi*$^-$] recipient species (Fig 43). Strong [*PSI*$^+$] transfected from *S. cerevisiae* into

S. paradoxus was found to propagate a stable strong [*PSI*$^{+}$] phenotype (See Table 12 (Appendix)) and was used in direct and reverse shuffle experiments and [*PSI*$^{+}$] interference studies.

Cell extract from the GT988-1A weak [*PSI*$^{+}$] *S. cerevisiae* strain generated weak, unstable [*PSI*$^{+}$] in *S. paradoxus*, but no prion was detected with the YPD color assay or –Ade suppression assay following transfection of weak [*PSI*$^{+}$] to S. *bayanus*. Interestingly, the conventional YPD color assay and –Ade suppression assay were less useful for [*PSI*$^{+}$] detection in *S. bayanus*, although a subtle [*PSI*$^{+}$]-dependent color difference was observed (for transfection of a strong variant) on synthetic media lacking uracil and tryptophan (-Ura-Trp). Because of this difference, a boiled-gel approach was effectively used for [*PSI*$^{+}$] screening in *S. bayanus* (Fig 43).

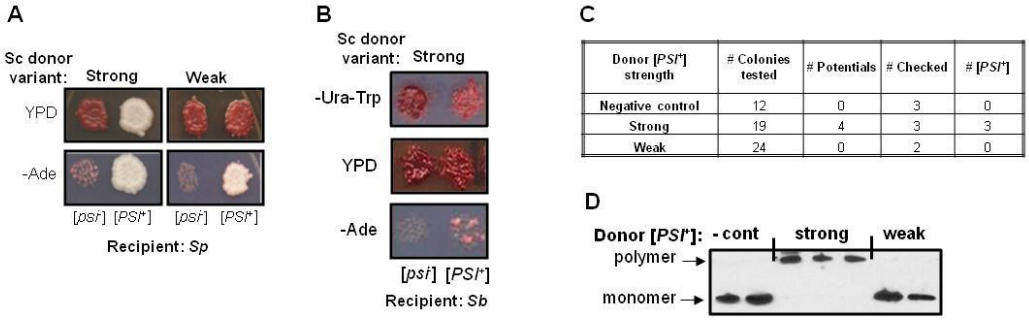

Donor [*PSI*$^{+}$] strength	# Colonies tested	# Potentials	# Checked	# [*PSI*$^{+}$]
Negative control	12	0	3	0
Strong	19	4	3	3
Weak	24	0	2	0

Figure 43: Cross-species prion transfection from *S. cerevisiae*. A — Cellular extract was transfected from either a strong or weak [*PSI*$^{+}$] *S. cerevisiae (Sc)* strain into a [*psi*$^{-}$] *S. paradoxus (Sp)* strain, expressing a version of Sup35 from *S. cerevisiae*. Representatives of [*PSI*$^{+}$] *S. paradoxus* transfectants obtained from either the strong (left) or weak (right) [*PSI*$^{+}$] donor strains are shown. Yeast were grown on YPD (for color assay) and on –Ade medium (for suppression assay) at 30°C for 8 days. **B —** Cellular extract was transfected from a strong [*PSI*$^{+}$] *S. cerevisiae (Sc)* strain into a [*psi*$^{-}$] *S. bayanus (Sb)* strain, expressing a version of Sup35 from *S. cerevisiae*. A Representative [*PSI*$^{+}$] *S. bayanus* transfectant obtained is shown. No [*PSI*$^{+}$] phenotype was observed for *S. bayanus* transfected with cellular extract from a weak [*PSI*$^{+}$] *S. cerevisiae* strain. Yeast were grown on YPD and –Ade medium at 25°C for X days.

A [*PSI*$^+$]-dependent color difference on –Ura-Trp was noted for the *S. bayanus* species. **C—** Transfectant potentials (Colonies transformed by the empty –Ura marker plasmid) were replica plated onto YPD, -Ade, and –Ura-Trp to look for potential [*PSI*$^+$] transfectants. The total number of colonies tested is recorded with those displaying a potential [*PSI*$^+$] phenotype labeled as "potentials". Colonies biochemically examined for [*PSI*$^+$] and numbers of verified [*PSI*$^+$] colonies are indicated. **D —** A "boiled gel" verified the [*PSI*$^+$] phenotype for *S. bayanus* transfected with cellular extract from a strong [*PSI*$^+$] *S. cerevisiae* strain. No aggregated Sup35 was observed for two randomly chosen *S. bayanus* colonies obtained after attempts to transfect cellular extract from a weak [*PSI*$^+$] *S. cerevisiae* strain. These 2 colonies obtained the *URA3* marker plasmid but may not have taken up the protein. A negative control having *S. bayanus* transfected without cellular extract did not show any aggregated Sup35.

4.5 CHAPTER 4 CONCLUSIONS:

- Cross-species prion transfection can be successfully performed to introduce a pre-formed aggregate into a different species.
- At least some underlying properties of prion variants are maintained after cross-species [*PSI*$^+$] transfection as far as the carrier protein is not changed.

\

CHAPTER 5: COMPARISON OF SPECIES BARRIER IN *S. PARADOXUS* VS *S. CEREVISIAE*

5.1 CHAPTER SUMMARY

As described in Chapter 3, a shuffle procedure performed in both a strong and a weak [*PSI*$^{+}$] *S. cerevisiae* variant produced a clear species barrier to prion transmission. We questioned whether the barriers obtained were due to interactions of the proteins, themselves, or could be partially attributed to factors present within the particular cell environment. To test this, the same experiments were performed in a different cell environment (*S. paradoxus*) and are presented in this chapter for comparison with results performed in S. cerevisiae.

5.2 MATERIALS

5.2.1 Plasmids

Centromeric plasmids expressing chimeric *SUP35* versions or complete *SUP35* versions originating from *S. cerevisiae, S. paradoxus,* or S. bayanus are described in Chapter 2.

5.2.2 Strains

S. cerevisiae, S. paradoxus, and *S. bayanus* strains used for plasmid shuffle, cytoduction, and transfection experiments are described in Chapter 2.

5.3 RESULTS AND DISCUSSION

5.3.1 The effect of cell environment on a species barrier

Comparison of cross-species transmission in strong [*PSI*$^+$] *S. paradoxus vs. S. cerevisiae* using direct shuffle

To begin with the same variant used in *S. cerevisiae*, cell lysate from a strong or weak $Sup35_{Sc}$ [*PSI*$^+$] variant was transfected into a haploid *S. paradoxus* strain that expressed the same $SUP35_{Sc}$ version (Fig 43, A). Next, a shuffle procedure was performed in the *S. paradoxus* strong [*PSI*$^+$] variant. Phenotypes in *S. paradoxus* produced from transmission to heterologous proteins are presented in Figure 44.

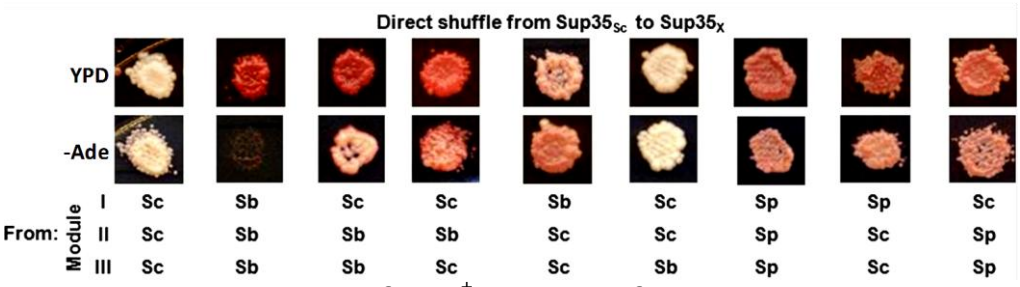

Figure 44: Phenotypes of [*PSI*$^+$] produced from direct transmission in *S. paradoxus.* Direct shuffle experiments for strong [*PSI*$^+$] and in *S. paradoxus* were performed as on Fig. 1 22).1. Numerals I, II, and III refer to the exchangeable modules of the PrD (Fig. "Sc", "Sp", and "Sb" refer to *S. cerevisiae*, *S. paradoxus*, and *S. bayanus*, respectively. Phenotypic patterns of strong prion variant are changed when transferred to the new protein. –Ade and YPD plates were photographed after 8 days.

Results listing the efficiency of prion transmission to different Sup35 PrDs are shown in the Appendix on Table 13 (Appendix) and are compared to results obtained in *S. cerevisiae* (Fig 45). For both cell environments, a very strong barrier was observed for Sup35 *S. cerevisiae* transmission to the Sup35 *S. bayanus* PrD. In fact, the barrier was absolute in the *S. paradoxus* cell environment (0% transmission in the *S. paradoxus* cell, versus 12% transmission in the *S. cerevisiae* cell). Notably, there was a weaker [*PSI*$^+$]

phenotype for $Sup35_{Sc}$ transmission to any Sup35 PrD chimera comprised of combinations of *S. cerevisiae* and *S. paradoxus*. Transmission to any Sup35 *S. cerevisiae*/*S. bayanus* PrD chimera that contained module II from *S. bayanus* created a weak prion with a dark pink color on YPD and noticeable darker brown phenotype on YPD and -Ade medium (Fig. 44)

A shuffle procedure from the weak [*PSI*$^+$] *S. paradoxus* variant to different PrDs was also attempted. However, a majority of colonies lost [*PSI*$^+$] during the transformation process, preventing analysis of transmission efficiency.

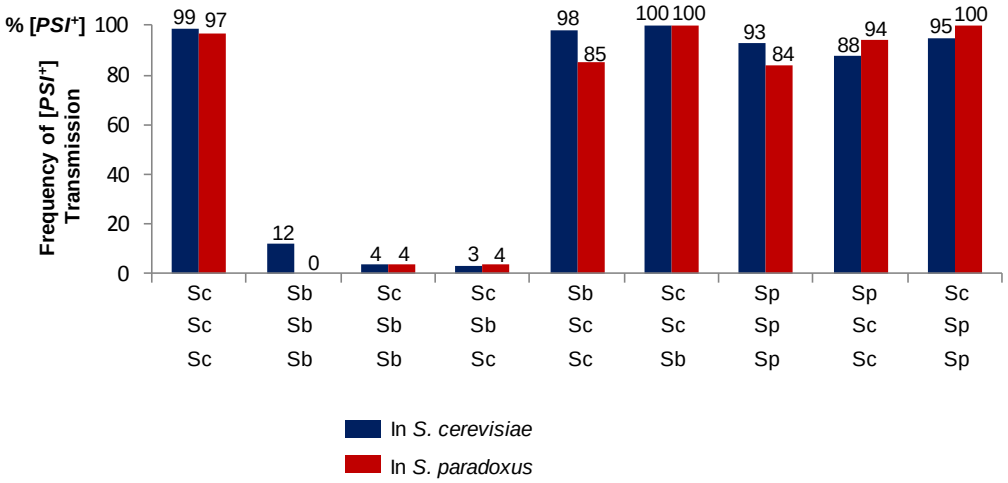

Figure 45: Comparison of prion transmission barriers in performed in *S. cerevisiae* and *S. paradoxus*. Direct shuffle experiments for strong [*PSI*$^+$] in *S. cerevisiae* (presented in Chapter 3) and in *S. paradoxus* were performed as on Fig 11. Numerals I, II, and III refer to the exchangeable modules of the PrD (Fig 22). "Sc", "Sp", and "Sb" refer to *S. cerevisiae*, *S. paradoxus*, and *S. bayanus*, respectively. Frequencies of prion transmission are shown above each bar. Red and blue bars indicate that the experiment was performed in the *S. cerevisiae* or *S. paradoxus* cell environments, respectively. See Tables 5 and Table 13 in the Appendix for actual numbers obtained

Reverse shuffle in *S. paradoxus*

Similar to results in *S. cerevisiae*, direct transmission produced weaker than the original strong [*PSI*$^{+}$] phenotypes when donor proteins had *S. paradoxus* and *S. bayanus* PrDs (Fig 44 and Fig 47) and for certain versions with *S. cerevisiae* /*S. paradoxus* or *S. cerevisiae*/ *S. bayanus* chimeric PrDs. We questioned whether this is caused by transitory interactions between the new protein and cellular factors or is due to a permanent structural change in the folding of the prion core. To test this, a reverse shuffle was performed to transfer the prion back to the original Sup35$_{Sc}$ protein (See Table 14 in the Appendix)

A comparison is made to reverse shuffle results obtained for *S. cerevisiae* (Chapter 3) in Figure 46. In general, reverse shuffle results for strong [*PSI*$^{+}$] in the *S. paradoxus* cell environment show similar trends to results obtained in *S. cerevisiae*. Reverse shuffle from the Sup35 *S. paradoxus* PrD or from chimeric PrD's comprised of modules from *S. cerevisiae* and *S. paradoxus* (having a weak [*PSI*$^{+}$] phenotype) to the *S. cerevisiae* PrD restored the original strong [*PSI*$^{+}$] variant. This implicates the efficiency of interactions between the *S. paradoxus* PrD with cellular factors as the cause for the weakened phenotype rather than a permanent structural change to the prion core. Conversely, reverse shuffle beginning with any version of chimeric Sup35 having module II originating from *S. bayanus* transmitted a weak [*PSI*$^{+}$] variant to the original Sup35$_{Sc}$ protein, suggesting a permanent structural change caused by propagation through the heterologous protein. It is important to note that no prion was transmitted in direct shuffle from the Sup35 *S. cerevisiae* PrD to the complete *S. bayanus* PrD, so only chimeric versions of the Sup35 PrD were tested for reverse transmission in *S. paradoxus*. Overall,

direct and reverse shuffle results showed that the major rules of a transmission barrier are generally invariant in *S. cerevisiae* and *S. paradoxus* host cells and do not depend on the presence of the [*PIN*$^+$] prion, although some specific numerical differences were detected. Therefore, both transmission barrier and conformational fidelity appear to be primarily determined by the protein itself rather than by the cell environment

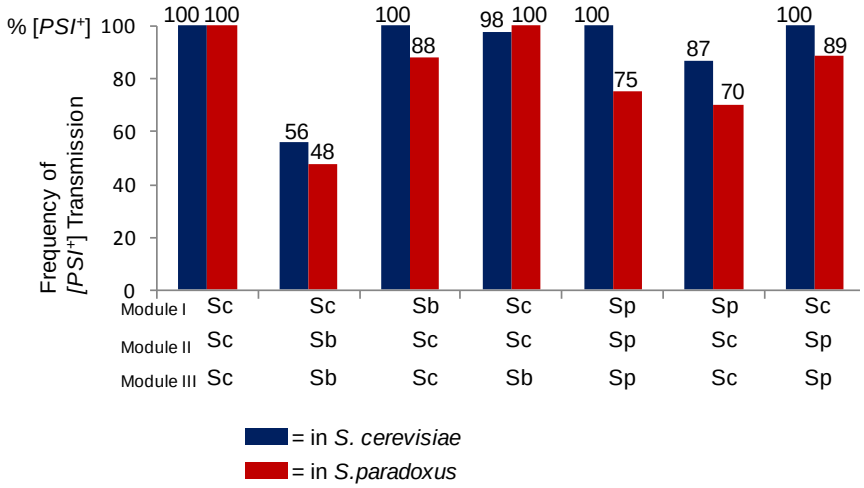

Figure 46: Comparison of reverse prion transmission for reverse shuffle in *S. cerevisiae* and *S. paradoxus*. Reverse shuffle experiments for strong [*PSI*$^+$] in *S. cerevisiae* and in *S. paradoxus* were performed as on Fig 11. Numerals I, II, and III refer to the exchangeable modules of the Sup35 PrD (Fig 22). "Sc," "Sp", and "Sb" refer to *S. cerevisiae*, *S. paradoxus*, and *S. bayanus*, respectively. Frequencies of prion transmission are shown above each bar. Red and blue bars indicate that the experiment was performed in the *S. cerevisiae* or *S. paradoxus* cell environments, respectively. Reverse transmission from the complete *S. bayanus* PrD was not possible, as no colonies were obtained from direct shuffle due to an absolute transmission barrier. Numbers showing reverse transmission from the Sc-Sb-Sc chimeric PrD was not presented due to few colonies available from direct shuffle for testing. See Tables 9 and 14 in the Appendix for actual numbers obtained.

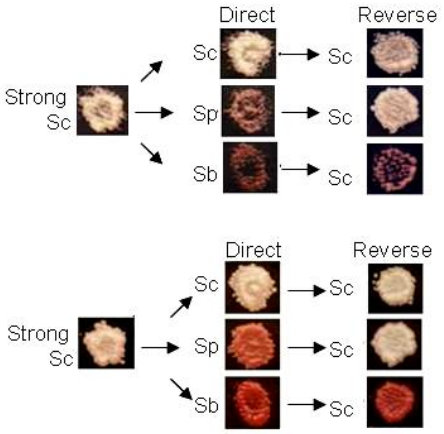

Figure 47: Reproduction and switch of prion variants in cross-species transmission in the *S. paradoxus* cell environment. Patterns of [*PSI*$^{+}$] isolates obtained from a strong *S. cerevisiae* prion variant in the *S. paradoxus* cell environment went through direct shuffle to the control *S. cerevisiae* Sup35 protein or chimeric proteins with either *S. paradoxus PrD* or *S. bayanus* Module II PrDs, followed by reverse shuffle back to *S. cerevisiae* Sup35 (Fig 11). "PrD_X" refers to PrDs of various origins as indicated. These data are representatives of direct shuffle results presented in Table 13 (Appendix) and reverse shuffle results presented in Table 14 (Appendix). Numbers of independent isolates obtained for each phenotype can be found on those tables. Unlike variations in phenotype observed for reverse shuffle from combinations with Sb module II performed in *S. cerevisiae*, no noticeable variations were observed for reverse shuffle from combinations with Sb module II in the *S. paradoxus* cell environment.

5.3.2 Comparison of the species barriers in transfection with the other assays

We previously demonstrated how a plasmid shuffle procedure or cytoduction assay is useful to detect and measure species-specific barriers to cross-species prion transmission (Chapter 3). Here we demonstrate that a cross-species transfection procedure also generates a species barrier, and the barrier produced is stronger than that observed for both a plasmid shuffle or cytoduction assay. With the transfection procedure, transfection of a strong [*PSI*$^{+}$] *S. cerevisiae* PrD variant produced in *S. cerevisiae* into a *S. paradoxus* strain expressing the same $Sup35_{Sc}$ protein yielded an efficiency of 19% to the *S. cerevisiae* PrD, and no transmission to the *S. paradoxus* and *S. bayanus* PrD versions (Table 15 (Appendix); Fig 48). Overall, a species barrier was clearly seen for transfection

from the strong $Sup35_{Sc}$ [PSI^+] variant to the *S. paradoxus* PrD version expressed in *S. paradoxus* (A), even though this strong barrier was not detected by either the plasmid shuffle (B) or cytoduction (C) procedures for the same strong variant. This result may be attributed to differences between the host and recipient cell environments or to the length of heterologous protein co-expression, as proteins were co-expressed for shorter intervals in transfection than for shuffle and cytoduction procedures. The shortened interaction time may prevent sufficient heterologous interactions needed to overcome a species barrier. The cross-species transfection procedure was also tested in parallel in a weak [PSI^+] variant. 7% transmission to the *S. cerevisiae* PrD was observed with no transmission to the *S. paradoxus* or *S. bayanus* PrDs.

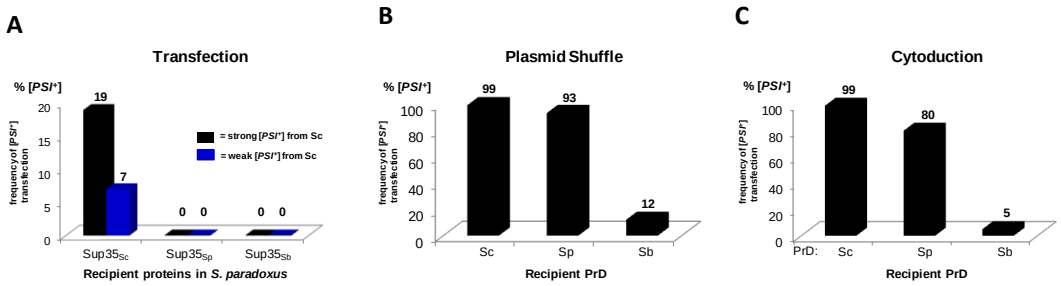

Figure 48. Comparison of cross-species transmission efficiency for transfection from *S. cerevisiae* to *S. paradoxus*. A— Cell lysate from either a *S. cerevisiae* strong or weak [PSI^+] variant was transfected into a [psi^-] *sup35Δ S. paradoxus* strain. The *S. paradoxus* strain produced Sup35 from a plasmid (originating from either *S. cerevisiae* (Sc), *S. paradoxus* (Sp), or *S. bayanus* (Sb)). The percentages of [PSI^+] colonies obtained are presented. Data shown are presented in Table 15 (Appendix). B—Direct cross-species transmission to heterologous Sup35 PrD's was performed in a strong *S. cerevisiae* variant (data previously presented in Table 5 (Appendix)). C—Cytoduction transmission to heterologous Sup35 PrD's was performed in a strong *S. cerevisiae* variant (data previously presented in Table 6 (Appendix)).

5.4 CHAPTER 5 CONCLUSIONS:

- A transmission barrier and conformational fidelity are primarily determined by the protein itself rather than the cell environment.
- A species barrier in transfection is stronger than in the plasmid shuffle or cytoduction assays, apparently due to a shorter period of coexistence of the heterologous proteins.

CHAPTER 6: PRION INTERFERENCE

6.2 MATERIALS

6.2.1 Plasmids

Centromeric plasmids expressing chimeric *SUP35* versions or complete *SUP35* versions originating from *S. cerevisiae*, *S. paradoxus*, or S. bayanus are described in Chapter 2 and Chapter 3.

6.2.2 Strains

S. cerevisiae, *S. paradoxus*, and *S. bayanus* strains used for interference studies and SDD-AGE are described in Chapter 2.

6.3 RESULTS AND DISCUSSION

6.3.1The effects of heterologous Sup35 co-expression on [*PSI*$^+$] propagation.

Modifications to the shuffle assay were made to study the effects of transient coexpression of heterologous proteins on [*PSI*$^+$] propagation (modifications described in Chapter 2, Fig 12). A [*PSI*$^+$] strain is transformed with plasmids carrying either homologous, heterologous, or chimeric *SUP35* versions. After a brief period of co-expression (6 days), the new plasmid is removed, and [*PSI*$^+$] propagation is checked to compare the percentage of [*psi*$^-$] colonies to the same strain receiving a homologous $Sup35_{Sc}$ copy. The terms "interference" and "poisoning" describe destabilization of the original prion after transient co-existence with a divergent protein. Notably, results showed that co-expression of a divergent Sup35 prion domain can strongly interfere with prion propagation. Table 16 (Appendix) provides a detailed list of all Sup35 versions tested for [*PSI*$^+$] interference in *S. paradoxus*. Figure 49 shows an example of

interference in the *S. paradoxus* strain. A strong [PSI^+] $Sup35_{Sc}$ variant produced in *S. paradoxus* presented 53% [PSI^+] loss after transient co-expression of Sup35 with the *S. paradoxus* PrD. Practically no interference (0.1% [PSI^+] loss) was observed for coexpression of Sup35 with the *S. cerevisiae* PrD.

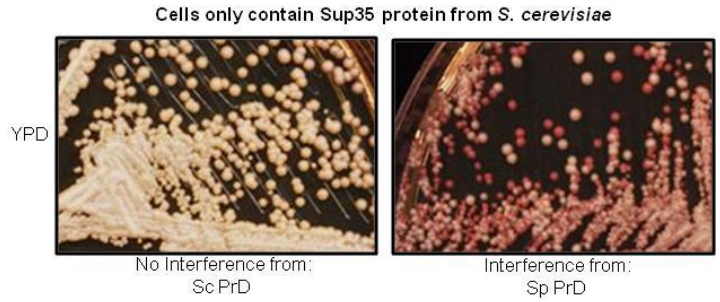

Figure 49: An example of prion interference in the *S. paradoxus* cell environment. This experiment was performed in a strong [PSI^+] *sup35Δ S. paradoxus* strain that expressed a *S. cerevisiae* version of *SUP35* from a plasmid. Either Sup35 having a PrD from *S. cerevisiae* (left) or *S. paradoxus* (right) protein was introduced and then removed (by expression on a centromeric plasmid) (See Figure 12). When the photograph was taken, the cells were only producing the original *S. cerevisiae* Sup35 protein. Red colonies are [psi^-]. White colonies retain the prion. Both white and red colonies produced after the loss of the interfering plasmid remained stable in subsequent passages on YPD.

6.3.2 The relationship between prion interference and a prion transmission barrier

As previously described, modifications to the plasmid shuffle procedure allow determination of both 1) the efficiency of prion transmission and 2) the extent of prion interference for the same protein (Fig. 11, Fig. 12). The results of both techniques were compared in the *S. paradoxus* cell environment by introducing Sup35 having the PrD from either *S. cerevisiae*, *S. paradoxus*, or *S. bayanus* (Fig. 50). A strong [PSI^+] variant produced in $Sup35_{Sc}$ was used as the starting variant. Prion transmission to Sup35 with the *S. cerevisiae* PrD was virtually complete (97% transmission) with no interference (0.1% [PSI^+] loss) observed. A minor transmission barrier (84% [PSI^+] transmission) was

observed for Sup35 with the *S. paradoxus* PrD. However, this protein exhibited high interference (53% [*PSI*$^+$] loss) after transient coexpression. Sup35 having the *S. bayanus* PrD, however, produced an absolute barrier (0% [*PSI*$^+$] transmission) yet exhibited almost no interference (1.2% [*PSI*$^+$] loss) in propagation of the original strong [*PSI*$^+$] variant. Therefore, we conclude that prion interference does not correlate with a prion transmission barrier when performed in the *S. paradoxus* cell environment. It should be noted that results for both transmission and interference experiments shown here are performed in haploid strains with 6 days of heterologous protein co-expression. Shorter periods of co-expression cause less interference, and differences in interference are observed when performed in diploid strains. (see Section 6.3.6).

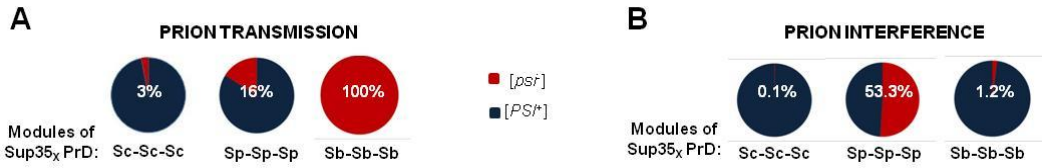

Figure 50: Comparison of prion transmission barriers and prion interference. A—Direct shuffle experiments for strong [*PSI*$^+$] in *S. paradoxus* were performed as on Fig. 11. Numerals I, II, and III refer to the exchangeable modules of PrD (Fig. 22). "Sc", "Sp" and "Sb" refer to *S. cerevisiae*, *S. paradoxus*, and *S. bayanus*, respectively. Frequencies of prion transmission and loss are shown on each chart. Blue sectors indicate the percentage of individual transformants displaying the [*PSI*$^+$] phenotype. Red sectors indicate the percentage of individual transformants that did not obtain the prion (percentage indicated on each chart). Data presented in panel A are also included in Figure 45 and Table 13 (Appendix). **B**—See Figure 12 for the prion interference scheme. PrD modules of protein transiently coexisting with Sc Sup35 are indicated below each chart. The percentages of [*psi*$^-$] cells after loss of coexisting plasmid are indicated. All data shown here are included in Table 16 (Appendix).

6.3.3 The influence of the cell environment on prion interference

We also questioned whether prion interference is caused by interactions of the proteins, themselves, or can be attributed to factors present within the *S. paradoxus* cell

environment. To test this, we performed a similar interference experiment in the *S. cerevisiae* cell environment, beginning with the strong [*PSI*$^+$] $Sup35_{Sc}$ variant used in the *S. paradoxus* experiments and co-expressed the same set of proteins (Fig, 51). Contrary to data obtained in *S. paradoxus,* no interference (0% [*PSI*$^+$] loss) was observed for Sup35 having the PrD from *S. cerevisiae*, *S. paradoxus* or *S. bayanus.* Based on the comparisons of the same experiments in the two species, we concluded that [*PSI*$^+$] interference depends on factors present within the cell environment. Again, the interference data obtained in the *S. cerevisiae* environment did not correlate to transmission data (Table 5 (Appendix); Fig. 15) obtained in the same species. (Specifically, there was only 12% [*PSI*$^+$] transmission from the *S. cerevisiae* PrD to the *S. bayanus* PrD, yet no interference was observed. In addition, there was a very slight reduction of transmission efficiency to the *S. paradoxus* PrD (93% transmission) when compared to homologous transmission (99% transmission to the *S. cerevisiae* PrD) but no interference by the *S. paradoxus* or *S. cerevisiae* PrD was observed in the *S. cerevisiae* cell environment.

Figure 51: Prion interference in the *S. cerevisiae* cell environment. See Figure 12 for the prion interference scheme. "Sc," "Sp," and "Sb" designate *S. cerevisiae*, *S. paradoxus*, and *S. bayanus*, respectively. The percentage of [*psi*$^-$] cells after loss of a coexisting plasmid are indicated as percentages. PrD modules of protein transiently coexisting with Sc Sup35 are indicated below each chart. The data are also included in Table 17 (Appendix).

6.3.4 The effects of PrD module exchange on [*PSI*$^+$] interference in *S. paradoxus*

To study the effects of particular Sup35 regions on prion interference, *SUP35* PrD's from *S. cerevisiae*, *S. paradoxus* and *S. bayanus* were divided into three exchangeable modules, with the sizes and sequence of each module described on Figure 22. Different modules were combined to create chimeric Sup35 proteins (all having M and C domains from *S. cerevisiae*) which were tested for prion interference. Results for all constructs are reported in Table 16 (Appendix) with graphs shown in Figure 52. As predicted, neither an additional dose of the original $Sup35_{Sc}$ protein (giving 0.1% [*PSI*$^+$] loss), nor the expression of an empty control plasmid (0% [*PSI*$^+$] loss) interfered with [*PSI*$^+$] propagation. Co-expression of the complete $Sup35_{Sp}$ protein (62% [*PSI*$^+$] loss) and the *S. paradoxus* PrD (53% [*PSI*$^+$] loss) gave the highest levels of interference. Surprisingly, both the complete $Sup35_{Sb}$ protein (0% [*PSI*$^+$] loss) and the *S. bayanus* PrD (1% [*PSI*$^+$] loss) showed little to no interference, despite complete $Sup35_{Sb}$ having the greatest sequence divergence from *S. cerevisiae*. For the *S. cerevisiae*/*S. paradoxus* PrD chimeric constructs, it was noted that sequence differences in Module I caused interference in prion transmission (26% [*PSI*$^+$] loss when module I from *S. cerevisiae* was exchanged with Module I from *S. paradoxus*). Sequence differences in both Modules I and II causing a synergistic effect for prion interference (Relatively no interference observed when Modules II and III from *S. cerevisiae* were exchanged for *S. paradoxus*, but there was 51% [*PSI*$^+$] loss when both were combined with the exchange of Module I from *S. paradoxus*). Differences in either Module I or Module II between *S. cerevisiae* and *S. bayanus* cause prion interference (22-24% [*PSI*$^+$] loss when either Module I or Module II from *S. cerevisiae* is switched with *S. bayanus*).

Figure 52: The effect of module exchange on prion interference in the *S. paradoxus* cell environment. All data shown here are included in Table 16 (Appendix). See Figure 12 for the prion interference scheme. PrD modules of protein transiently coexisting with SC Sup35 are indicated below each chart. The % of [*psi*$^-$] cells after loss of coexisting plasmid are indicated

6.3.5 The identity of a single residue influences prion interference

The discovery that sequence differences of particular modules has a profound effect on prion interference led us to question the influence that identity of short stretches or even individual residues may have on prion interference. Previous data showed that exchange of module 1 from *S. cerevisiae* to *S. paradoxus* presented a barrier to prion transmission and contributed to interference (Fig 52), so it was of interest to investigate the effects at the order of a single residue. Only one residue (at position 12) is conserved between *S. cerevisiae* and *S. bayanus* (asparagine) but differs in *S. paradoxus* (serine), so site-directed mutagenesis was used to exchange this residue. Interestingly, this residue lies within residues 9-14 which in *S. cerevisiae* meets the criteria for a universal consensus sequence (Fig 22) thought to be crucial for amyloid formation [74]. Though the asparagine residue at position 12 in *S. cerevisiae* or *S. bayanus* conforms to the residue requirement needed at this position, the serine at position 12 in *S. paradoxus* is predicted to disrupt the consensus (Fig 53, A). We exchanged this residue to document its effects on prion interference in the *S. paradoxus* cell environment (Fig 53, B). Here, the

S12N mutation is sufficient to eliminate prion interference. In reverse, the N12S mutation induced interference in the context of the Sc-Sp-Sp chimera (No interference was observed when it was exchanged in the Sup35 Sc-Sc-Sc PrD) which seems to indicate a synergistic effect from residue 12 in module I and one or more regions of module II or III. Overall, we concluded that the identity of a specific residue influences prion interference.

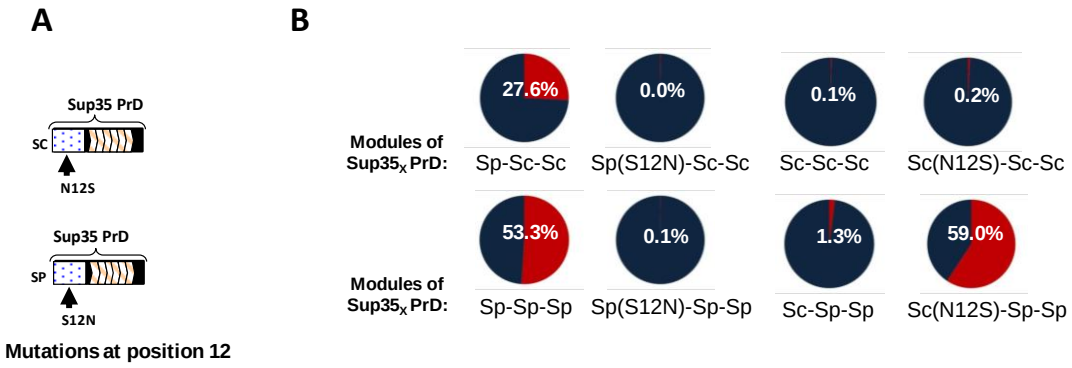

Figure 53: The effect of single amino acid substitutions on prion interference in the *S. paradoxus* cell environment. A—Note species-specific differences at residue 12 that were exchanged for these experiments. **B—**All data shown here are included in Table 16 (Appendix). See Figure 12 for the prion interference scheme. PrD modules of protein transiently coexisting with SC Sup35 are indicated below each chart. The % of [*psi*$^-$] cells after loss of the coexisting plasmid are indicated

An explanation for differences between prion transmission and prion interference may be that divergence in key stretches of Sup35 are required for interaction with and then incorporation of the soluble protein into an aggregate. The *S. bayanus* and *S. cerevisiae* PrDs share 77% sequence similarity, yet no transmission from the *S. cerevisiae* PrD to the complete *S. bayanus* PrD was observed. Interference by the *S. bayanus* PrD was also not observed. Perhaps the same regions of divergence preventing incorporation of $Sup35_{Sb}$ PrD's into the aggregate also prevents efficient interactions with Sup35Sc aggregates that would interfere with its [*PSI*$^+$] propagation. A drastic difference is seen

for the $Sup35_{Sp}$ PrD which shares a higher sequence similarity (94%) with the $Sup35_{Sc}$ PrD. Interestingly [*PSI*$^+$] is transferred from $Sup35_{Sc}$ to $Sup35_{Sp}$ with a high efficiency of 84% and yet shows high levels of Sup35Sc [*PSI*+] interference (53.3%). This would be explained by similarity in key stretches that would allow interaction with and incorporation with the aggregate, but the heteroaggregate formed is hypothesized to be less efficiently propagated (see section 6.3.7).

6.3.6 The effects of co-expression length and Hsp104 dosage on [*PSI*$^+$] interference

[*PSI*$^+$] interference by heterologous proteins was observed in *S. paradoxus* but not in *S. cerevisiae*. This was attributed to environmental factors such as chaperones that may vary in concentration and sequence among species. One hypothesis states that different Hsp104 levels or perhaps species-specific Hsp104/ Ssa ratios may affect [*PSI*$^+$] propagation of the same protein differently in particular cell environments. Numerous attempts to compare Hsp104 and Ssa chaperone levels using western blot with densitometry were not sensitive enough to accurately detect reproducible differences. Therefore, a mating interference technique was used to document the effects of Hsp104 dosage on [*PSI*$^+$] interference. The mating procedure (Fig. 54) involves crossing a [*PSI*$^+$] haploid *MATa* strain (expressing $Sup35_{Sc}$ from a plasmid) to a [*psi*$^-$] haploid *MATα* strain expressing different *SUP35* versions from *URA3* plasmids. The strains were crossed on YPD and incubated for fixed amounts of time, with diploids obtained by velveteening the yeast onto “drop-out” media selective for both plasmids. Then the *URA3* plasmid coding for the desired Sup35 protein was removed by replica plating onto 5-FOA medium. Hsp104 dosage was manipulated by creating a *hsp104Δ* deletion in one mating type strain

(see Chapter 4), allowing comparison of diploids having one or two functional *HSP104* gene copies.

In addition to Hsp104 dosage comparisons, the length of heterologous protein co-expression in the diploid system was also compared. The previously described plasmid shuffle procedure for assessing transmission and interference (Fig. 12), required 6 days of protein co-expression before the newly introduced plasmid could be removed (4 days to obtain colonies after plasmid transformation and 2 days growth on a master plate), but the mating interference procedure enabled even shorter lengths of coexpression (a minimum of 1.5 days coexpression). In general, little interference was detected for shorter length of heterologous co-expression (Fig. 55, Table 18 (Appendix)); however, subtle color differences were observed in [*PSI*$^+$] colonies (Table 19, Appendix). Ultimately, our results comparing 1.5 vs. 6 days of heterologous protein co-expression showed a profound difference in levels of prion interference with the Sup35 Sp PrD (24% [*PSI*$^+$] loss after 1.5 days, with 97% [*PSI*$^+$] loss after 6 days of coexpression.) Co-expression of the Sup35$_{Sb}$ PrD showed 0% [*PSI*$^+$] loss after 1.5 days, but 21% [*PSI*$^+$] loss after 6 days of coexpression.) (see Fig. 55) showing data obtained.) Overall, we concluded that the length of heterologous Sup35 co-expression is positively correlated with [*PSI*$^+$] interference and that deletion of one out of two *HSP104* copies from a diploid *S. paradoxus* strain decreases prion interference.

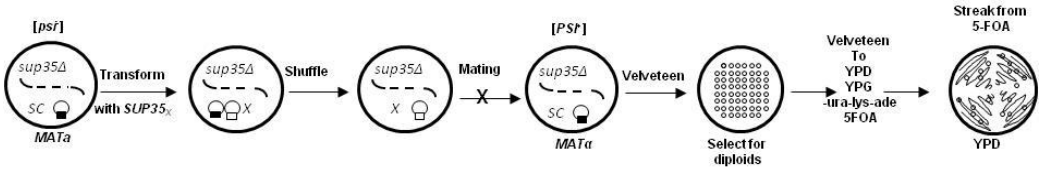

Figure 54: Mating interference scheme. A—a [*psi*$^-$] *sup35*Δ strain with the *S. cerevisiae SUP35* gene on a *LYS2* plasmid was transformed with a *URA3* plasmid bearing a variable *SUP35* construct. Transformants were obtained on medium lacking uracil to selective for the new plasmid. The original *LYS2* plasmid was lost, and the strain was mated to a [*PSI*$^+$] *sup35*Δ strain of the opposite mating type having *SUP35* gene on a *LEU2* plasmid. Individual transformants having the *URA3* plasmid were mixed with the [*PSI*$^+$] strain of the opposite mating type for either 8 hours (short-term) or longer on YPD and then velveteened to –Ura-Leu media to select for diploids. Diploids were replica plated onto YPD (color assay), YPG (petite screen), -ura-lys-ade (diploid selection) and 5-FOA (for loss of *URA3* plasmid) media. Each patch was streaked from 5-FOA media to YPD to assess prion loss. Numbers of white or pink [*PSI*$^+$] vs red [*psi*$^-$] were counted.

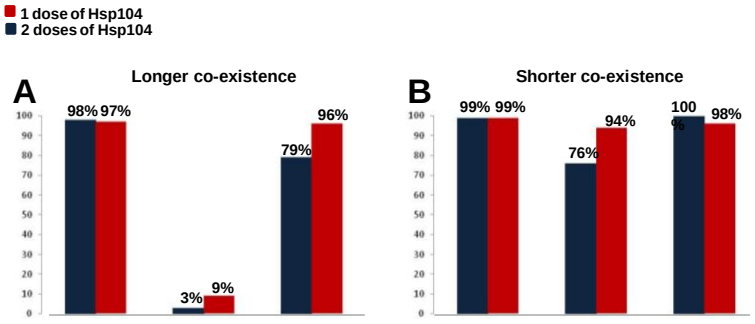

Figure 55: Effects of Hsp104 copy number and length of heterologous protein co-existence on prion interference in *S. paradoxus*. Mating interference experiments were performed as shown on Fig. 54. Diploid strains either had one (red) or two functioning copies (blue) of the *HSP104* gene with strains designated by color. Percentages above each bar represent the percentage of individual transformants retaining the [*PSI*$^+$] phenotype following either a long-term **(panel A)** or short-term **(panel B)** co-existence with a heterologous protein.

6.3.7 Models for [*PSI*$^+$] interference

Both white and red colonies were obtained from interference by $Sup35_{Sp}$ protein co-expression. The white colonies displayed a strong and stable [*PSI*$^+$] variant, having the same characteristics as the initial variant present before the interfering protein was

introduced; the red colonies were found to be [*psi*$^-$]. Based on this result, it was hypothesized that heterologous proteins may less efficiently (due to differences in key sequence stretches) compete with homologous protein to join onto the ends of prion seeds, "capping" them to prevent addition of Sup35 monomers. White colonies would, therefore, represent yeast obtaining homologous $Sup35_{Sc}$ aggregates and red [*psi*$^-$] colonies would arise from cells receiving "capped" aggregates that cannot efficiently propagate. Thus, this "amyloid capping" model predicts the presence of shorter aggregates and is presented in Figure 56. A semi-denaturing detergent agarose gel electrophoresis procedure (SDD-AGE) (Described in section 2.4.6) was employed to measure aggregate size in a *S. paradoxus* strain co-expressing either two homologous Sup35Sc copies (negative control) or one $Sup35_{Sc}$ and one $Sup35_{Sp}$ copy. Surprisingly, aggregates co-expressing both $Sup35_{Sc}$ and $Sup35_{Sp}$ were larger than those expressing two Sup35Sc copies (control) (Fig. 57), thus failing to support the amyloid capping model.

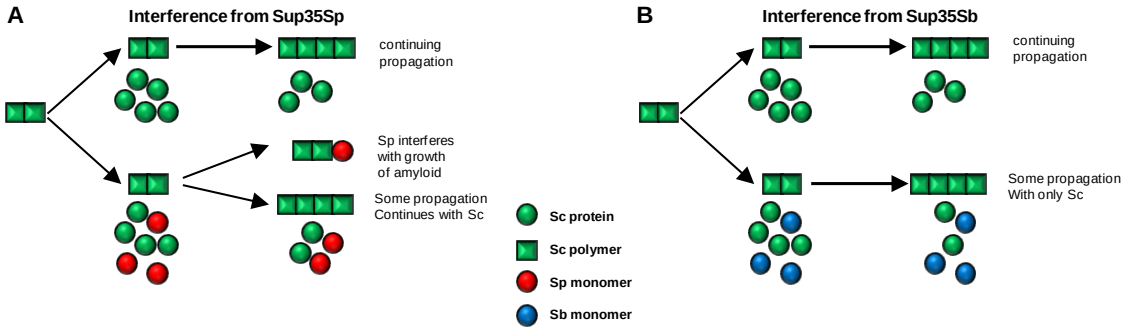

Figure 56: Amyloid capping model. A—In the amyloid capping model, high $Sup35_{Sc}$ and $Sup35_{Sp}$ sequence similarity is proposed to facilitate $Sup35_{Sp}$ interaction with $Sup35_{Sc}$ aggregates. Sup35Sp monomers would theoretically join to the ends of Sup35Sc aggregates, capping them and preventing aggregate growth. **B—**The amyloid capping model suggests that high sequence divergence between some regions of $Sup35_{Sc}$ and $Sup35_{Sb}$ would prevent interactions of $Sup35_{Sb}$ with $Sup35_{Sc}$ aggregates, thus aggregates are not capped, and no interference is observed.

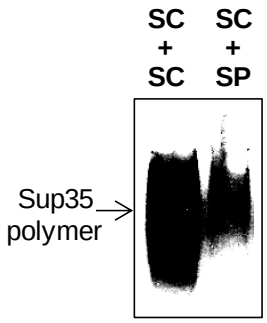

Figure 57: Aggregate size from heterologous Sup35 co-expression. A *sup35Δ S. paradoxus* strain having a strong [*PSI+*] variant produced $Sup35_{Sc}$ from a centromeric plasmid. This strain was transformed with another centromeric plasmid to produced either $Sup35_{Sc}$ (control) or $Sup35_{Sp}$. Following a period of heterologous co-expression, the total cell lysate was extracted and run on a semi-denaturing detergent agarose gel electrophoresis (SDD-AGE) gel (see Chapter 2 methods). Aggregates were transferred to a nitrocellulose membrane by capillary action and were probed with Sup35M antibody.

Based on the findings that larger aggregates are produced from heterologous $Sup35_{Sc}$/$Sup35_{Sp}$ co-expression than produced by homologous Sup35Sc/Sup35Sc co-expression, a different interference model was proposed. This "interference fragmentation" model (Fig 58) highlights the impaired interactions of cellular factors in the propagation of [PSI^+] heteroaggregates. Specifically, this model suggests that homologous aggregates (left of figure) are more efficiently propagated by more favorable interactions with cellular components (such as Hsp104) that fragment aggregates to generate prion "seeds" for later cycles of propagation. Less efficient disaggregation would produce fewer seeds leading to larger aggregates and, ultimately, impairing [PSI^+] propagation. Hsp104 is one cellular chaperone implicated, as it has an established role in [PSI^+] propagation and is known to disaggregate [PSI^+] (see Fig 58). In this model, heterologous Sup35 co-expression of more divergent proteins ($Sup35_{Sc}$/ $Sup35_{Sb}$) might fail to generate interference, as the protein divergence at key regions prevents successful

interactions leading to incorporation of the divergent protein ($Sup35_{Sb}$) into the $Sup35_{Sc}$ aggregates. However, interactions of key regions of more similar sequences in heterologous Sup35 proteins may provide sufficient opportunities for interaction between the aggregate and the protein (Sup35Sp) and allow incorporation into the aggregate. Yet, growth of the heteroaggregate would cause less efficient interactions with the endogenous Hsp104 may sufficiently reduce disaggregation causing fewer and larger seeds. Fewer seeds lessens the efficiency of future rounds of [*PSI*$^+$] propagation and larger aggregates may not be transferred as frequently to daughter cells, ultimately producing a destabilization and eventual [*PSI*$^+$] curing.

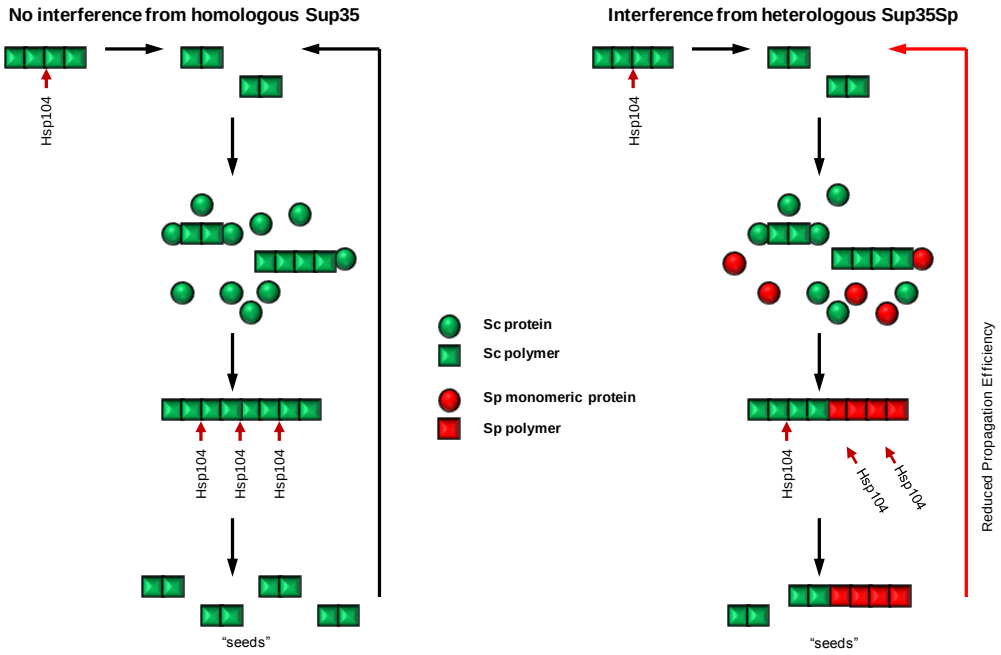

Figure 58: Interference fragmentation model. A—In the prion model, homologous Sup35Sc monomers join onto the ends of Sup35Sc aggregates or "seedsm" causing aggregate growth. Cellular factors including Hsp104 interact with the aggregates and fragment them to form additional "seeds" which continue the propagation cycle. **B**— The interference fragmentation model proposes that sequence similarities may allow heterologous proteins to be incorporated into the aggregates but may interact less efficiently with cellular factors such as Hsp104 that fragment the aggregates. Heterologous aggregates would remain larger and provide fewer seeds for propagation, thus producing a weaker [*PSI*$^+$] phenotype.

Additionally, larger aggregates might also be less efficiently transmitted to daughter cells.

6.4 CHAPTER 6 CONCLUSIONS:

- Co-expression of a divergent Sup35 prion domain can interfere with prion propagation
- Prion interference does not correlate with a prion transmission barrier.
- [*PSI*$^{+}$] interference is dependent on factors present within a cell environment.
- In *S. paradoxus*, different PrD regions are primarily responsible for prion interference in different cross-species combinations
- The identity of specific residues (sequences), rather than the overall level of PrD homology is crucial for determining prion interference. Prion interference is not directly correlated with the overall PrD divergence.
- Overall, deletion of one out of two *HSP104* copies from a diploid *S. paradoxus* strain decreases prion interference
- The length of heterologous Sup35 co-expression is positively correlated with [*PSI*$^{+}$] interference
- Co-expression of a divergent Sup35 prion domain can interfere with prion propagation
- Prion interference does not correlate with a prion transmission barrier.
- [*PSI*$^{+}$] interference is dependent on factors present within a cell environment.

6.5 CHAPTER 6 ACKNOWLEDGEMENTS:

I would like to thank my students Ankita Tippur, David Deng, Illene Del Valle, and Kudo Jang for assisting in the construction of a plasmid and for helping me obtain some prion intereference results presented in this chapter.

CHAPTER 7: THE INFLUENCE OF DIFFERENT [*PIN*$^+$]-INDEPENDENT INDUCERS ON CROSS-SPECIES PRION INFECTIVITY IN *S. PARADOXUS*

7.1 CHAPTER SUMMARY

S. paradoxus and *S. bayanus* strains used for this work were previously found to be [*pin*$^-$] (Results by B. Chen). Different [*PIN*$^+$]-independent inducers (constructed by B. Chen) were overexpressed in attempts to induce [*PSI*$^+$] *de novo* in [*psi*$^-$] *S. paradoxus* and *S. bayanus* strains that produce Sup35 from various origins. The characteristics of the [*PSI*$^+$] variants successfully produced in *S. paradoxus* were documented for each type of variant observed from different combinations of inducee and inducer. Throughout this chapter, the term "inducee" refers to the version of Sup35 expressed in the *sup35Δ* strain, and this Sup35 version is originated from either *S. cerevisiae*, *S. paraodoxus*, or *S. bayanus*. "Inducer" refers to the Sup35NM-Hpr6.6 version overexpressed to facilitate *de novo* [*PSI*$^+$] formation. The [*PSI*$^+$] variants obtained then served as initial prions for plasmid shuffle and cytoduction assays, allowing us to document the importance of inducer sequence and protein origin on the types of variants produced by *de novo* [*PSI*$^+$] formation in *Saccharomyces*.

.

7.2 MATERIALS

7.2.1 Plasmids

Plasmids pmCUP-NMSB-HRP6.6, pmCUP-NMSC-HRP6.6 , and pmCUP-NMSP-HRP6.6 were used as described in section 7.2.3 to induce [*PSI*$^+$] *de novo* by serving as artificial [*PIN*$^+$]-independent factors. Plasmids pRS317-PS-SUP35SC, pRS317-PS-SUP35SP, and pRS317-PS-SUP35SB were transformed into *sup35Δ s*trains as an essential source of Sup35, a factor required for viability.

7.2.2 Strains

The *S. paradoxus* strain GT1320-5B was a haploid derivative of SP7-1D with the following genotype: *S. paradoxus MATα ura3-P2 lys2 Δho::KanMX6 ade1SP::ade1-14SC [LYS2 SUP35S$_X$]*. This strain contained the *sup35*Δ*::natNT2* transplacement on the chromosome (constructed as described in Chapter 4), and was maintained alive by *S. cerevisiae – E. coli* shuttle plasmids bearing the *SUP35* gene originating from either *S. cerevisiae*, *S. paradoxus*, or *S. bayanus*. [*PSI*$^+$] of varying strengths was induced in Sup35 of different origins by various Sup35NM-Hpr6.6 [*PIN*$^+$]-independent inducers. The karyogamy-deficient recipient strains for cytoduction were constructed on the basis of the previously described (Chen *et al.*, 2007) strain 1B-D910 *(MA*T**a** *ade1–14 his3 leu2 trp1 ura3 cyh R kar1–1sup35Δ::HIS3* [*rho*$^-$ *psi*$^-$ *pin*$^-$]), by substituting the original plasmid bearing the *S. cerevisiae SUP35* gene by plasmids with a *LEU2* marker, each carrying *SUP35* originating from either *S. cerevisiae, S. paradoxus,* or *S. bayanus*.

7.2.3 [*PIN*$^+$]-independent inducers

[*PSI*$^+$] formation was induced *de novo* in *S. paradoxus* and *S. bayanus* for the following experiments using artificial [*PIN*$^+$]-independent inducers (constructed by B. Chen), as [*PIN*$^+$] is not present in these species. Each inducer consisted of *SUP35NM* from either *S. cerevisiae*, *S. paradoxus*, or *S. bayanus* fused to the human membrane progesterone receptor (*HPR6.6)* gene that codes for a 195 amino acid human protein having a transmembrane domain (Fig. 59). This artificial inducer was placed under P_{CUP1} promoter control. The Hpr6.6 transmembrane domains of homologous chimeras were predicted to interact, thus bringing Sup35NM proteins into contact, facilitating [*PSI*$^+$] nucleation. Once formed, the aggregate was expected to adopt a [*PIN*$^+$]-like role to cross seed aggregation of full length Sup35 produced. The inducers (on plasmids) were over expressed to facilitate *de novo* [*PSI*$^+$] formation in a *sup35Δ S. paradoxus* strain producing either $Sup35_{Sc}$, $Sup35_{Sp}$ or $Sup35_{Sb}$ from a plasmid. The inducer plasmid was then removed. Descriptions and images of [*PSI*$^+$] versions obtained using various combinations of Sup35 origin and inducer are shown in Table 20 and on Figures 60 and 61. *De novo* [*PSI*$^+$] variants in *S. paradoxus* were then used as starting prions for plasmid shuffle and cytoduction assays to measure cross-species prion transmission.

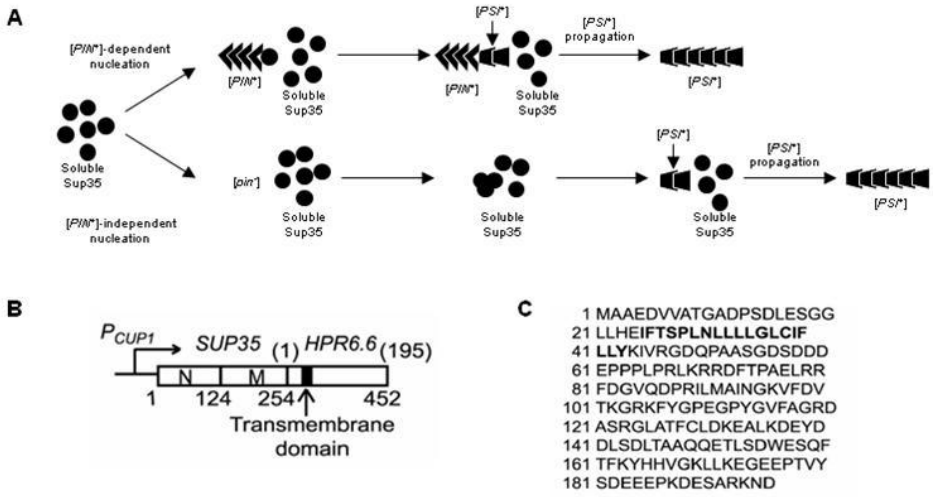

Figure 59: The creation of a [*PIN*$^+$]-independent induction system. A —The presence of an inducing factor (such as [*PIN*$^+$]) promotes efficient induction of the [*PSI*$^+$] prion by serving as a template for Sup35 aggregation (top scheme). Sup35 may rarely formn [*PSI*$^+$] without an aggregation factor (bottom scheme). **B** —Each [*PIN*$^+$]-independent inducer was constructed by fusing *SUP35NM* from either *Saccharomyces cerevisiae*, *Saccharomyces paradoxus*, or *Saccharomyces bayanus* to the human membrane progesterone receptor (*HPR6.6)* gene. The *HPR6.6* gene codes for a 195 aa human protein having a transmembrane domain (black sector). This artificial inducer was placed under the control of a copper-inducible promoter (P_{CUP1}). Numbers correspond to aa positions, with aa's from Hpr6.6 shown in parentheses. **C** —the amino acid sequence for the Hpr6.6 protein is shown with the transmembrane domain highlighted in bold.

7.3 RESULTS AND DISCUSSION

7.3.1 *De novo* [*PSI*$^+$] induction

De novo [*PSI*$^+$] induction in *S. paradoxus*

To generate [*PSI*$^+$] *de novo* in S. paradoxus using different inducers, a *S. paradoxus sup35ΔnatNT2* strain expressing a plasmid copy of *SUP35*, from either *S. cerevisiae*, *S. paradoxus*, or *S. bayanus,* were transformed with plasmids expressing versions of Sup35NM-Hpr6.6 inducers from either *S. cerevisiae*, *S. paradoxus*, or *S.*

bayanus. This gave 9 different combinations of Sup35 protein / inducer. Transformants were plated on –Ade medium containing 25 μM $CuSO_4$ to cause overexpression of the inducer and were incubated at 25°C for 21 days. Ade^+ papillae (Fig 60) were checked for [PSI^+] using a YPD color test, a –Ade suppression test, and a GuHCl curability assay. Results obtained for specific papillae for each of the 9 Sup35 / inducer combinations are presented in Table 20. Pictures of different [PSI^+] phenotypes obtained are shown in Figure 61.

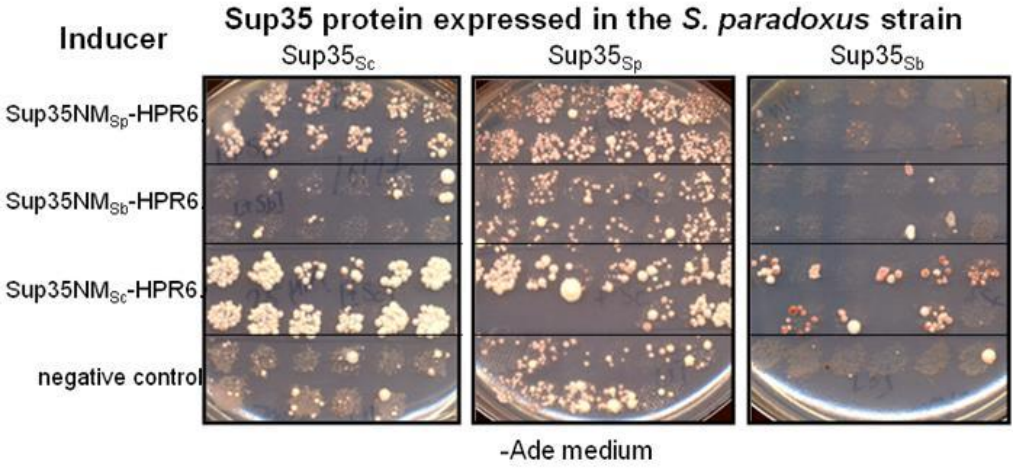

Figure 60: [*PSI*$^+$] *de novo* induction in *S. paradoxus*. Different versions of *SUP35NM-HPR6.6* inducers were overexpressed in a [*psi*$^-$, *pin*$^-$] *S. paradoxus* strain to induce *de novo* [*PSI*$^+$] formation in a target Sup35 protein. The *S. paradoxus* strain had only one version of the Sup35 protein present, which was either from *S. cerevisiae* (Sc), *S. paradoxus* (Sp), or *S. bayanus* (Sb). The strain, producing a version of the Sup35 target protein, was transformed with different versions of the *SUP35-HPR6.6* inducer constructs or an empty plasmid (negative control) under control of the P_{CUP1} promoter. Cells were plated on media lacking adenine and containing 25 μM $CuSO_4$ for promoter induction. Images shown were taken after 21 days of incubation at 30°C

Inducee	Inducer	Isolate #	Strength
SC	SC	#1	Strong
		#2	Strong
		#3	Strong
	SP	#1	Weak
		#2	Strong
	SB	#1	Weak
		#2	Weak
		#3	Weak
		#4	Weak
		#5	Weak
SP	SC	#1	Weak
		#2	Weak
		#3	Weak
		#4	Weak
		#5	Weak
	SP	#1	Strong
		#2	Weak
		#3	Weak
	SB	#1	Weak
		#2	Weak
		#3	Medium
		#4	Weak
SB	SC	#1	Weak
		#2	Weak
		#3	Weak
		#4	Weak
		#5	Weak
	SP	#1	Strong
	SB	#1	Strong

Table 20: Properties of *de novo* induced [*PSI*$^+$] in *S. paradoxus* A haploid *S. paradoxus* strain, produced Sup35 from either *S. cerevisiae* (Sc), *S. paradoxus* (Sp) , or *S. bayanus* (Sb) on a plasmid (inducee). Each version was transformed with three different *SUP35NM-HPR6.6 [PIN*$^+$]-independent inducers (containing Sup35NM from either *S. cerevisiae*, *S. paradoxus*, *or S. bayanus*) to create 9 different combinations. Each combination was plated on -Ade media containing 25 μM $CuSO_4$ for overexpression of the [*PIN*$^+$]-independent inducers. Individual Ade$^+$ papillae (Figure 60) were screened for [*PSI*$^+$] on –Ade medium and by guanidine hydrochloride sensitivity. Representative [*PSI*$^+$] samples from the 9 different combinations were assigned isolate numbers and are listed in this table and shown on Figure 61. Some were used to perform shuffle and cytoduction assays shown in this chapter..

Characteristics of [*PSI*$^+$] induced *de novo* in *S. paradoxus* Sup35

Overall, the $Sup35_{Sc}$ protein induced by $Sup35_{Sc}$-Hpr6.6 exclusively produced strong [*PSI*$^+$], but induction by $Sup35_{Sp}$-Hpr6.6 generated both strong and weak [*PSI*$^+$]. Induction by $Sup35_{Sb}$-Hpr6.6 produced only weak [*PSI*$^+$].

The $Sup35_{Sp}$ protein induced by $Sup35_{Sc}$-Hpr6.6 exclusively generated weak [*PSI*$^+$]; however, induction with $Sup35_{Sp}$-Hpr6.6 or $Sup35_{Sb}$-Hpr6.6 produced either strong or weak [*PSI*$^+$].

The $Sup35_{Sb}$ protein induced with $Sup35_{Sc}$-Hpr6.6 exhibited both strong and weak [*PSI*$^+$], but produced only detectable strong [*PSI*$^+$] when induced with $Sup35_{Sp}$-Hpr6.6 or $Sup35_{Sb}$-Hpr6.6.

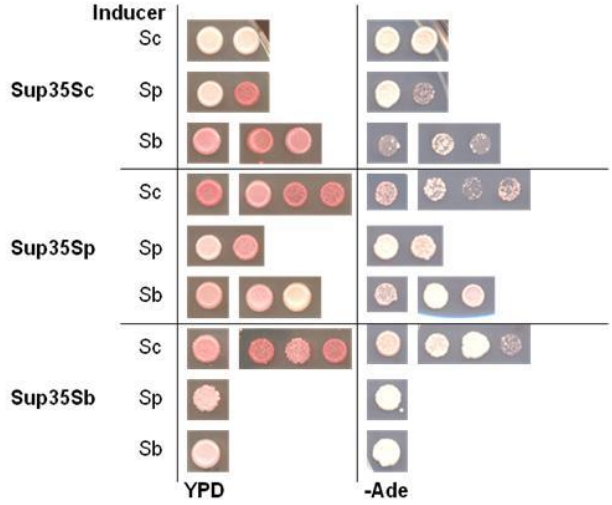

Figure 61: *de novo* [*PSI*$^+$] in *S. paradoxus* generated from [*PIN*$^+$]-independent inducers. A haploid *S. paradoxus* strain, expressed *SUP35* from either *S. cerevisiae* (Sc), *S. paradoxus* (Sp) , or *S. bayanus* (Sb) on a plasmid. Each version was transformed with three different *SUP35NM-HPR6.6 [PIN*$^+$]-independent inducers (containing Sup35NM from either *S. cerevisiae, S. paradoxus, or S. bayanus*) under P_{CUP} promoter control to create 9 different combinations. Each combination was plated on -Ade media containing 25 μM $CuSO_4$ for overexpression of the *[PIN*$^+$]-independent inducers . Individual Ade$^+$ papillae were screened for [*PSI*$^+$] using synthetic "drop-out" media and by performing 3 passages on YPD containing guanidine hydrochloride (GnHCl) to check for GnHCl sensitivity and [*PSI*$^+$] curing. Representative [*PSI*$^+$] samples from the 9

different combinations, described in table 4.X, are shown here. The Sup35 version being expressed by the strain is indicated to the left in bold. The version of the *SUP35NM-HPR6.6 [PIN$^+$]*-independent inducer used in denoted by either "Sc", "Sp", or "Sb." Colonies were spotted on YPD or –Ade media and were incubated at 30°C.

Attempts to induce [*PSI*$^+$] *de novo* in *S. bayanus*

A similar attempt was made to induce [*PSI*$^+$] in the *S. bayanus* species, but the prion was not detected by the YPD color assay or by suppression on –Ade medium (result by B. Chen). Later, a prion transfection procedure (described in Section2.2.4) was used to successfully introduce a pre-formed strong [*PSI*$^+$] variant into *S. bayanus*. Interestingly, the strong [*PSI*$^+$] phenotype obtained through transfection was detected on –Ura-Trp medium and by biochemical analysis, but was not readily visible from the YPD color assay and –Ade suppression assay for the same prion propagated in *S. cerevisiae* and *S. paradoxus*. Thus, we propose that *de novo* [*PSI*$^+$] may have been generated in *S. bayanus*, but was not detected by typical screening methods for [*PSI*$^+$]. Further screening is needed to determine whether [*PIN*$^+$]-independent inducers can be used to generate [*PSI*$^+$] *de novo* in *S. bayanus* and to determine the type of variant formed.

7.4 THE INFLUENCE OF PRION INDUCER ON CROSS-SPECIES TRANSMISSION

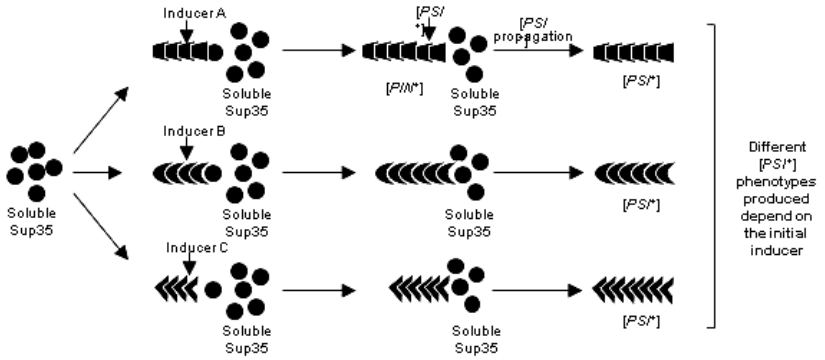

Figure 62: The proposed influence of different [*PIN*$^+$]-independent inducers on *de novo* [*PSI*$^+$] formation —The presence of a [*PIN*$^+$]-inducing factor (such as a prion form of the Rnq1 protein) promotes efficient induction of the [*PSI*$^+$] prion by serving as a template for Sup35 aggregation. Different versions of the [*PIN*$^+$]-independent inducing factor, created by fusing the N and M domains of *SUP35* from either *S.cerevisiae*, *S. paradoxus*, or *S. bayanus* to the human membrane progesterone receptor (*HPR6.6)* gene, were predicted to affect the type of [*PSI*$^+$] variant formed. The artificial inducers (under the control of a copper-inducible promoter (P_{CUP1}) were overexpressed in a *S. paradoxus* strain producing either full length Sup35Sc, Sup35Sp or Sup35 Sb.

Five different direct shuffle experiments were performed, each beginning with a [*PSI*$^+$] variant induced *de novo* by a unique combination of Sup35 protein and Sup35NM-Hpr6.6 inducer (see Figure 59 and Figure 61). All variants were checked for efficiency of [*PSI*$^+$] transmission to Sup35 having the PrD from either *S. cerevisiae*, *S. paradoxus*, and *S. bayanus* prion domains. Results are presented for each inducee/ inducer combination in Tables 21-25.

7.4.2 Plasmid shuffle from [*PSI*$^+$] formed in Sup35 having the *S. cerevisiae* PrD

The following results measure transmission from [*PSI*$^+$] in $Sup35_{Sc}$ generated with different inducers:. Results showed [*PSI*$^+$] was transmitted with 100% efficiency to

Sup35 having a prion with the *S. cerevisiae* PrD that was induced by Sup35NM$_{Sc}$Hpr6.6 but with 80% efficiency when induced by Sup35NM$_{Sp}$-Hpr6.6 or Sup35NM$_{Sb}$-Hpr6.6.

[*PSI*$^{+}$] was transmitted with reduced efficiency to Sup35 having a prion with the *S. paradoxus* PrD, when induced by Sup35NM$_{Sc}$Hpr6.6 (55%) or Sup35NM$_{Sp}$-Hpr6.6 (40%) but with 94% efficiency when induced by Sup35NM$_{Sb}$-Hpr6.6.

Finally, use of the Sup35NM$_{Sc}$-Hpr6.6 inducer produced no transmission to a prion having the *S. bayanus* PrD, but efficiencies of 17% and 85% were observed from use of the Sup35NM$_{Sp}$-Hpr6.6 and Sup35NM$_{Sp}$-Hpr6.6 inducers, respectively.

7.4.3 Plasmid shuffle from [*PSI*$^{+}$] formed in Sup35 having the *S. paradoxus* PrD

The following results measure transmission from [*PSI*$^{+}$] in Sup35$_{Sp}$ generated with different inducers. Results showed [*PSI*$^{+}$] was transmitted with 91% efficiency to Sup35 having the *S. cerevisiae* PrD, when induced by Sup35NM$_{Sc}$Hpr6.6 but with 88% efficiency when induced by Sup35NM$_{Sp}$-Hpr6.6.

[*PSI*$^{+}$] was transmitted with increased efficiency to Sup35 having the *S. paradoxus* PrD, when induced by Sup35NM$_{Sc}$Hpr6.6 (97%) and with absolute efficiency (100%) by Sup35NM$_{Sp}$-Hpr6.6.

Finally, use of either the Sup35NM$_{Sc}$-Hpr6.6 or the Sup35NM$_{Sp}$-Hpr6.6 inducer produced no transmission to Sup35 having the *S. bayanus* PrD.

Overall, differences in transmission was observed for experiments performed in [*PSI*$^{+}$] generated under various conditions of inducer and inducee, suggesting that inducers may reflect the *de novo* [*PSI*$^{+}$] variants formed.

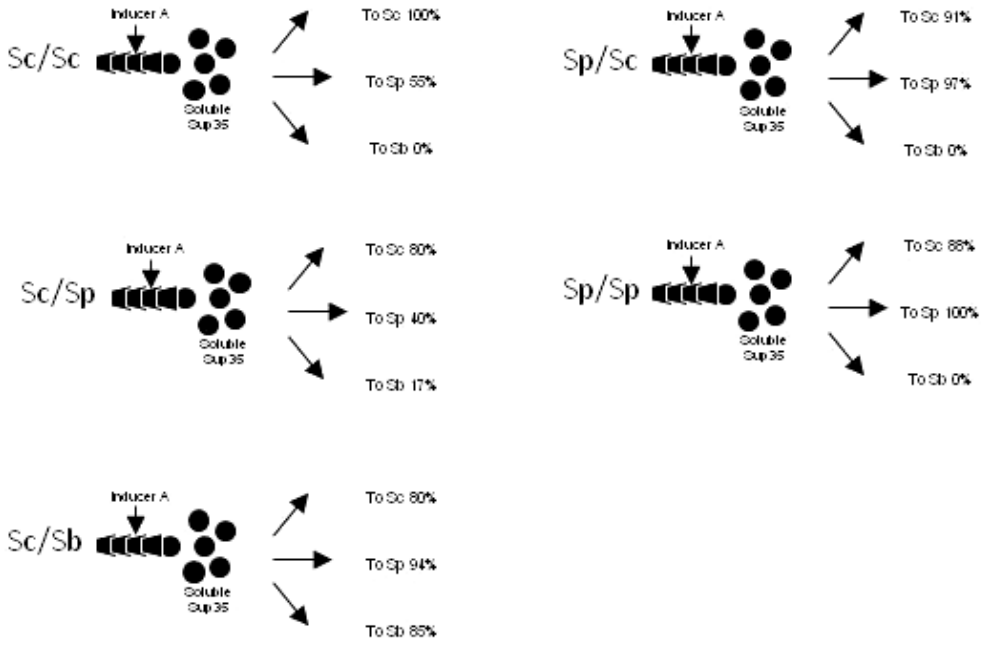

Figure 63: Prion transmission in *S. paradoxus* [*PSI*$^+$] generated with different combinations of Sup35 origin and [*PIN*$^+$]-independent inducers — Prion shuffle experiments were performed in *S. paradoxus* [*PSI*$^+$] strains. Different combinations of [*PIN*$^+$]-independent inducers were used to produce [*PSI*$^+$] in Sup35 originating from either *S. cerevisiae*, *S. paradoxus*, or *S. bayanus*. The efficiency of [*PSI*$^+$] transmission to Sup35 from either *S. cerevisiae* ($Sup35_{Sc}$), *S. paradoxus* ($Sup35_{Sp}$) or *S. bayanus* ($Sup35_{Sb}$) is recorded for each. See data presented in Tables 21-25 (Appendix).

7.5 THE INFLUENCE OF PRION INDUCER ON CYTOPLASMIC [*PSI*$^+$] EXCHANGE

Cytoduction experiments were performed in *S. paradoxus* to study effects of Sup35 sequence and inducer sequence on [*PSI*$^+$] characteristics such as infectivity. [*psi*$^-$] cytoductants received cytoplasm (but not the donor nucleus) from a [*PSI*$^+$] donor strain by a process detailed in Chapter 2 (Fig 12). Prion transfer was detected by growth on synthetic ethanol glycerol (SEG) medium lacking adenine with added cycloheximide (cyc). Donor [*PSI*$^+$] variants (*S. paradoxus*) were generated as previously described in a *sup35Δ* strain expressing either $SUP35_{Sc}$, $SUP35_{Sp}$, or $SUP35_{Sb}$ (inducee) from a plasmid.

[*PSI*$^+$] was induced by overexpression of *SUP35NM-HPR6.6 [PIN*$^+$]-independent inducers. [*PSI*$^+$] or [*psi*$^-$] (control) *S. paradoxus* donor strains were then crossed to a [*psi*$^-$] *S. cerevisiae sup35Δ* recipient strain expressing either $SUP35_{Sc}$, $SUP35_{Sp}$, or $SUP35_{Sb}$ from a plasmid. Rare colonies getting *URA3* plasmid from the donor were excluded.

7.5.1 Cytoduction from [*PSI*$^+$] formed in Sup35 having the *S.cerevisiae* PrD

The following results detail cytoduction from [*PSI*$^+$] in $Sup35_{Sc}$ generated with different inducers. Results showed that [*PSI*$^+$] (induced by $Sup35NM_{Sc}Hpr6.6$ or $Sup35NM_{Sp}Hpr6.6$) was transmitted efficiently to Sup35 having the *S. cerevisiae* PrD, but not to Sup35 having the *S. paradoxus* or *S. bayanus* PrD. However, [*PSI*$^+$] (induced by $Sup35NM_{Sb}Hpr6.6$) was transmitted much more efficiently to Sup35 having the *S. paradoxus* PrD than to Sup35 with the *S. cerevisiae* or *S. bayanus* PrDs.

7.5.2 Cytoduction from [*PSI*$^+$] formed in Sup35 having the *S. paradoxus* PrD

The following results detail cytoduction from [*PSI*$^+$] in $Sup35_{Sp}$ generated with different inducers. Results showed that [*PSI*$^+$] (induced by $Sup35NM_{Sc}Hpr6.6$ or $Sup35NM_{Sp}Hpr6.6$) was transmitted in a decreasing order of efficiency to Sup35 having the *S. cerevisiae* PrD, the *S. paradoxus* PrD, and then to Sup35 having the *S. bayanus* PrD. However, [*PSI*$^+$] (induced by $Sup35NM_{Sp}Hpr6.6$ or $Sup35NM_{Sb}Hpr6.6$ or) was transmitted most efficiently to Sup35 having the *S. paradoxus* PrD than to Sup35 with the *S. cerevisiae* or *S. bayanus* PrDs.

7.5.3 Cytoduction from [*PSI*$^+$] formed in Sup35 having the *S. bayanus* PrD

The following results detail cytoduction from [*PSI*$^+$] in Sup35$_{Sb}$ generated with different inducers. Results showed that [*PSI*$^+$] (induced by Sup35NM$_{Sc}$Hpr6.6) was transmitted most efficiently to Sup35 having the *S. paradoxus* PrD than to Sup35 with the *S. cerevisiae* or *S. bayanus* PrDs.

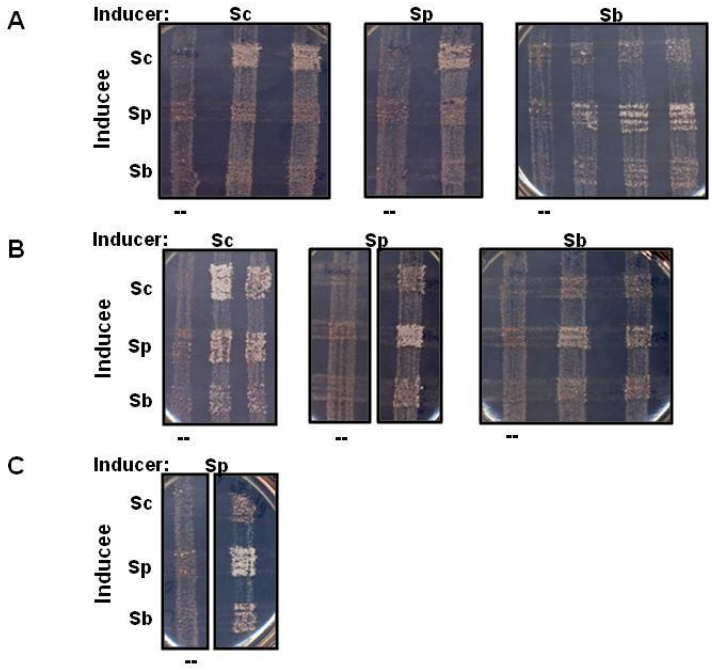

Figure 64: The effect of Sup35 origin and [*PIN*$^+$]-independent inducer on cytoplasmic [*PSI*$^+$] transfer from *S. paradoxus* to *S. cerevisiae.* Cytoduction was used to study the effect of the origin of *SUP35NM-HPR6.6 [PIN*$^+$]-independent inducers on the type of [*PSI*$^+$] formed. *De novo* [*PSI*$^+$] was generated in a haploid *sup35Δ S. paradoxus* strain expressing *SUP35* (inducee) from either *S. cerevisiae* (Sc), *S. paradoxus* (Sp), or *S. bayanus* (Sb) on a plasmid. [*PSI*$^+$] was induced, in each, by overexpression of a Sc, Sp, or Sb version of a *SUP35NM-HPR6.6 [PIN*$^+$]-independent inducer. Different [*PSI*$^+$] or [*psi*$^-$] (control) *S. paradoxus* donor strains were crossed to a [*psi*$^-$] *S. cerevisiae sup35Δ* recipient strain expressing either a *SUP35$_{Sc}$* (Panel A), *SUP35$_{Sp}$* (Panel B), or *SUP35$_{Sb}$* (Panel C) version from a plasmid. Cytoductants received the donor cytoplasm but not the donor nucleus in a process previously described on Figure 13. [*PSI*$^+$] transfer was detected by growth on synthetic ethanol glycerol (SEG) medium lacking adenine with added cycloheximide (cyc). The supression efficiency can be compared with respect to the negative

control that was mated to a [*psi*$^-$] donor strain (marked with a dash). Plates were incubated at 30°C.

7.6 CHAPTER 7 CONCLUSIONS:

- The prion inducer does influence prion characteristics that determine cross-species infectivity

7.7 CHAPTER 7 ACKNOWLEDGEMENTS:

I would like to thank my student David Deng for helping me obtain prion transmission data presented in this chapter. I would also like to thank Buxin Chen for preparing the inducer constructs.

CHAPTER 8: ANALYSIS OF SUP35 BARRIERS TO AGGREGATION *IN VITRO*

8.1 CHAPTER SUMMARY

All evidence presented in previous chapters for species barriers and heterologous prion interference was obtained *in vivo*, and was caused by the interplay between cellular factors and the protein sequence divergence. To specifically determine the influence of protein sequence on these processes, it becomes helpful to study these processes with purified Sup35NM *in vitro*, thus eliminating influences of cellular factors. In this chapter, bacterial purified Sup35NM from *S. cerevisiae*, *S. paradoxus*, and *S. bayanus* were aggregated under different conditions (with and without seeding by a pre-existing amyloid seed) to assess the impact of the cell environment on aggregation. In particular, cross-seeding aggregation was performed to generate species barriers between proteins from different *Saccharomyces* species.

8.2 MATERIALS

8.2.1 Strains

Yeast strains GT17, GT671, GT256-23C, GT988-1A and bacterial strains HMS174 and the *E. coli* gammabody expression strain BL21(DE3)pLysS are described in Chapter 2.

8.2.2 Plasmids

The *E. coli* expression vectors pET20b-SUP35NM, pET20b-SUP35NMSpar, and pET20b-SUP35NMSbay containing *SUP35*NM from the species indicated are described in Chapter 2. The *E. coli* gammabody expression vectors pGBSup35$_{12\text{-}21}$, pGBSup35$_{7\text{-}26}$, and pGBSup35$_{7\text{-}17}$ contain short *SUP35* sequences grafted into a variable domain of the gammabody and are described in Chapter 2.

8.3 RESULTS AND DISCUSSION

8.3.1 transfection of *in vitro* generated amyloid into yeast

Purified Sup35NM(His)$_6$ was aggregated *in vitro* with rotation to generate "seeds" for future experiments to investigate the influence of aggregation conditions and protein sequence on species barriers and amyloid interference. Sup35NM(His)$_6$ originating from *S. cerevisiae* or *S. bayanus* was purified from *E. coli* (Methods sections 2.4.7) and was incubated at either 4° or 37°C until aggregated to produce prion "seeds" (Section 2.4.8). The aggregated protein was sonicated and transfected into the *S. cerevisiae* yeast strain GT17 (Methods section 2.2.4). The phenotype and transfection efficiencies of each were analyzed. Figure 65 shows images of representative phenotypes. Interestingly, Sup35NM$_{Sc}$(His)$_6$ aggregated at 4°C showed an exclusively strong phenotype, whereas, aggregation under the same conditions at 37°C yielded a weak phenotype. However, Sup35NM$_{Sb}$(His)$_6$ produced a weak phenotype when aggregated at both 4°C and 37°**C** (See Table 26). Overall, we concluded that transfection of *in-vitro* generated amyloid into yeast produces different prion strains depending on the initial amyloid formation.

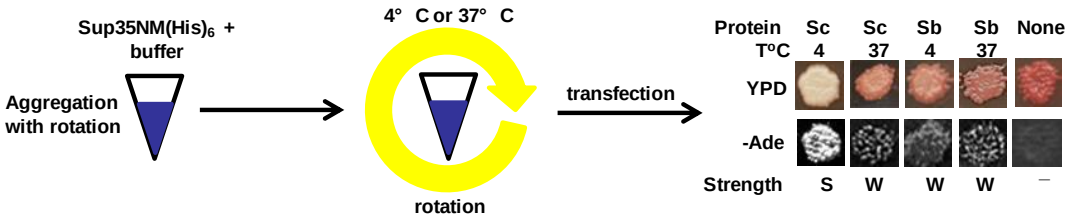

Figure 65 Patterns of Sup35NM amyloids obtained *in vitro*. Sup35NM(His)$_6$ from either *S. cerevisiae* (Sc) or *S. bayanus* (Sb) was aggregated at 4°C or 37°C with rotation. Transfection of the aggregates into yeast produces different prion strains depending on the initial amyloid.

Table 26 Phenotypes of yeast transfected with Sup35NM(His)$_6$ seeds.

Sup35 source	Incubation T°	# [*PSI*$^+$], %	Total #	Phenotype
Sc	4°	13 (12%)	106	All strong
	37°	4 (4%)	108	All weak
Sb	4°	12 (13%)	94	All weak
	37°	12 (11%)	107	All weak

"Sc" and "Sb" refer to *S. cerevisiae* and *S. bayanus*, respectively. Sup35NM(His)$_6$ protein was aggregated *in vitro* at the indicated incubation temperature with rotation (See Figure 65). Transfection of seeds into the *S. cerevisiae* yeast strain GT17 produced different prion variant phenotypes, dependent upon the protein sequence and the aggregation kinetics for different conditions.

8.3.2 The effects of rotation conditions on aggregate seeding *in vitro*

Four different Sup35NM$_{Sc}$(His)$_6$ and Sup35NM$_{Sb}$(His)$_6$ "seeds" (described in Section 8.3.1) were used to attempt to seed aggregation of Sup35NM$_{Sc}$(His)$_6$ protein. Samples were aggregated with rotation *in vitro* at either 4°C or 37°C until polymerized. A control (without seed) was also aggregated until polymerized. Each sample was then transfected into *S. cerevisiae* strains GT17 and GT671, and the transfection efficiency and phenotype for each combination were recorded.

Virtually all seeding reactions performed at 4°C produced a strong [*PSI*$^+$] phenotype, regardless of the origin or variant of the seeds (see Table 27 and Table 28). All [*PSI*$^+$] obtained from the 4°C aggregation control (without seed) also produced a strong phenotype. However, aggregation at 37°C rarely produced transfectants. Only two colonies were obtained from all 37°C aggregation reactions with *S. cerevisiae* seed, and these exhibited a strong phenotype like the strong seed used. (Table 27). One colony was obtained from the 37°C aggregation using *S. bayanus* seed and was weak like the phenotype of the *S. bayanus* seed (Table 28).

Table 27 Phenotypes of yeast transfected with *S. cerevisiae* seeded Sup35NM$_{Sc}$(His)$_6$ aggregates.

Incubation T°	Seed used	# [*PSI*$^+$], %	Total #	Phenotype
4°	none	10 (11%)	91	All strong
	Sc 4°	8 (15%)	54	All strong
	Sc 37°	3 (3%)	108	All strong
37°	none	0 (%)	106	NA
	Sc 4°	2 (2%)	108	All strong
	Sc 37°	0 (0%)	107	NA

"Sc" refers to *S. cerevisiae* protein. Sup35NM$_{Sc}$(His)$_6$ seeds (described in Table 26) were used to attempt to seed the aggregation of monomeric Sup35NM$_{Sc}$(His)6 protein *in vitro* at different temperatures using rotation. The aggregates were transfected into the *S. cerevisiae* yeast strain GT17 and produced the indicated variant phenotypes.

Table 28 Phenotypes of yeast transfected with *S. bayanus* seeded Sup35NM$_{Sc}$(His)$_6$ aggregates.

Incubation T°	Seed used	# [*PSI*$^+$], %	Total #	Phenotype
4°	none	10 (11%)	91	All strong
	Sb 4°	43 (40%)	108	42 strong, 1 weak
	Sb 37°	23 (22%)	106	All strong
37°	none	0 (0%)	106	NA
	Sb 4°	0 (0%)	101	NA
	Sb 37°	1 (1%)	106	All weak

"Sc" refers to *S. cerevisiae* protein. Sup35NM$_{Sb}$(His)$_6$ seeds (described in Table 26) were used to attempt to seed the aggregation of monomeric Sup35NM$_{Sc}$(His)6 protein *in vitro* at different temperatures using rotation. The aggregates were transfected into the *S. cerevisiae* yeast strain GT17 and produced the indicated variant phenotypes. Heterologous seeding (if present) was not apparent due to the competition of homologous *de novo* aggregation reaction by Sup35ScNM(His)6.

Overall, our results suggest that a strong prion is favored for aggregation conditions at 4°C and a weak prion is favored for aggregation conditions at 37°C (See Table 26, Figure 65). When seeded aggregation is performed with rotation, a competition exists between seeded aggregation and *de novo* aggregation of the monomer. Reaction conditions (such as temperature) may favor one aggregation type over the other, thus, influencing the dominant variant produced. Therefore at 4°C in the presence of weak

homologous seed, the strong *de novo*-formed prion proliferates faster and outcompetes a slow growing prion seeded by the weak seed. Conversely, in conditions favoring *de novo* formation of a weak prion (37°C), *de novo* produced prions are weak. Therefore a stronger prion produced from the homologous strong seed overtakes.

Heterologous seeding is predicted to be less efficient than homologous seeding due to impaired interactions between the divergent proteins, but provides similar competition between *de novo* homologous aggregation and heterologous seeded aggregation. This hypothesis is supported by $Sup35_{Sc}(His)_6$ seeded by *S. bayanus* seed. Transfected *S. bayanus* seed alone produces a weak variant, but when used to seed aggregation, virtually all strong colonies were obtained (with the exception of one weak colony out of 214 observed). Alternatively, *S. bayanus* seed may rather serve a [PIN^+]-like role, to sequester $Sup35_{Sc}(His)_6$, facilitating that proteins' interactions to more efficiently form homologous *de novo* $Sup35_{Sc}(His)_6$ [PSI^+].

8.3.3 Quiescent aggregation conditions

As noted, rotation conditions for *in vitro* aggregation facilitated high rates of unseeded aggregation and thwarted attempts to compare the effect of the type of seed used on the phenotype and species barrier. Thus we sought conditions that would enrich for seeded but eliminate unseeded aggregation. A quiescent protocol (see Methods in Chapter 2), lacking the rotation element, was found to produce the desired conditions and was used for the following experiments (Fig. 66, Fig. 67, Fig 68).

8.3.4 Seeding to generate in vitro aggregates produces a species barrier

Species barrier presented by heterologous proteins

Seeded aggregation, but not *de novo* aggregation, was successfully detected for quiescent aggregation reactions performed to measure the kinetics of cross-species seeding effects. As seen from Figure 66, the unseeded monomeric control failed to aggregate, while seeded reactions did generate polymerized protein. In addition, a species barrier was observed for quiescent conditions when $Sup35NM_{Sc}(His)_6$ and $Sup35NM_{Sb}(His)_6$ were incubated with seed prepared at 37°C (see Fig. 66). Overall, it was observed that homologous seeding (*S. cerevisiae* by *S. cerevisiae* and *S. bayanus* by *S. bayanus*) was more efficient than heterologous seeding (*S. cerevisiae* by *S. bayanus*). Other results revealed that $Sup35NM_{Sp}(His)_6$ seeds also seeded the *S. cerevisiae* monomer less efficiently overall (Fig 67). Furthermore, our results were reproduced in a different species when $Sup35NM_{Sb}(His)_6$ seeded by amyloid from either *S. cerevisiae*, *S. paradoxus*, or *S. bayanus* showed a significantly higher efficiency of homologous seeding (*S. bayanus* by *S. bayanus*) than for seeding by *S. cerevisiae* or *S. paradoxus* (Fig. 68). Thus aggregation kinetics were used to detect a species barrier for heterologous seeding *in vitro*.

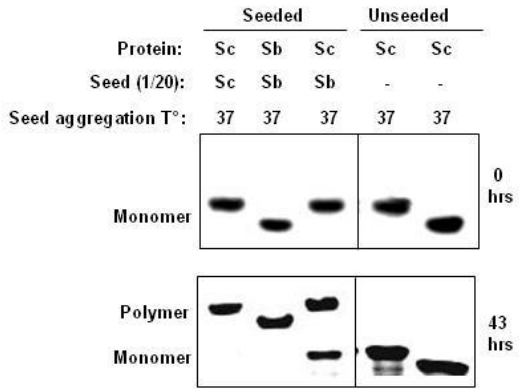

Figure 66. A Species barrier observed under quiescent aggregation conditions *in vitro*. After 43 hrs without rotation at 37°, Sup35NM is polymerized only with pre-existing seed. Homologous seeding (Sc by Sc and Sb by Sb) is more efficient than heterologous seeding (Sc by Sb).

Effects of seed aggregation temperature on aggregation kinetics

Interestingly, differences in aggregation kinetics were detected for seeds prepared using the same Sup35NM$_{Sc}$(His)$_6$ protein but under different conditions. Seed prepared at 4°C, for example, seeded homologous aggregation to completion However, seed prepared at 37°C was less efficient under the same conditions, leaving a majority of the protein detected in the soluble fraction (Fig. 67). Sup35NM$_{Sp}$(His)$_6$ seed prepared at 25°C also seeded aggregation of Sup35NM$_{Sp}$(His)$_6$ slightly more efficiently than seeds prepared at 4°C (Fig. 67 and Fig. 68).

The effect of seed temperature on aggregation efficiency appears to agree with results obtained from transfection of different seeds into yeast (section 8.3.1). Upon transfection, Sup35NM$_{Sc}$(His)$_6$ seeds produced at 4°C exhibited a strong [*PSI*$^+$] phenotype that is correlated with shorter prion core length and mostly polymerized protein. Weaker transfection phenotypes were observed for Sup35NM$_{Sc}$(His)$_6$ seed produced at 37°C and for Sup35NM$_{Sb}$(His)$_6$ seed produced at both 4°C and 37°C. This weak phenotype is associated with a longer prion core and protein in both polymerized

and monomeric fractions. Such was observed for aggregation using $Sup35NM_{Sc}(His)_6$ seed produced at 37°C and for $Sup35NM_{Sb}(His)_6$ seeds aggregated at both temperatures. Lastly, in addition to aggregation kinetics, transfection of aggregates generated in these studies into yeast provides additional verification of the strengths of variants produced and are ongoing experiments.

Results presented in Figures 67 and 68 were obtained by K. Jang and K. Bruce.

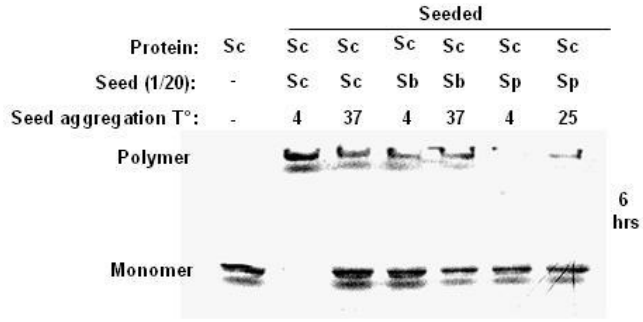

Figure 67. Seed aggregation conditions affect the species barrier for $Sup35_{Sc}NM(His)_6$ aggregation. After 6 hrs at 4°C without rotation, $Sup35NM_{Sc}$ is polymerized only with pre-existing seed. Aggregation efficiency depended on the temperature used to aggregate seeds. (faster aggregation for Sc seed prepared at 4°C rather than 37°C, but faster aggregation for Sp seed prepared at 25°C rather than 4°C. Results were obtained by K. Jang and K. Bruce.

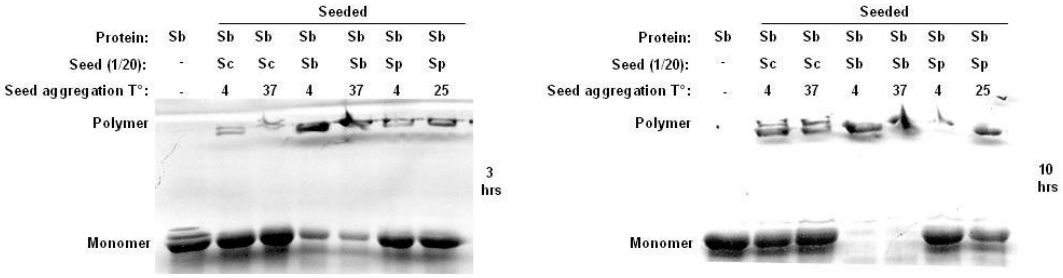

Figure 68. Seed aggregation conditions affect the species barrier for $Sup35_{Sc}NM(His)_6$ aggregation. After 3 or 10 hrs without rotation at 4°C , $Sup35NM_{Sb}$ is polymerized only with pre-existing seed. Homologous seeding (Sb by Sb) is more efficient than heterologous seeding (Sb by Sc or Sp). Aggregation efficiency depended on the temperature used to

aggregate seeds (faster aggregation for Sp seed prepared at 25°C than at 4°C). Results were obtained by K. Jang and K. Bruce.

Use of purified Sup35 aggregates from *S. cerevisiae* to seed *in vitro* $Sup35NM_{Sc}$ aggregation

Previously described rotation and quiescent seeding experiments were performed using protein purified from *E. coli* and with seed completely generated *in vitro*. Such reactions provide valuable insight into the role of protein sequence and aggregations conditions on amyloid nucleation, amyloid growth and seeding mechanisms, in general. However, the lack of cellular factors normally present within a cell environment may generate conditions and aggregates that differ from those formed *in vivo.* To remedy this, a *LEU2* plasmid producing $Sup35NM_{Sc}(His)_6$ was transformed into a strong [PSI^+] *sup35Δ* strain producing full length Sup35 from a *URA3* plasmid. $Sup35NM_{Sc}(His)_6$ aggregates were purified using Ni-NTA His-bind® resin and eluted in phosphate buffer with imidazole. Different amounts of aggregated $Sup3_{Sc}NM(His)^6$ (or no seed for the control) was added to seed aggregation, and aliquots were periodically removed and ran on a boiled gel assay to measure the seeding effects (Fig. 69). Overall, the in vivo aggregated protein did seed aggregation of the $Sup35NM_{Sc}(His)_6$ monomer, and the seeding effect was dose dependent. This experiment was twice performed by K. Jang. Currently, experiments are underway to compare seeding from protein purified from different variants should reveal whether the extracted variant phenotype is retained in the *in vitro* system. The phenotypes will be checked by transfecting seeded aggregates from the experiment into yeast.

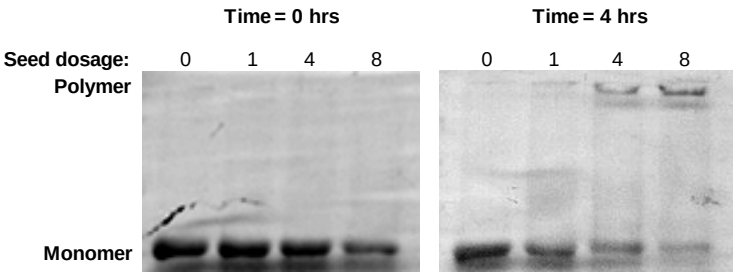

Figure 69 Seeing of Sup35NMSc by purified strong [*PSI*$^+$] Sup35NM$_{Sc}$(His)$_6$ aggregates: Sup35NM$_{Sc}$(His)$_6$ was purified from a stong [*PSI*$^+$] *S. cerevisiae* strain using nickel-NTA resin. Varying doses of the purified yeast aggregate (or a negative control without seed) were use to seed the aggregation of *E. coli* purified Sup35$_{Sc}$NM(His)$_6$ monomer. The aggregation was performed at 4°C under quiescent conditions (described in Chapter 2), and samples were taken at different times and run on a boiled gel to assess the progress of aggregation (see Methods section 2.4.4, Fig 14). (results by K. Jang)

8.3.5 Gammabody analysis

Typically, amyloid aggregation is thought to involve initial recognition interactions between an existing aggregate and key residues or "stretches" of a homologous monomer. Following successful recognition, the monomer uses the aggregate as a structural template, adopts its folding pattern, and is incorporated as a part of the aggregate. It was further hypothesized that the key recognition sequences are prion variant-specific, thus, identifying these stretches would be extremely useful for prion variant typing and for uncovering mechanisms of protein misfolding and propagation. We, therefore, attempted to use grafted amyloid-motif antibodies ("gammabodies") for studies of [*PSI*$^+$] recognition sequences. (See Fig. 70). Gammabodies are actually antibodies, having desired short regions of a target protein sequence grafted in [98]. If particular grafted sequences include the recognition element(s) required for a monomer to interact with a particular variant, this gammabody is also predicted to become incorporated into the aggregate, thus "detecting" the aggregate. It was previously shown, for example, that gammabodies having various grafts from the Aß peptide exhibited

different sensitivities of detection to Aß soluble oligomers vs. fibrils [98, 99]. Conversely, grafted sequences that are outside of key recognition elements would not facilitate interactions with the aggregate, so these gammabodies would not bind to or "detect" the aggregate. Monomers are not detected by gammabodies, for example, as there is no aggregate for a monomer to become incorporated into.

To date, we have shown that the gammabody grafted with the 7-26 or 12-21 fragment of Sup35N recognize aggregated, but not the monomeric form of $Sup35NM_{Sc}(His)_6$ *in vitro* (Fig 70, Fig 71,). We have also shown that these gammabodies exhibit a higher sensitivity to the "stronger" variant generated at 4^oC than a variant generated at $37\ ^oC$ (or sometimes 25^oC) in the same protein (Fig 71). Interestingly, an initial gammabody experiment also showed binding to proteins extracted from both *S. cerevisiae* strong and weak [PSI^+] variants, but no detection of extract from the same [psi^-] strain (**Interference in *S. paradoxus* [PSI^+] propagation.**
Binding of $Sup35NM_{Sp}(His)_6$ and $Sup35NM_{Sc}(His)_6$ aggregates but not to their monomers was also observed for this experiment.

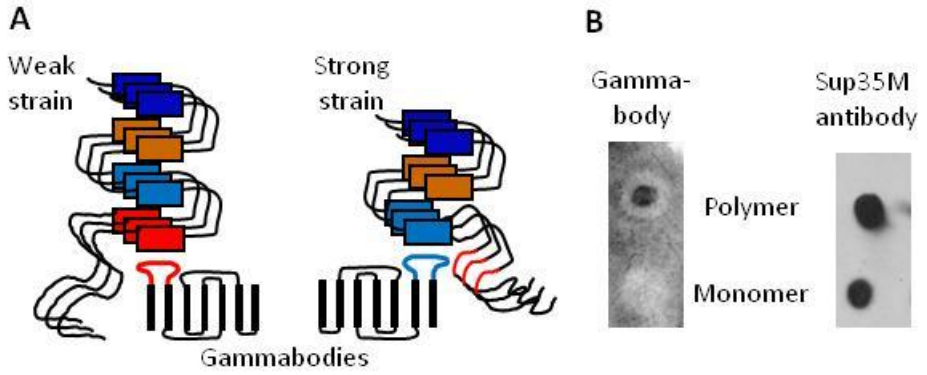

Figure 70. Gammabodies and Detection of $Sup35NM(His)_6$. A – expected recognition of different exposed β-strands in different prion strains by gammabodies with different grafts. **B –** 7-26 gammabody recognizes the amyloid polymer but not monomer. Sup35M antibody is used as a control.

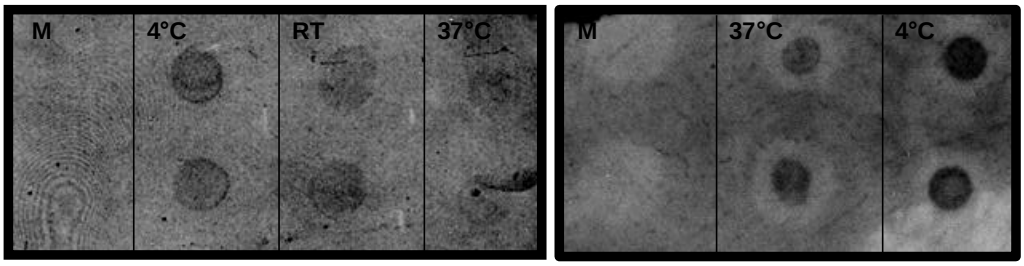

Figure 71 Gammabody 12-21 detection of *in vitro* aggregated Sup35NM$_{Sc}$(His)$_6$ protein. Sup35NM$_{Sc}$(His)$_6$ aggregated at either 4°C, room temperature (RT), or 37°was spotted on a nitrocellulose membrane and detected with a gammabody incorporating the 12-21 fragment of Sup35Sc. A monomer (M) was also spotted. The gammabody used incorporated Sup35 residues 12-21.

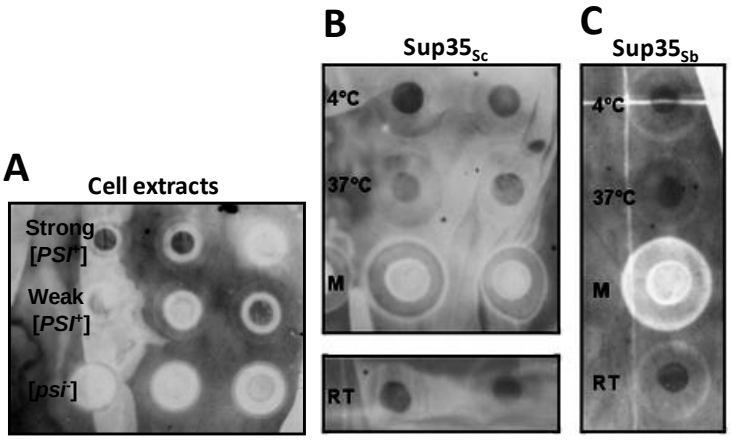

Figure 72 Gammabody detection of *S. cerevisiae* cell extracts and *in vitro* aggregated Sup35NM(His)$_6$ protein. "Sc" and "Sb" refer to *S. cerevisiae* and *bayanus*, respectively. **A —***S. cerevisiae* yeast total lysate isolated from a strong or weak [*PSI*$^+$] strain and a [*psi*$^-$] strain **B —** Sup35NM$_{Sc}$(His)$_6$ aggregated at 4°C, room temperature, 37°C, and monomeric protein (control). **C—**Sup35NM$_{Sb}$(His)$_6$ aggregated at 4°C, 37°C, room temperature, and monomeric protein (control).

8.4 CHAPTER 8 CONCLUSIONS:

- Transfection of *in-vitro* generated amyloid into yeast produces different prion strains depending on the conditions of amyloid formation, thus confirming results by the Weissman lab
- For aggregation performed with rotation, a competition exists between seeded aggregation and *de novo* aggregation of the monomer. The reaction conditions may favor one aggregation type over the other, influencing the dominant variant produced.

- A quiescent protocol can be used to separate a seeded from an unseeded aggregation reaction.
- A species barrier was observed for *in vitro* quiescent conditions as homologous seeding was more efficient than heterologous seeding
- The temperature of the seed aggregation dictates the type of strain formed, thus a barrier *in vitro*, depends on the strain (like a barrier *in vivo*).
- 7-26 gammabody and 12-21 recognize the amyloid polymer but not monomer.

CHAPTER 9: OVERALL CONCLUSIONS AND FUTURE PERSPECTIVES

9.1 OVERALL CONCLUSIONS:

- It is possible to transfect and propagate [*PSI*$^{+}$] into *S. bayanus* and *S. paradoxus*
- The specificity of prion transmission is determined by the protein itself rather than the cell environment
- Variant-specific prion patterns can be altered irreversibly during cross-species transmission through *S. bayanus* Module II
- A divergent protein can "interfere" with [*PSI*$^{+}$] propagation and is dependent on the cell environment
- The identity of specific regions, rather than the overall level of PrD homology is crucial for determining cross-species transmission and interference
- Prion interference does not correlate with a prion transmission barrier

9.2 FUTURE PERSPECTIVES

The results presented in this work highlight the contributions of both protein sequence and cell environment to the efficiency of cross-species prion transmission and interference in *Saccharomyces* species. The effects of sequence divergence were tested by exchanging different modules of the Sup35 PrD, and our focus was narrowed further to show the significance of individual amino acid residues. To date, the individual contributions of additional residues differing between these species remain untested and may shed light on protein interactions crucial for conversion of monomers into the prion fold. Knowledge of these interactions may further aid in predicting the specific mechanisms of protein misfolding. In addition, our tests of divergent Sup35 versions that

interfere with [*PSI*$^{+}$] propagation were performed only in the context of full length Sup35 proteins. Future work to identify the minimal residues necessary for Sup35 prion interference may provide insight into engineering interfering peptides to prevent or slow progression of similar amyloid and prion diseases in mammals.

Our work performing cross-species transmission and interference experiments *in vitro* using purified Sup35 proteins provides further insight into the role of protein sequence in these processes and is independent of contributing factors of the yeast cell environment. Effects generated by manipulation of temperature and other aggregation conditions are also explored. Additional *in vitro* seeding experiments are useful to assess whether variant-specific properties are maintained *in vitro*, in the absence of these cellular factors. These experiments would be performed by seeding *in vitro* purified Sup35 with purified Sup35 in the [*PSI*$^{+}$] state isolated from yeast. The protein aggregated *in vitro* (absent of the presence of cellular factors) will then be transfected into yeast using methods described in Chapter 4, and the stringency of the prion variant will be compared to the original variant generated *in vivo*.

Furthermore, we have shown that cross-species transfer of a *S. cerevisiae* prion through chimeric proteins containing module II from *S. bayanus* and back to *S. cerevisiae* permanently weakened the stringency of the prion strain. Potentially, therapies targeting strain conversion may be useful in slowing, delaying, or preventing amyloid or prion disease in mammals by permanently converting the conformation of a protein fold to a desired variant that is consistent with longer incubation periods, slower progression of disease or is associated with different areas of the brain.

APPENDIX:

Table 1: Yeast **s**trains used in this work.

Strain	Genotype/description
GT17	*S. cerevisiae* 74-D694-a ade1-14 his3-Δ200 leu2-3, 112 trp1-289 ura3-52 [*psi*$^-$] [*pin*$^-$]
GT81-1C	*S. cerevisiae MATa ade1-14$_{SC}$ his3-Δ200 lys2 leu2-3,112 trp1-Δ ura3-52* [*PSI*$^+$][*PIN*$^+$]
GT255-2A	*S. cerevisiae MATα ade1-14 $_{SC}$ his3Δ (or 11,15) lys2 leu2-3,112 trp1 ura3-52 sup35::HIS3* [*psi*$^-$][*PIN*$^+$] [*CEN LEU2 SUP35$_{SC}$*]
GT256-23C	*S. cerevisiae MATα ade1-1$_{SC}$ 4 his3Δ (or 11,15) lys2 leu2-3,112 trp1 ura3-52 sup35::HIS3* [*PSI*$^+$][*CEN LEU2 SUP35$_{SC}$*]
GT671	*S. cerevisiae MATα ade1-14 his3Δ (or 11,15) lys2 ura3-52 leu2-3,112 trp1 sup35::HIS3* [*CEN LEU2 SUP35*] [*psi-*][*pin*$^-$]
GT749-1B	*S. paradoxus MATα/MATa lys2/lys2 ura3-P2/ura3-P2*
GT983	*S. paradoxus MATα/MATa lys2/lys2 ura3-P2/ura3-P2 HO/ho::KANMX6*
GT983-2A	*S. paradoxus MATa lys2 ura3-P2 ho::KANMX6*
GT986	*S. bayanus MATa ade1::URA3$_{SC}$ ura3-1, ho::KANMX4*
GT988-1A	*S. cerevisiae MATα ade1-14$_{SC}$ his3Δ (or 11,15) lys2 leu2-3,112 trp1 ura3-52 sup35::HIS3* weak [*PSI*$^+$][*CEN LEU2 SUP35$_{SC}$*]
GT991	*S. bayanus MATa ade1::ADE1$_{SC}$ ura3-1, ho::KANMX4*
GT992	*S. paradoxus MATa ade1::URA3$_{SC}$ lys2 ura3-P2 ho::KANMX6*
GT1020	*S. bayanus MATα, ura3-1 lys2 ho::KANMX4*
GT1028	*S. bayanus MATa ade1::ade1-14$_{SC}$ ura3-1 ho::KANMX4*
GT1037	*S. paradoxus MATa ade1::ura3$_{SC}$ lys2 ura3-P2 ho::KANMX6*
GT1041	*S. bayanus MATα/MATa ADE1/ade1::ade1-14$_{SC}$ LYS2/lys2 ura3-1/ura3-1 ho::KANMX4/ ho::KANMX4*
GT1041-7A	*S. bayanus MATa ade1::ade1-14$_{SC}$ lys2 ura3-1 ho::KANMX4*
GT1085	*S. cerevisiae MATa ade1-14$_{SC}$ his3Δ leu2-3,112 trp1-289 ura3 kar1 cyh^R sup35::HIS3* [*rho*$^-$] [*psi*$^-$] [*PIN*$^+$] [*CEN URA3 SUP35N$_{SC}$MC$_{SC}$*]
GT1088	*S. cerevisiae MATa ade1-14$_{SC}$ his3Δ leu2-3,112 trp1-289 ura3 kar1 cyh^R sup35::HIS3* [*rho*$^-$] [*psi*$^-$] [*PIN*$^+$] [*CEN URA3 SUP35(NI)$_{SC}$(NII,III)$_{SP}$(MC)$_{SC}$*]
GT1089	*S. cerevisiae MATa ade1-14$_{SC}$ his3Δ leu2-3,112 trp1-289 ura3 kar1 cyh^R sup35::HIS3* [*rho*$^-$] [*psi*$^-$] [*PIN*$^+$] [*CEN URA3 SUP35(NI)$_{SP}$(NII,III)$_{SB}$(MC)$_{SC}$*]
GT1090	*S. cerevisiae MATa ade1-14$_{SC}$ his3Δ leu2-3,112 trp1-289 ura3 kar1 cyh^R sup35::HIS3* [*rho*$^-$] [*psi*$^-$] [*PIN*$^+$] [*CEN URA3 SUP35(NI)$_{SB}$(NII,III,MC)$_{SC}$*]
GT1091	*S. cerevisiae MATa ade1-14$_{SC}$ his3Δ leu2-3,112 trp1-289 ura3 kar1 cyh^R sup35::HIS3* [*rho*$^-$] [*psi*$^-$] [*PIN*$^+$] [*CEN URA3 SUP35(NI)$_{SB}$(NII,III)$_{SP}$(MC)$_{SC}$*]
GT1092	*S. cerevisiae MATa ade1-14$_{SC}$ his3Δ leu2-3,112 trp1-289 ura3 kar1 cyh^R sup35::HIS3* [*rho*$^-$] [*psi*$^-$] [*PIN*$^+$] [*CEN URA3 SUP35(NI)$_{SP}$(NII,III,MC)$_{SC}$*]
GT1093	*S. cerevisiae MATa ade1-14$_{SC}$ his3Δ leu2-3,112 trp1-289 ura3 kar1 cyh^R sup35::HIS3* [*rho*$^-$] [*psi*$^-$] [*PIN*$^+$] [*CEN URA3 SUP35(NI)$_{SC}$(NII-III)$_{SB}$(MC)$_{SC}$*]
GT1216-2C	*S. paradoxus MATα ura3-P2 lys2 Δho::KanMX6 Δsup35::ClonNAT* [*LYS2 SUP35$_{Sc}$*]
GT1116	*S. paradoxus MATa ade1::ADE1$_{SC}$ lys2 ura3-P2 ho::KANMX6*
GT1122	*S. bayanus MATα/MATa ADE1/ade1::ade1-14$_{SC}$ LYS2/lys2 ura3-1/ura3-1 ho::KANMX4/ ho::KANMX4 SUP35/sup35ΔnatNT2*
GT1122-4B	*S. bayanus MATα ade1::ade1-14$_{SC}$ lys2 ura3-1 ho::KANMX4 sup35ΔnatNT2* [*hphNT1 SUP35$_{SP}$*]
GT1131	*S. bayanus MATα ade1::ade1-14$_{SC}$ lys2 ura3-1 ho::KANMX4 sup35ΔnatNT2* [*LYS2 SUP35$_{SP}$*]
GT1132	*S. bayanus MATα ade1::ade1-14$_{SC}$ lys2 ura3-1 ho::KANMX4 sup35ΔnatNT2* [*LYS2 SUP35$_{SB}$*]
GT1133	*S. bayanus MATα ade1::ade1-14$_{SC}$ lys2 ura3-1 ho::KANMX4 sup35ΔnatNT2* [*LYS2 SUP35$_{SC}$*]
GT1144	*S. bayanus MATα ade1::ade1-14$_{SC}$ lys2 ura3-1 ho::KANMX4 sup35ΔnatNT2* [*hphNT1 SUP35$_{SC}$*]
GT1188	*S. paradoxus MATa ade1::ade1-14$_{SC}$ lys2 ura3-P2 ho::KANMX6*
GT1320-5B	*S. paradoxus MATα ade1SP::ade1-14$_{SC}$ (UGA) lys2 ura3-52 Δsup35::ClonNAT* [*PSI$_+$*] *[SUP35]*

GT1320-36A	*S. paradoxus MATa ade1SP::ade1-14$_{SC}$ (UGA) lys2 ura3-52 Δsup35::ClonNAT* [*PSI$_{+}$*] *[SUP35]*
OT23 (SP7-1D)	*S. paradoxus*
OT227 (FM361)	*S. bayanus*
OT294 (Su1A)	*S. bayanus MATa, ura3-1, ho::KANMX4*
OT295 (Su1B)	*S. bayanus MATα, ura3-1, ho::KANMX4*

Table 2: Plasmids used in this work.

***SUP35* Plasmids used in this study**

			Origin of *SUP35* domains				
			SUP35 N			*SUP35 M*	*SUP35 C*
Plasmid name	Yeast marker	Promoter	Module I	Module II	Module III		
pBC105	*URA3*	P_{SUP35}	*Sc*	*Sp*	*Sp*	*Sc*	*Sc*
pBC107	*URA3*	P_{SUP35}	*Sb*	*Sc*	*Sc*	*Sc*	*Sc*
pBC109	*URA3*	P_{SUP35}	*S*	*Sc*	*Sc*	*Sc*	*Sc*
pBC110	*URA3*	P_{SUP35}	*Sc*	*Sb*	*Sb*	*Sc*	*Sc*
pBC111	*URA3*	P_{SUP35}	*Sc*	*Sb+1*	*Sb*	*Sc*	*Sc*
pKB102	*URA3*	P_{SUP35}	*Sc*	*Sb+1*	*Sc*	*Sc*	*Sc*
pBC112	*URA3*	P_{SUP35}	*Sc*	*Sc*	*Sb*	*Sc*	*Sc*
pBC113	*URA3*	P_{SUP35}	*Sp(S12N)*	*Sc*	*Sc*	*Sc*	*Sc*
pBC114	*URA3*	P_{SUP35}	*Sc(N12S)*	*Sc*	*Sc*	*Sc*	*Sc*
pBC106	*URA3*	P_{SUP35}	*Sp*	*Sb*	*Sb*	*Sc*	*Sc*
pBC108	*URA3*	P_{SUP35}	*Sb*	*Sp*	*Sp*	*Sc*	*Sc*
pBC103[1]	*URA3*	P_{SUP35}	*Sp*	*Sp*	*Sp*	*Sc*	*Sc*
pBC104[2]	*URA3*	P_{SUP35}	*Sb*	*Sb*	*Sb*	*Sc*	*Sc*
pBC102[3]	*URA3*	P_{SUP35}	*Sc*	*Sc*	*Sc*	*Sc*	*Sc*
pGN100	*URA3*	P_{SUP35}	*Sc*	*Sb(P50Y)*	*Sb*	*Sc*	*Sc*
pGN102	*URA3*	P_{SUP35}	*Sc*	*Sc(Y49P)*	*Sc*	*Sc*	*Sc*
pGN103	*URA3*	P_{SUP35}	*Sb*	*Sb(P50Y)*	*Sb*	*Sc*	*Sc*
pKB103	*URA3*	P_{SUP35}	*Sb*	*Sc*	*Sb*	*Sc*	*Sc*
pKB100	*URA3*	P_{SUP35}	*Sc*	*Sb*	*Sc*	*Sc*	*Sc*
pKB101	*URA3*	P_{SUP35}	*Sp(S12N)*	*Sp*	*Sp*	*Sc*	*Sc*
pBC100[4]	*URA3*	P_{SUP35}	*Sp*	*Sp*	*Sp*	*Sp*	*Sp*
pBC101[5]	*URA3*	P_{SUP35}	*Sb*	*Sb*	*Sb*	*Sb*	*Sb*
pASB2	*LEU2*	P_{SUP35}	*Sc*	*Sc*	*Sc*	*Sc*	*Sc*
pET20b-SUP35NM		*T7*	*Sc*	*Sc*	*Sc*	*Sc*	---
pET20b-SUP35NMSpar		*T7*	*Sp*	*Sp*	*Sp*	*Sp*	---
pET20b-SUP35NMSbay		*T7*	*Sb*	*Sb*	*Sb*	*Sb*	--
pmCUP1MCSC		P_{CUP1}	---	---	--	*Sc*	*Sc*
pmCUP-NMSB-HRP6.6	*URA3*	P_{CUP1}	*Sb*	*Sb*	*Sb*	*Sb*	---
pmCUP-NMSC-HRP6.6	*URA3*	P_{CUP1}	*Sc*	*Sc*	*Sc*	*Sc*	---
pmCUP-NMSP-HRP6.6	*URA3*	P_{CUP1}	*Sp*	*Sp*	*Sp*	*Sp*	---
pRS317-PS-SUP35SC	*LYS2*	P_{SUP35}	*Sc*	*Sc*	*Sc*	*Sc*	*Sc*
pRS317-PS-SUP35SP	*LYS2*	P_{SUP35}	*Sp*	*Sp*	*Sp*	*Sp*	*Sp*
pRS317-PS-SUP35SB	*LYS2*	P_{SUP35}	*Sb*	*Sb*	*Sb*	*Sb*	*Sb*

Other plasmids used in this study

Plasmid name	Yeast marker	Promoter	Gene of interest
pRS316-GAL	URA3	PGAL	---
pGBSup3512-21	---	T7	SUP35aa 12-21
pGBSup357-26	---	T7	SUP35aa 7-26
pGBSup357-17	---	T7	SUP35aa 7-17
PFA6a-kanMX6	---	SP6	KANMX6
pBluescript-URA3 I			URA3
pRS303N	natNT2		NatNT2
pRS303H	hphNT1		HYG
pRS317	LYS2		---

[1] Also called p316-PS-SUP35NSP-MCSC
[2] Also called p316-PS-SUP35NSB-MCSC
[3] Also called p316-PS-SUP35NSC-MCSC
[4] Also called p316-PS-SUP35SP
[5] Also called p316-PS-SUP35SB

Table 3: Primers used in this work.

Name	Sequence	Usage
SUP35-PAR-F	5'-TATCGGATCCCTAGCAACAATGTCGGATTCA-3'	Forward primer for module I of *Sc*, contains *Bam*HI site
SP-S12N-R	5' CACGGCCACCTTGTGGATTGA 3'	Reverse primer for module II *Sb* and includes the *Pfl*MI site
SB-Insertion-R	5'-TACCACGGCCACCTTGTGGGTTGAATTGCTGTTGGTAACCGCCTTGAGGATTGTACTGTTGATAGCCGCCTTGAGCGTTGTATTGTTGTTGGTAACCTGCTTCCGGG-3'	Reverse primer for module II *Sb* which adds 1 OR and includes the *Pfl*MI site
SP-S12N-F#2	5'-TATCGGATCCCTAGCAACAATGTCGGATTCAAACCAAGGTAACAATCAGCAAAACTACCAGCAATACGGCCAAAACTCT-3'	Forward primer for module I *Sp* which includes the mutation S12N and *Bam*HI site
NSC-R-BglII-SacI	5'-AGTCGAGCTCAGATCTACCTTGAGACTGTGGTTGGA-3'	Reverse primer for module III *Sc* which includes the *Bgl*II and *Sac*I site
NSC-MCSC(N12S)	5'-AGCAGGATCCCTAGCAACAATGTCGGATTCAAACCAAGGCAACAATCAGCAAAGCTACCAGCAATACAGCCAGAA-3'	Forward primer for module I *Sc* which includes the N12S mutation and *Bam*HI site
NSB(P50Y)-F	5'-TATCAAGCTTACAATGCTCAAGCCCAACAACCTGCAGGTGGCTATTACCAAAACTACCAAGGTTACGCTGGCTACCAACA-3'	Forward primer for module I *Sc* which includes the P50Y mutation and *Hind*III site
Sup35Rev 517	5'-CTTCCTCTTTCTTATCAG-3'	Reverse primer for module III *Sc* and *Sb*
NSC(Y49P)-F	5'-TATCAAGCTTACAATGCTCAAGCCCAACCTGCAGGTGGGTACTACCAAAATCCCCAAGGTTATTCTGGGTACCAACA-3'	Forward primer for module I *Sc* which includes the Y49P mutation and *Hind*III site

Hsp104-HYGF	5’- AAGAAAAAGCAATCAACTACACG TGCAATAAAACATACAGAATATGAAT TCGAGCTCGTTAAAGC-3’	Forward primer to amplify the *HYG* gene. This primer has flanking $Hsp104_{Sp}$ ends
Hsp104-HYGR	5'- TCACGGATTCTTATCCAAAAATTTT CTATACGAATCACACTAAATGCAG GTCGACGGATCCCCGG-3'	Reverse primer to amplify the *HYG* gene. This primer has flanking $Hsp104_{Sp}$ ends

Table 4: The effects of sonication on transfection efficiency of *in vitro* generated aggregates.

Yeast strain	Sc aggregate	[*PSI*$^+$], %	Total number
GT671	Control	1 (1%)	109
	4°, unsonicated	51 (49%)	104
	4°, sonicated	16 (15%)	108
	37°, unsonicated	4 (4%)	102
	37°, sonicated	9 (9%)	103
GT17	Control	0 (0%)	28
	4°, unsonicated	6 (40%)	15
	4°, sonicated	7 (32%)	22
	37°, unsonicated	0 (0%)	24
	37°, sonicated	3 (13%)	24

Sup35NM$(His)_6$ protein originated from *S. cerevisiae* (Sc) was purified from *E. coli* and aggregated at either 4° or 37° C. The protein was transfected into two yeast strains, either with prior sonication (S) or without (NS) sonication. The numbers of transfectants obtained were recorded with percentages of [*PSI*$^+$] shown. Yeast having no protein transfected was also included as a negative control. The yeast strain GT17 carried a chromosomal copy of *SUP35,* while GT671 was chromosomally deleted for *SUP35* but carried a copy on a plasmid.

Table 5: Results of direct transmission for the strong [*PSI*$^+$] strain

Construct shuffled in	Shuffle results		
	# [*PSI*$^+$]	% [*PSI*$^+$], Confidence limits	Total number
Sc-Sc-Sc	196	99% (97.6-100.0)	198
Sp-Sp-Sp	95	93% (88.1-97.9)	102
Sp-Sc-Sc	75	88% (81.1-94.9)	85
Sc-Sp-Sp	52	95% (88.9-100.0)	55
Sb-Sb-Sb	15	12% (6.5-17.5)	130
Sb-Sc-Sc	83	98% (94.7-100.0)	85
Sc-Sb-Sb	3	5% (0.1-9.9)	67
Sc-Sb-Sc	1	3% (0.0-8.9)	33
Sb-Sc-Sb	35	100% (96.7-100.0)	35
Sc-Sc-Sb	77	100% (97.8-100.0)	77
Sc-Sb+1-Sb	4	11% (1.0-21.0)	37
Sc-Sb+1-Sc	15	46% (29.0-63.1)	33
Sb-Sp-Sp	34	90% (80.2-99.8)	38
Sp-Sb-Sb	3	6% (0.0-12.7)	49
Sp(S12N)-Sp-Sp	63	98% (94.9-100.0)	64
Sp(S12N)-Sc-Sc	71	99% (96.3-100.0)	72
Sc(N12S)-Sc-Sc	33	57% (44.3-69.7)	58
Sb-Sb(P50Y)-Sb	13	65% (44.0-86.0)	20
Sc-Sb(P50Y)-Sb	7	30% (11.2-48.8)	23
Sc-Sc(Y49P)-Sc	21	75% (58.9-91.1)	28

Direct shuffle was performed in the strain GT256-23C as shown on Plasmid shuffle scheme Fig 11.

Table 6: Results of cytoduction for the strong [*PSI*$^{+}$] strain.

PrD for [*psi*$^{-}$] recipient strain	Cytoduction Results	
	[*PSI*$^{+}$] (%)	Total numbers
Sc-Sc-Sc	96 (99%)	97
Sp-Sp-Sp	79 (80%)	99
Sp-Sc-Sc	48 (81%)	59
Sc-Sp-Sp	51 (94%)	54
Sb-Sb-Sb	4 (5%)	83
Sb-Sc-Sc	48 (81%)	59
Sc-Sb-Sb	0	68
Sc-Sb-Sc	2 (6%)	32
Sc-Sb+1-Sb	0	58
Sb-Sp-Sp	51 (59%)	87
Sp-Sb-Sb	8 (9%)	86

Cytoduction was performed in the strain GT256-23C as shown in Cytoduction scheme Fig 12.

Table 7. Results of direct transmission for the weak [*PSI*$^+$] strain.

Construct shuffled in	Shuffle results		
	# [*PSI*$^+$]	% [*PSI*$^+$], Confidence limits	Total number
Sc-Sc-Sc	100	92% (86.9-97.1)	109
Sp-Sp-Sp	16	27% (15.8-38.2)	60
Sp-Sc-Sc	26	39% (27.2-50.8)	67
Sc-Sp-Sp	30	86% (74.4-97.6)	35
Sb-Sb-Sb	24	26% (17.0-35.0)	92
Sb-Sc-Sc	39	83% (72.2-93.8)	47
Sc-Sb-Sb	10	15% (6.2-23.8)	65
Sc-Sb-Sc	1	2% (0-6.9)	64
Sb-Sc-Sb	12	67% (45.2-88.8)	18
Sc-Sc-Sb	22	88% (75.3-100.0)	25
Sc-Sb+1-Sb	24	51% (36.7-65.3)	47
Sc-Sb+1-Sc	21	58% (41.9-74.1)	36
Sb-Sp-Sp	19	100% (95.5-100.0)	19
Sp-Sb-Sb	0	0% (0-3.14)	37
Sp(S12N)-Sp-Sp	26	58% (43.5-72.5)	45
Sp(S12N)-Sc-Sc	52	77% (67.0-87.0)	68
Sc(N12S)-Sc-Sc	76	70% (61.4-78.6)	109
Sb-Sb(P50Y)-Sb	20	48% (32.9-63.1)	42
Sc-Sb(P50Y)-Sb	28	80% (66.7-93.3)	35
Sc-Sc(Y49P)-Sc	35	95% (87.8-100.0)	37

Directshuffle was performed in the strain GT256-23C as shown in Plasmid shuffle scheme Fig 11.

Table 8. Results of cytoduction for the weak [*PSI*$^+$] strain.

PrD for [*psi*$^-$] recipient strain	Cytoduction Results	
	[*PSI*$^+$] (%)	Total Numbers
Sc-Sc-Sc	87 (68%)	128
Sp-Sp-Sp	8 (10%)	81
Sp-Sc-Sc	18 (21%)	87
Sc-Sp-Sp	79 (93%)	85
Sb-Sb-Sb	48 (60%)	80
Sb-Sp-Sp	88 (79%)	111
Sp-Sb-Sb	2 (2%)	92

Cytoduction was performed in the strain GT988-1A as shown in figure Cytoduction scheme Fig 12.

Table 9: Results of reverse shuffle for the strong [*PSI*$^+$] strain.

Construct shuffled out	Reverse shuffle results			
	Number of isolates tested	# [*PSI*$^+$]	% [*PSI*$^+$], Confidence limits	Number tested
Sc-Sc-Sc	5	174	100% (98.4-100.0)	174
Sb-Sc-Sc	2	130	100% (98.2-100.0)	130
Sc-Sc-Sb	3	63	98% (94.9-100.0)	64
Sc-Sb-Sc	1	16	76% (57.8-94.2)	21
Sc-Sb-Sb	3	9	56% (31.7-80.3)	16
Sb-Sb-Sb	4	76	45% (37.6-52.5)	170
Sp-Sp-Sp	4	56	100% (97.5-100.0)	56
Sp-Sc-Sc	4	39	87% (77.0-97.0)	45
Sc-Sp-Sp	4	56	100% (97.5-100.0)	56
Sp(S12N)-Sp-Sp	4	50	96% (90.7-100.0)	52
Sp(S12N)-Sc-Sc	3	42	100% (97.1-100.0)	42
Sc(N12S)-Sc-Sc	4	36	82% (80.8-83.2)	44
Sb-Sb(P50Y)-Sb	2	7	13% (4.18-21.8)	55
Sc-Sb(P50Y)-Sb	2	6	11% (2.96-19.0)	56
Sc-Sc(Y49P)-Sc	2	49	98% (94.1-100.0)	50
Sc-Sb+1-Sb	2	0	0% (0.0-3.14)	40

[*PSI*$^+$] isolates obtained by direct shuffle (Plasmid shuffle scheme Fig 11~~2.3~~) were used in the reverse shuffle to *S. cerevisiae SUP35*. Several independent isolates were analyzed per each construct in most cases, as indicated. Total numbers are shown.

Table 10 Results of the reverse shuffle for the weak [*PSI*$^+$] strain.

Construct shuffled out	Reverse shuffle results			
	Number of isolates tested	# [*PSI*$^+$]	% [*PSI*$^+$], Confidence limits	Number tested
Sc-Sc-Sc	2	30	100% (96.5-100.0)	30
Sb-Sb-Sb	1	8	73% (46.7-99.3)	11
Sc-Sc-Sb	1	11	100% (94.1-100.0)	11
Sp-Sp-Sp	3	31	100% (96.5-100.0)	31
Sp-Sc-Sc	1	30	100% (96.5-100.0)	30
Sp(S12N)-Sp-Sp	3	17	90% (76.3-100.0)	19
Sp(S12N)-Sc-Sc	2	47	98% (93.9-100.0)	48
Sc(N12S)-Sc-Sc	3	29	85% (73.0-97.0)	34

[*PSI*$^+$] isolates obtained by direct shuffle (plasmid shuffle scheme Fig. 2.X) were used in the reverse shuffle to *S. cerevisiae SUP35*. Several independent isolates were analyzed per each construct in most cases, as indicated. Total numbers are shown.

Table 11: Mitotic stability for selected Sup35 prion isolates generated by chimeric Sup35 protein.

S. cerevisiae strain background	PrD (I-II-III)	# of isolates	% [psi$^-$]	# of colonies per isolate
Strong	Sc-Sc-Sc	3	0	50-90
	Sp-Sp-Sp	4	0	33-98
	Sp-Sc-Sc	3	0	32-78
	Sc-Sp-Sp	2	0	50-80
	Sb-Sb-Sb	2	0	44-50
		1	17.9	39
		1	56.7	60
	Sb-Sp-Sp	3	0	35-64
		1	35.0	40
Weak	Sc-Sc-Sc	3	0	89-106
		1	0.6	161
	Sp-Sp-Sp	1	0	75
		2	1.4-1.9	53-69
		1	80.0	50
	Sp-Sc-Sc	1	0	50
	Sb-Sb-Sb	1	0	98
		1	68.8	32
		1	90	50
	Sb-Sp-Sp	2	1.2-3.7	54-81

Independent [*PSI*$^+$] isolates obtained from direct shuffle (see Figures 1E, SIII, and SV) in either a strong or weak [*PSI*$^+$] strain were streaked-out through three passages on YPD. This corresponds to approximately 20-40 cell divisions. The numbers of [*PSI*$^+$] and [*psi*$^-$] colonies were counted as shown here. Mosaic colonies (usually rare in stable [*PSI*$^+$] isolates) were counted as [*PSI*$^+$]. Strain background refers to the stringency of the prion strain in which the experiment was performed, either strong (GT256-23C) or weak (GT988-1A).

Figure 35: Construction of the *SUP35* genes with chimeric SUP35N domains

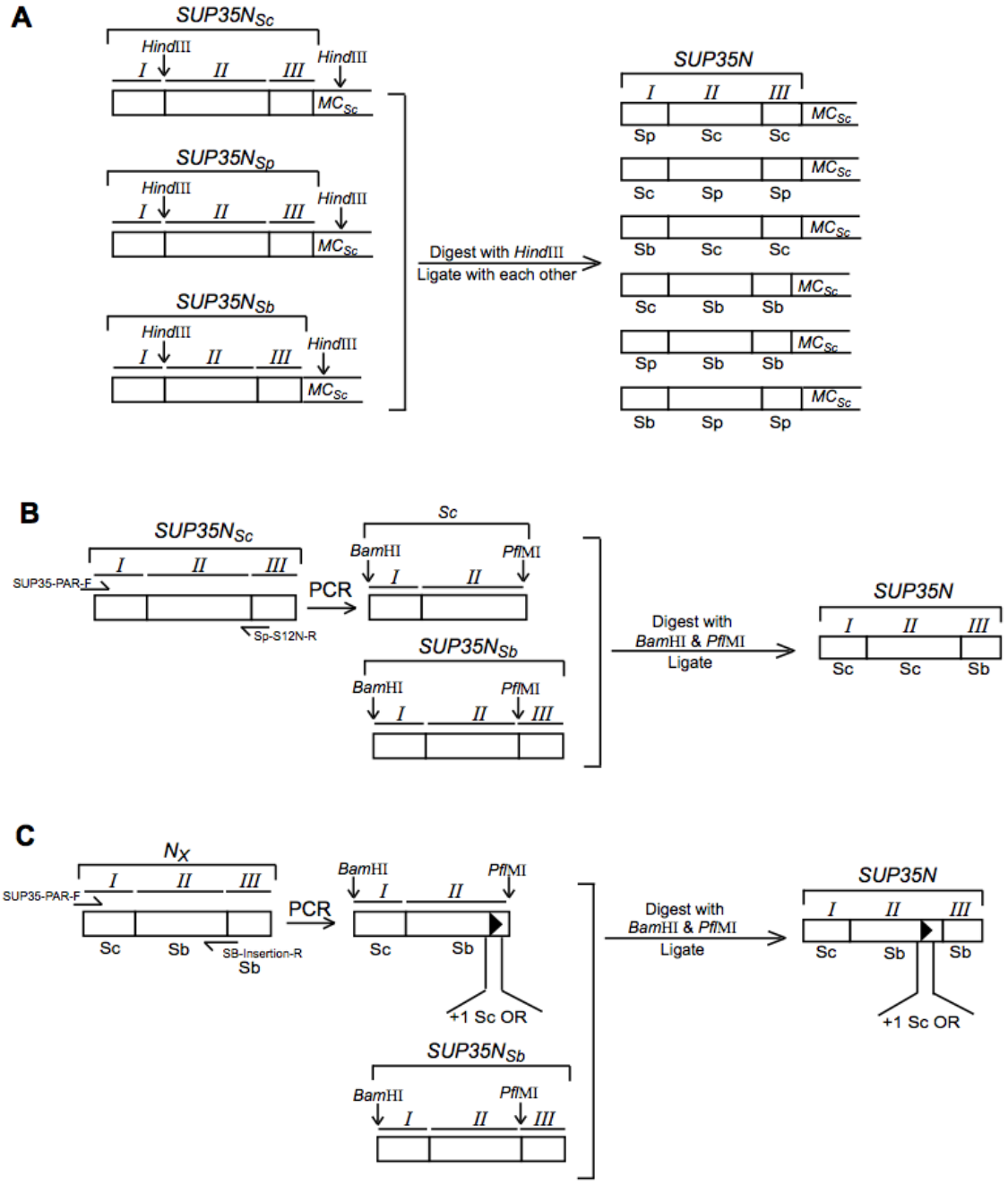

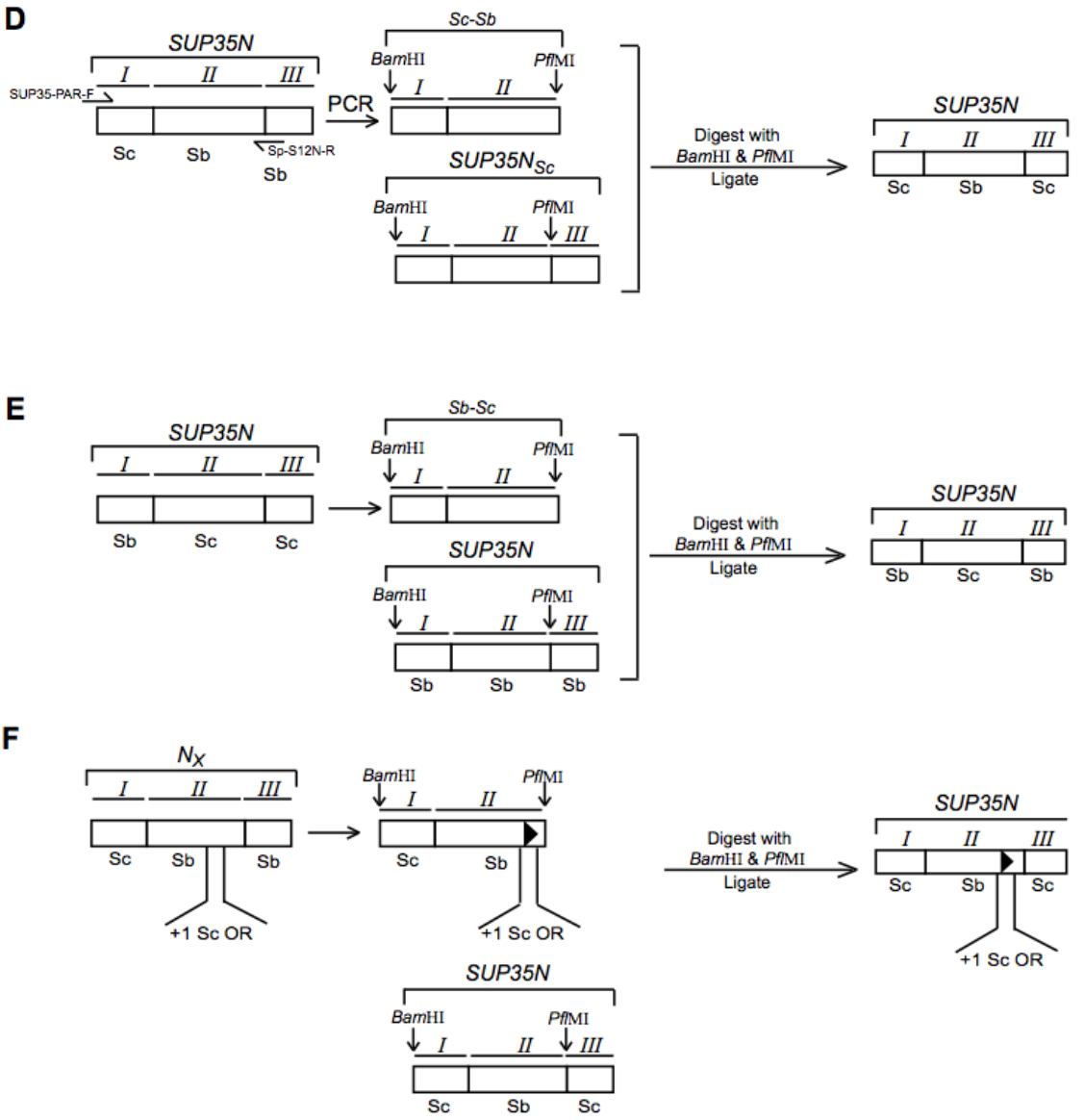

Figure 35: Construction of the *SUP35* genes with chimeric SUP35N domains. Designations "Sc," "Sp" and "Sb" refer to *S. cerevisiae*, *S. paradoxus* and *S. bayanus*, respectively. Designations *N*, *M* and *C* refer to *SUP35N*, *SUP35M* and *SUP35C* domains, respectively. Modules of *SUP35N* domain (Fig 22) are designated by Roman numerals. **A**—Plasmids pBC102, pBC103 and pBC104 (Table 2) were digested with *Hin*dIII, and the 0.3 kb fragments containing modules II and III of different origins in conjunction with the small portion of *S. cerevisiae SUP35M* region were exchanged between plasmids. **B**—To construct the plasmid bearing modules I and II of *S. cerevisiae* in conjunction with module III of *S. bayanus*, the *S. cerevisiae* fragment corresponding to modules I and II has been PCR-amplified with primers SUP35-PAR-F and SP-S12N-R (Table 3), containing *Bam*HI and *Pfl*MI sites, cut with *Bam*HI and *Pfl*MI and inserted into plasmid pBC102 at the same sites with the *Bam*HI site upstream of the *SUP35* ORF and cut with the same enzymes. **C**—In order to generate a plasmid bearing *S. cerevisiae* module I in conjunction with modules II and III of *S. bayanus* with an extra repetitive

unit of *S. cerevisiae* added to the ORs region, the fragment encompassing module I of *S. cerevisiae* and module II of *S. bayanus* was PCR-amplified from the *S. cerevisiae* / *S. bayanus* chimeric construct generated as described above with primers SUP35-PAR-F and SB-Insertion-R (Table 3), respectively, including the region with *Bam*HI site ahead of the ORF, and the region before (and including) *Pfl*MI site with an artificially added sequence corresponding to one *S. cerevisiae* repetitive unit. This fragment was inserted into the plasmid pBC102 cut with *Bam*HI and *Pfl*MI. **D**—In order to generate a plasmid bearing *S. cerevisiae* modules I and III flanking module II of *S. bayanus*, the fragment encompassing module I of *S. cerevisiae* and module II and III of *S. bayanus* was PCR-amplified from the *S. cerevisiae* / *S. bayanus* chimeric construct generated as described above with primers SUP35-PAR-F and SP-S12N-R (Table 3), containing *Bam*HI and *Pfl*MI sites, cut with *Bam*HI and *Pfl*MI and inserted into plasmid pBC102 at the same sites with the *BamHI* site upstream of the *SUP35* ORF and cut with the same enzymes. **E**—In order to generate a plasmid bearing *S. bayanus* modules I and III flanking module II of *S. cerevisiae*, the fragment encompassing module I and II was cut from plasmid PBC107 with *Bam*HI and *Pfl*MI and inserted into plasmid pBC104 at the same sites with the *Bam*HI site upstream of the *SUP35* ORF and cut with the same enzymes. **F**—In order to generate a plasmid bearing *S. cerevisiae* module I and III in conjunction with modules II of *S. bayanus* with an extra repetitive unit of *S. cerevisiae* added to the Ors region, the fragment encompassing module I of *S. cerevisiae* and module II of *S. bayanus* with the extra repetitive unit was cut from plasmid pBC111 with *Bam*HI and *Pfl*MI and inserted into plasmid pKB100 at the same sites with the *Bam*HI site upstream of the *SUP35* ORF and cut with the same enzymes.

Figure 36: Construction of the *SUP35* derivatives with a mutation at position 12

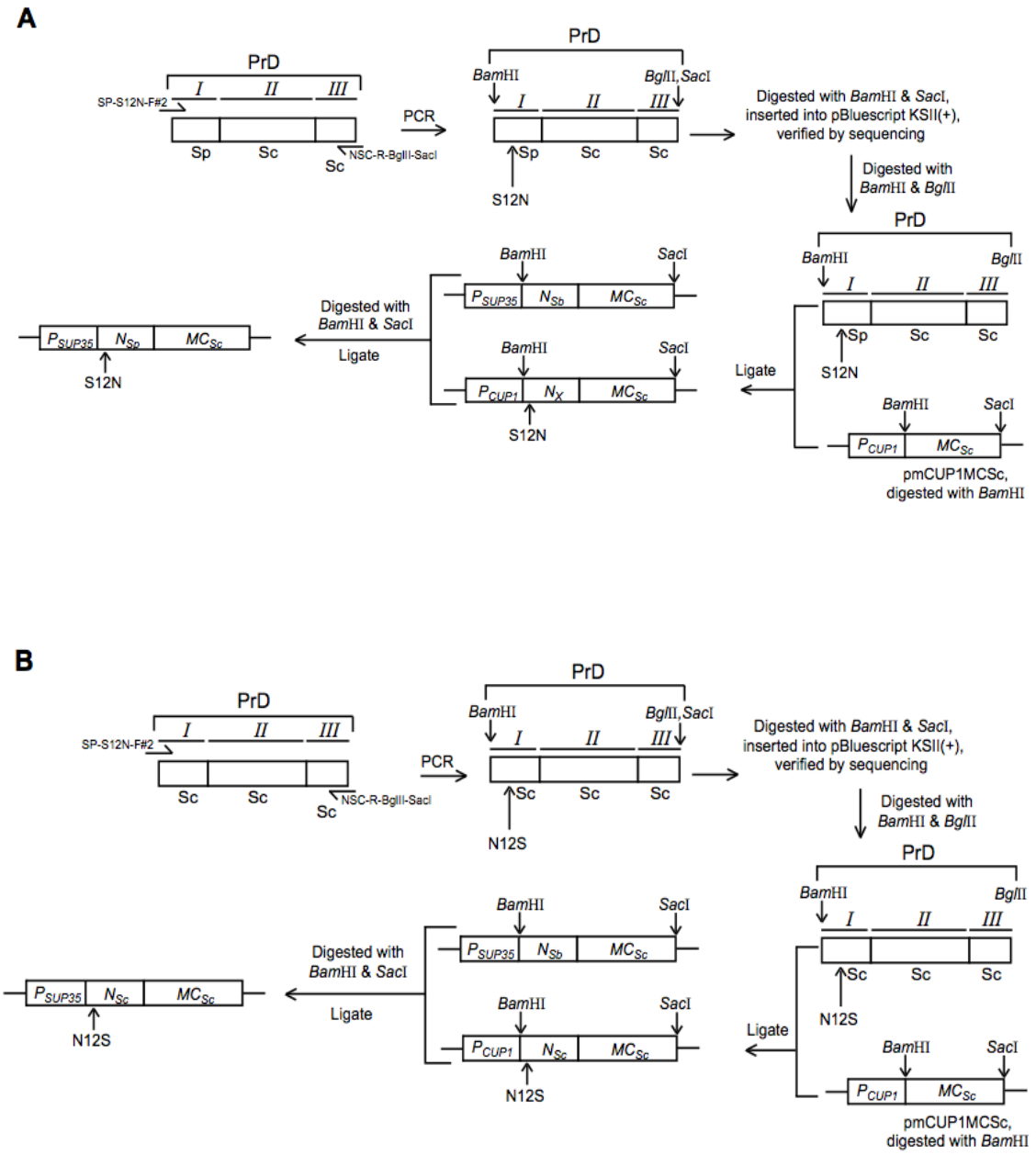

Figure 36: Construction of the *SUP35* genes with chimeric SUP35N domains. For designations of the *SUP35* domain and modules, see Figure 35 legend. **A**—Plasmid pBC109 (Table 2) was PCR-amplified using primers SP-S12N-F#2 and NSC-R-BglII-SacI (Table 3). The former primer introduces a G to A substitution at nucleotide position 35, changing coding capacity of codon 12 from serine (S) to asparagine (N). Resulting fragment was digested by *Bam*HI and *Sac*I, inserted into plasmid pBluescript KSII (+) from Stratagene (cut with the same enzymes), verified by sequencing, digested with

*Bam*HI and *Bgl*II, fused to the *SUP35MC* region of *S. cerevisiae* by inserting into pmCUP1MCSC (Table 2) cut with *Bam*HI, and the BamHI-SacI fragment encompassing full-size gene of chimeric SUP35 bearing the S12N was inserted into plasmid pBC104 (Table 2) bearing *PSUP35* promoter cut with *Bam*HI and SacI. A similar strategy was used for construction of pKB101 (Table 2). **B**—Plasmid pBC102 (Table 2) was PCR-amplified using primers NSC-MCSC(N12S) and NSC-R-BglII-SacI (Table 3). The former primer introduces an A to G substitution at nucleotide position 35, changing coding capacity of codon 12 from asparagine (N) to serine (S). Resulting fragment was digested with *Bam*HI and *Sac*I, inserted into plasmid pBluescript KSII (+) from Stratagene (cut with the same enzymes), verified by sequencing, digested with *Bam*HI and *Bgl*II, fused to the *SUP35MC* region of *S. cerevisiae* by inserting into pmCUP1MCSC (Table SI) cut with *Bam*HI, and the *Bam*HI-*Sac*I fragment encompassing the full-size gene of *SUP35* of *S. cerevisiae* bearing the N12S was inserted into plasmid pBC104 (Table 2) bearing *PSUP35* promoter cut with *Bam*HI and *Sac*I.

Figure 37: Construction of the *SUP35* derivatives with a mutation at position 49/50

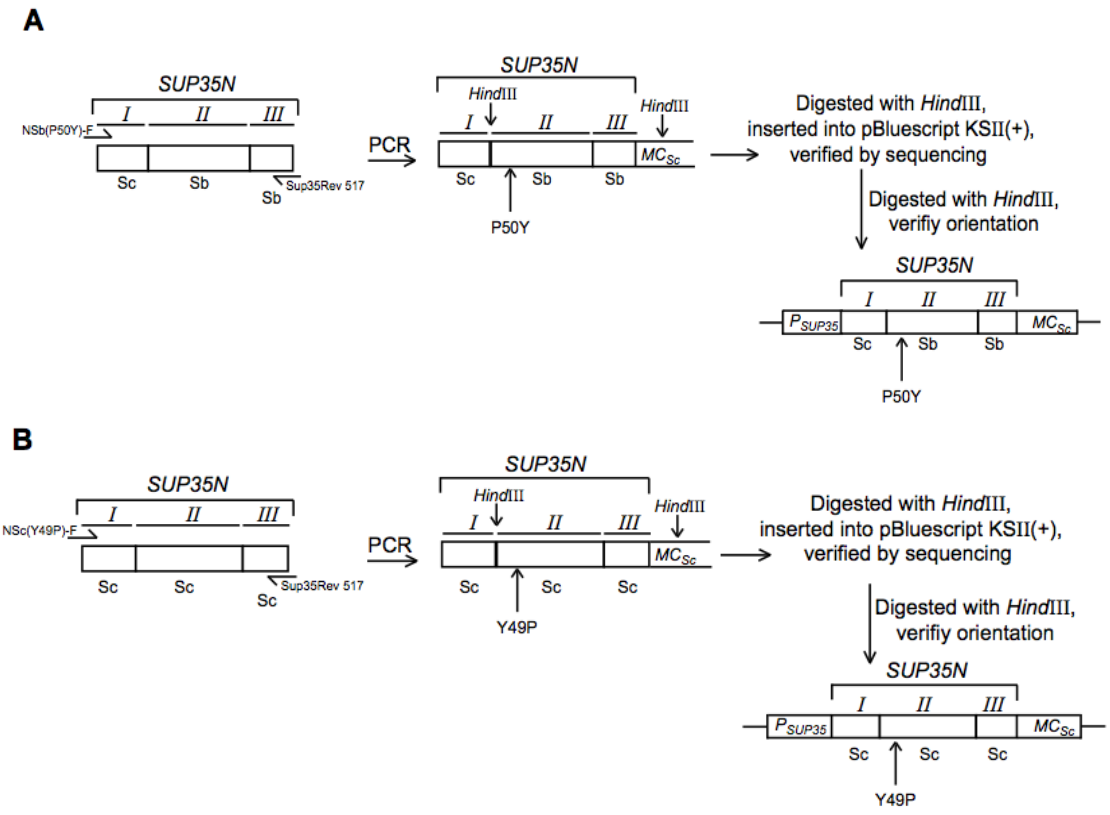

Figure 37: Construction of the *SUP35* derivatives with a mutation at position 19/50. For designations of the *SUP35N* domains and modules, see Fig. S8 legend. **A**—Plasmid pBC110 (Table SI) was PCR-amplified using primers NSB(P50Y)-F and SUP35REV-517 (Table SII). The former primer also introduces a CC to TA substitution at nucleotide position 148 and 149, changing coding capacity of codon 50 from proline to tyrosine. Resulting fragment was digested with *Hind*III, inserted into plasmid pBluescript KSII (+) from Stratagene (cut with the same enzyme), verified by sequencing, digested with *Hind*III, inserted into plasmid pBC110 (Table SI) cut with *Hind*III and verified orientation of the insert. A similar strategy was performed to construct the plasmids pGN101 and pGN103 (Table SI). **B**—Plasmid pBC102 (Table SI) was PCR-amplified using primers NSC(Y49P)-F and SUP35REV-517 (Table SII). The former primer also introduces a TA to CC substitution at nucleotide position 145 and 146, changing coding capacity of codon 49 from tyrosine to proline. Resulting fragment was digested with *Hind*III, inserted into plasmid pBluescript KSII (+) from Stratagene (cut with the same enzyme), verified by sequencing, digested with *Hind*III, inserted into plasmid pBC102 (Table SI) cut with *Hind*III and verified orientation of the insert.

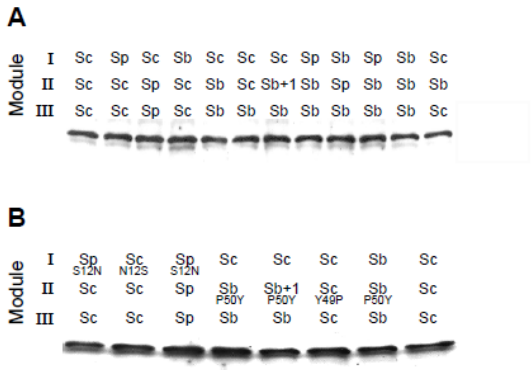

Figure 38: Levels of the Sup35 protein produced by the chimeric or mutant constructs. Proteins were isolated from the derivatives of the strain GT256-23C (see materials and methods) bearing *URA3* plasmids with either chimeric or mutant SUP35 PrDs fused to the MC regions of *S. cerevisiae* and expressed from the P_{SUP35} promoter. Protein isolation and western analysis were as described in Chapter 2. **A**—and **B**—refer to two different gels, each containing the Sc control (Sc-Sc-Sc). Each Sup35 chimeric construct was produced at the same level as the control.

Table 12: Stability of strong [*PSI*$^+$] transfected to *S. paradoxus* from GT256-23C.

Colony #	Stability of Transfected strong [*PSI*$^+$] In *S. paradoxus*				
	# Light pink	# Medium pink	# red	Total number	% [*PSI*$^+$]
A	299	0	3	302	99%
B	338	0	1	339	100%
C	415	0	0	415	100%
D	349	0	0	349	100%
E	220	0	1	221	100%

[*PSI*$^+$] from *S. cerevisiae* strain GT256-23C was transfected into *S. paradoxus* to produce the strong [*PSI*$^+$] strain used for direct and reverse transmission experiments and interference studies. [*PSI*$^+$] colonies were streaked out on YPD medium and numbers of each phenotype were recorded.

Table 13: Efficiencies of cross-species transmission performed in a *S. paradoxus* strong [*PSI*$^+$] variant.

PrD shuffled in	Direct shuffle results		
	# [*PSI*$^+$]	% [*PSI*$^+$], Confidence limits	Total number
Sc-Sc-Sc	75	97% (93.3-100.0)	77
Sp-Sc-Sc	64	94% (88.3-99.7)	68
Sc-Sp-Sp	52	100% (97.3-100.0)	52
Sp-Sp-Sp	26	84% (71.1-96.9)	31
Sb-Sb-Sb	0	0% (0.0-3.2)	61
Sc-Sb-Sb	3	4% (0-8.5)	74
Sc-Sb-Sc	2	4% (0-9.3)	51
Sb-Sc-Sc	46	85% (75.4-94.6)	54
Sc-Sc-Sb	22	100% (95.9-100.0)	22
Sp-Sb-Sb	9	12% (4.8-19.3)	77
Sb-Sp-Sp	**11**	**31% (15.9-46.1)**	**36**

A direct shuffle procedure was performed beginning with a strong [*PSI*$^+$] variant obtained from transfection.

Table 14: Efficiencies of cross-species reverse transmission performed in a *S. paradoxus* strong [*PSI*$^+$] variant.

PrD shuffled from	Reverse shuffle results		
	# [*PSI*$^+$]	% [*PSI*$^+$], Confidence limits %	Total number
Sc-Sc-Sc	21	100% (95.7-100.0)	21
Sc-Sb-Sb*	7	41% (17.6-64.4)	17
Sb-Sc-Sc	14	88% (72.1-100.0)	16
Sc-Sc-Sb	7	100% (86.3-100.0)	7
Sp-Sp-Sp*	6	38%(14.2-61.8)	16
Sp-Sc-Sc	7	70% (41.6-98.4)	10
Sc-Sp-Sp	8	89% (68.6-100.0)	9
Sb-Sp-Sp	7	47% (21.7-72.3)	15

[*PSI*$^+$] isolates obtained by direct shuffle (see Table 13~~5.1~~) were used in the reverse shuffle to $Sup35_{Sc}$ in the *S. paradoxus sup35Δ::natNT2* strain. Several independent isolates were analyzed per each construction in some cases, as indicated. Total numbers tested are shown. *Reverse transmission was checked for three different isolates from Sc-Sb-Sb and for two different isolated from Sp-Sp-Sp. Data from these individual isolates are combined.

Table 15: Efficiency of cross-species transmission from *S. cerevisiae* to *S. paradoxus*.

Sup35 version in *S. paradoxus*	Transfection from *S. cerevisiae* to *S. paradoxus*			
	Lysate from	# [*PSI*$^+$]	% [*PSI*$^+$], Confidence limits	Total number
Sup35$_{Sc}$	**Strong *S. cerevisiae* strain**	5	19% (3.9-34.1)	26
Sup35$_{Sp}$		0	0% (0-5.2)	37
Sup35$_{Sb}$		0	0% (0-5.7)	34
Sup35$_{Sc}$	**Weak *S. cerevisiae* strain**	3	7% (0-14.6)	43
Sup35$_{Sp}$		0	0% (0-4.6)	42
Sup35$_{Sb}$		0	0% (0-7.7)	25

Cell lysate from either a *S. cerevisiae* strong or weak [*PSI*$^+$] variant was transfected into a [*psi*$^-$] *sup35Δ::natNT2 S. paradoxus* strain. The *S. paradoxus* strain produced Sup35 (originating from either *S. cerevisiae*, *S. paradoxus*, or *S. bayanus*) on a centromeric plasmid. Following transfection, cells were plated on –Ura media to select for colonies likely receiving the protein (Colonies successfully transformed by the control plasmid had a greater likelihood of also receiving the transfected protein.) Ura$^+$ colonies were checked for the presence of [*PSI*$^+$], and the numbers and percentage of [*PSI*$^+$] colonies are recorded. The results were presented as a graph in Figure 47.

Table 16: Interference in *S. paradoxus* [*PSI*$^+$] propagation.

Interfering PrD	[*PSI*$^+$] Interference in *S. paradoxus*		
	# showing [*PSI*$^+$] loss	% interference (% [*psi*$^-$])	Total number
Empty vector	4	0.0%	110
Sc-Sc-Sc	2	0.1%	25
Sp-Sc-Sc	41	27.6%	42
Sc-Sp-Sp	11	1.3%	37
Sp-Sp-Sp	60	53.3%	60
Sb-Sb-Sb	11	1.2%	44
Sc-Sb-Sb	30	19.1	34
Sc-Sb-Sc	50	21.4%	51
Sb-Sc-Sc	48	23.7%	50
Sc-Sc-Sb	0	0.0%	23
Sp-Sb-Sb	20	0.4%	24
Sc(N12S)-Sc-Sc	13	0.2%	42
Sc(N12S)-Sp-Sp	37	59.3%	37
Sp(S12N)-Sc-Sc	2	0.0%	22
Sp(S12N)-Sp-Sp	3	0.1%	23
Sp complete	28	62.2%	28
Sb complete	0	0.0%	48

"Sc," "Sp" and "Sb" denote *S. cerevisiae*, *S. paradoxus*, and *S. bayanus*, respectively. Rates of interference by a heterologous Sup35 PrD or complete Sup35 version are recorded as percentages. Not all colonies exhibited [*PSI*$^+$] loss; however, numbers of colonies showing some degree of [*psi*$^-$] colonies are recorded together with the total number of colonies tested.

Table 17: Interference in *S. cerevisiae* strong [*PSI*$^+$] propagation.

Interfering PrD	[*PSI*$^+$] Interference in *S. cerevisiae* strong [*PSI*$^+$]		
	# showing [*PSI*$^+$] loss	% interference (% [*psi*$^-$])	Total number
Empty vector	0	0.0%	18
Sc-Sc-Sc	0	0.0%	16
Sp-Sp-Sp	0	0.0%	24
Sb-Sb-Sb	0	0.0%	4

"Sc," "Sp" and "Sb" denote *S. cerevisiae*, *S. paradoxus*, and *S. bayanus*, respectively. Rates of interference by a second homologous or heterologous Sup35 PrD are recorded as percentages. "Total number" refers to the number of independently transformed isolates tested for interference. For those tested, No colonies exhibited [*PSI*$^+$] loss;

Table 18. *HSP104* copy number and length of heterologous protein co-existence on prion interference in *S. paradoxus*.

Length of co-expression	Hsp104 copy number	Interfering PrD	# of independent isolates showing [*PSI*$^{+}$] loss	% interference (% [*psi*$^{-}$])	Total of independent isolates tested
Long term (6 days)	1 copy	Sc	6	2.7%	8
		Sp	8	90.8%	8
		Sb	7	3.8%	7
	2 copies	Sc	8	1.6%	8
		Sp	8	97.0%	8
		Sb	8	21.0%	8
Short term (1.5 days)	1 copy	Sc	4	1.3%	6
		Sp	5	5.7%	6
		Sb	6	2.1%	6
	2 copies	Sc	4	0.8%	6
		Sp	6	24.5%	6
		Sb	1	0.2%	6

"Sc," "Sp" and "Sb" denote *S. cerevisiae*, *S. paradoxus*, and *S. bayanus*, respectively. Rates of interference by a second homologous or heterologous Sup35 PrD are recorded as percentages. "Total number" refers to the number of independently transformed isolates tested for interference. Mating interference experiments were performed as shown on Fig. 54. Diploid strains either had one two functioning copies of the *HSP104* gene.

\

Table 19: Phenotypical differences for short-term heterologous Sup35 co-expression in *S. paradoxus*.

Hsp104 copy #	PrD	Phenotype for interference (short co-expression) in *S. paradoxus* from mating interference protocol					
		#	# Light Pink	# Medium Pink	# Red	Total #	
2 copies Hsp104	Sc	1	0	99	0	99	0% Light pink 99% Medium pink 1% Red
		2	0	136	1	137	
		3	0	72	0	72	
		4	0	133	2	135	
		5	0	130	1	131	
		6	0	70	1	71	
1 copy Hsp104		1	30	46	0	76	35% Light pink 64% Medium pink 1% Red
		2	47	71	1	119	
		3	27	72	4	103	
		4	6	84	1	91	
		5	25	11	1	37	
		6	46	53	0	99	
2 copies Hsp104	Sp	1	0	71	33	104	0% Light pink 76% Medium pink 25% Red
		2	0	69	47	116	
		3	0	76	8	84	
		4	0	91	17	108	
		5	0	84	18	102	
		6	0	56	22	78	
1 copy Hsp104		1	31	50	6	87	27% Light pink 67% Medium pink 6% Red
		2	25	74	3	102	
		3	36	82	4	122	
		4	13	91	0	104	
		5	31	60	6	97	
		6	20	33	14	67	
2 copies Hsp104	Sb	1	0	40	0	40	0% Light pink 100% Medium pink 0% Red
		2	1	96	0	97	
		3	0	82	0	82	
		4	0	73	0	73	
		5	0	148	0	148	
		6	0	165	1	166	
1 copy Hsp104		1	22	57	2	81	35% Light pink 63% Medium pink 2% Red
		2	17	59	4	80	
		3	39	46	2	87	
		4	41	113	1	155	

		5	46	78	3	127	
		6	70	75	2	147	

"Sc," "Sp" and "Sb" denote *S. cerevisiae*, *S. paradoxus*, and *S. bayanus*, respectively. "PrD" refers to prion domain. A mating interference experiment was performed to look for evidence of interference caused by a heterologous PrD. Following a short period (1.5 days) of homologous (negative control) or heterologous Sup35 co-expression, differences in phenotype was observed.

Table 21 Results of Direct Transmission for the *S. paradoxus* strain having [*PSI*$^+$] induced de novo with the *S. cerevisiae* inducee and the *S. cerevisiae* inducer.

PrD shuffled in	Direct Shuffle results		
	[*PSI*$^+$] (%)	Standardized error %	Total number
Sc-Sc-Sc	22 (100%)	(2.1)	22
Sp-Sc-Sc	22 (100%)	(2.1)	22
Sc-Sp-Sp	29 (100%)	(1.8)	29
Sp-Sp-Sp	11 (55%)	(11.1)	20
Sb-Sb-Sb	0 (0%)	(1.8)	29
Sc-Sb-Sb	4 (14%)	(6.6)	28
Sc-Sb-Sc	2 (7%)	(4.7)	30
Sb-Sc-Sc	12 (57%)	(10.8)	21
Sc-Sc-Sb	23 (100%)	(2.1)	23
Sp-Sb-Sb	6 (21%)	(7.6)	29
Sb-Sp-Sp	8 (31%)	(9.1)	26

Table 22. Results of Direct Shuffle for the *S. paradoxus* [*PSI*$^+$] strain having the Sc/Sp (inducee/inducer)

PrD shuffled in	Direct Shuffle results		
	[*PSI*$^+$] (%)	Standardized error %	Total number
Sc-Sc-Sc	8 (80%)	(12.6)	10
Sp-Sp-Sp	8 (40%)	(11.0)	20
Sb-Sb-Sb	0 (17%)	(9.1)	17

Table 23: Results of Direct Shuffle for the *S. paradoxus* [*PSI*$^+$] strain having the Sc/Sb (inducee/inducer)

PrD shuffled in	Direct Shuffle results		
	[*PSI*$^+$] (%)	Standardized error %	Total number
Sc-Sc-Sc	20 (80%)	(8.0)	25
Sp-Sp-Sp	29 (94%)	(4.3)	31
Sb-Sb-Sb	28 (85%)	(6.2)	33

Table 24: Results of Direct Shuffle for the *S. paradoxus* [*PSI*$^+$] strain #119 having the Sp/Sc (inducee/inducer)

PrD shuffled in	Direct Shuffle results (1 plasmid stage)		
	[*PSI*$^+$] (%)	Standardized error %	Total number
Sc-Sc-Sc	21 (91%)	(6.0)	23
Sp-Sp-Sp	35 (97%)	(2.8)	36
Sb-Sb-Sb	0 (0%)	(2.3)	18

Table 25: Results of Direct Shuffle for the *S. paradoxus* [*PSI*$^+$] strain #152 having the Sp/Sp (inducee/inducer)

PrD shuffled in	Direct Shuffle results		
	[*PSI*$^+$] (%)	Standardized error %	Total number
Sc-Sc-Sc	21 (88%)	(6.6)	24
Sp-Sp-Sp	21 (100%)	(2.2)	21
Sb-Sb-Sb	0 (0%)	(2.5)	16

REFERENCES:

[1] Wickner RB, Shewmaker F, Kryndushkin D and Edskes HK. Protein inheritance (prions) based on parallel in-register β-sheet amyloid structures. *BioEssays* 2008; **30:** 955–64.

[2] Fowler DM, Koulov AV, Balch WE, and Kelly JW. Functional amyloid – from bacteria to humans.*Trends Biochem Sci* 2007; **32:** 217–224.

[3] Inge-Vechtomov SG, Zhouravleva GA and Chernoff YO. Biological Roles of Prion Domains *Prion* 2007; **1:** 228-35.

[4] Dobson CM. Protein folding and misfolding. *Nature* 2003; **426:** 884–890.

[5] Kane MD, Lipinski WJ, Callahan MJ, Bian F, Durham RA, Schwarz RD, Roher AE and Walker LC. (2000) Evidence for seeding of beta -amyloid by intracerebral infusion of Alzheimer brain extracts in beta -amyloid precursor protein-transgenic mice. *J Neurosci* 2000; **20:** 3606-11.

[6] Eisele YS, Obermüller U, Heilbronner G, Baumann F, Kaeser SA, Wolburg H, *et al.* Peripherally applied Aβ-containing inoculates induce cerebral β-amyloidosis. *Science* 2010; **330:** 980–982

[7] Qian J, Yan J, Ge F, Zhang B, Fu X, Tomozawa H, *et al.* Mouse senile amyloid fibrils deposited in skeletal muscle exhibit amyloidosis-enhancing activity. *PLoS Pathog* 2010; **6:** e1000914.

[8] King C and Diaz-Avalos R. Protein-only transmission of three yeast prion strains. *Nature* 2004; **428:** 319-23.

[9] Tanaka M, Chien P, Naber N, Cooke R and Weissman JS. Conformational variations in an infectious protein determine prion strain differences. *Nature* 2004; **428:** 323-28.

[10] Bruce ME. TSE strain variation. *Br Med Bull* 2003; **66:** 98–108.

[11] Morales R, Abid K and Soto C. The prion strain phenomenon: molecular basis and unprecedented features. *Biochim Biophys Acta* 2006; **1772:** 681-91.

[12] Collinge J and Clarke AR. A general model of prion strains and their pathogenicity. *Science* 2007; **318:** 930-36.

[13] Moore, RA, Vorberg I and Priola SA. Species barriers in prion diseases–brief review. *Arch Virol* Suppl 2005; **19:** 187-2.

[14] Wickner RB. [*URE3*] as an altered URE2 protein: evidence for a prion analog in *Saccharomyces cerevisiae. Science* 1994; **264:** 566–569.

[15] Derkatch IL, Bradley ME, Zhou P, Chernoff YO, and Liebman SW. Genetic and environmental factors affecting the *de novo* appearance of the [*PSI*$^{+}$] prion in *Saccharomyces cerevisiae. Genetics* 1997; **2:** 507–519.

[16] Derkatch IL, Bradley ME, Hong JY and Liebman SW. Prions Affect the Appearance of Other Prions: The Story of [*PIN*$^{+}$]. *Cell* 2001; **106:** 171-82.

[17] Sondheimer N, Lopez N, Craig EA, and Lindquist S. The role of Sis1 in the maintenance of the [*RNQ*$^{+}$] prion. *EMBO* 2001; 20:2435–2442.

[18] Du Z, Park KW, Yu H, Fan Q, and Li L. Newly identified prion linked to the chromatin-remodeling factor Swi1 in *Saccharomyces cerevisiae. Nat Genet* 2008; 40: 460–465.

[19] Alberti S, Halfmann R, King O, Kapila A, and Lindquist S. A systematic survey identifies prions and illuminates sequence features of prionogenic proteins. *Cell* 2009; **137:** 146–158.

[20] Nemecek J, Nakayashiki T, and Wickner RB. A prion of yeast metacaspase homolog (Mca1p) detected by a genetic screen. *Proc Natl Acad Sci USA* 2009; **106:** 1892–1896.

[21] Patel BK, Gavin-Smyth J, and Liebman SW. The yeast global transcriptional co-repressor protein Cyc8 can propagate as a prion. *Nat Cell Biol* 2009; **11:** 344–349.

[22] Rogoza T, Goginashvili A, Rodionova S. Ivanov M, Viktorovskaya O, Rubel A, *et al.* Non-Mendelian determinant [*ISP+*] in yeast is a nuclear-residing prion form of the global transcriptional regulator Sfp1. *Proc Natl Acad Sci USA 2010*; **107:** 10573–10577.

[23] Halfmann RH and Lindquist S. Epigenetics in the extreme: prions and the inheritance of environmentally acquired traits. *Science* 2010; **330:** 629-32.

[24] Wickner RB, Liebman SW, and Saupe SJ. Prions of yeast and filamentous fungi: [URE3], [PSI^{+}], [PIN^{+}], and [Het-s]. S.B. Prusiner (Ed.), *Prion biology and diseases* (2nd ed.), Cold Spring Harbor Laboratory Press, Cold Spring Harbor, NY. 2004; Chapter 7: 305–372.

[25] True HL and Lindquist SL. A yeast prion provides a mechanism for genetic variation and phenotypic diversity. *Nature* 2000; **407:** 477-83.

[26] Chernoff, YO. Stress and prions: lessons from the yeast model. *FEBS Lett* 2007; **581:** 3695-701.

[27] Chernoff YO, Galkin AP, Lewitin E, Chernova TA, Newnam GP and Belenkiy SM. Evolutionary conservation of prion-forming abilities of the yeast Sup35 protein. *Mol Microbiol* 2000; **35:** 865-76.

[28] Nakayashiki T, Ebihara K, Bannai H and Nakamura Y. Yeast [*PSI*$^{+}$] "Prions" that Are Crosstransmissible and susceptible beyond a species barrier through a quasi-prion state. *Molecular Cell* 2001; **7:** 1121-30.

[29] Resende CG, Outeiro TF, Sands L, Lindquist S, and Tuite MF. Prion protein gene polymorphisms in *Saccharomyces cerevisiae*. *Mol Microbiol* 2003; **49:** 1005-17.

[30] Chernoff YO. Mutation processes at the protein level: is Lamarck back? *Mutat Res* 2001; **488:** 39-64.

[31] Derkatch IL, Chernoff YO, Kushnirov VV, Inge-Vechtomov SG and Liebman SW. Genesis and Variability of [*PSI*$^{+}$] Prion Factors in *Saccharomyces cerevisiae.* *Genetics* 1996; **144:** 1375-86.

[32] Schlumpberger M, Pruisner SB, and Herskowitz I. Induction of Distinct [*URE3*] Yeast Prion Strains. *Mol Cell Biol* 2001; **21:** 7035-46.

[33] Bradley ME, Edskes HK, Hong JY, Wickner RB and Liebman SW. Interactions among prions and prion "strains" in yeast. *Proc Natl Acad Sci USA* 2002; **99:** 16392-99.

[34] Borchsenius AS, Muller S, Newnam GP, Inge-Vechtomov SG and Chernoff YO. Prion variant maintained only at high levels of the Hsp104 disaggregase. *Curr Genet* 2006; **49:** 21-29.

[35] Zhou P, Derkatch IL, Uptain SM, Patino MM Lindquist S and Liebman SW. The yeast non-Mendelian factor [*ETA*$^{+}$] is a variant of [*PSI*$^{+}$], a prion-like form of release factor eRF3. *EMBO* 1999; **18:** 1182-91.

[36] Tanaka M, Collins SR, Toyama BH and Weissman JS. The physical basis of how prion conformations determine strain phenotypes. *Nature* 2006; **442:** 585-89.

[37] Kryndushkin DS, Alexandrov IM, Ter-Avanesyan MD and Kushnirov VV. Yeast [PSI+] prion aggregates are formed by small Sup35 polymers fragmented by Hsp104. *J Biol Chem* 2003; **278:** 49636-49643.

[38] Toyoma BH, Kelly MJS, Gross JD, Weissman JS. The structural basis of yeast prion strain variants. *Nature* 2007; **449**: 233-38.

[39] Derdowski A, Sindi SS, Klaips CL, DiSalvo S, and Serio TR. A size threshold limits prion transmission and establishes phenotypic diversity. *Science* 2010; **330:** 680-83.

[40] Kushnirov VV, Kochneva-Pervukhova NV, Chechenova MB, Frolova NS and Ter-Avanesyan MD. Prion properties of the Sup35 protein of yeast *Pichia methanolica. EMBO* 2000; **19:** 324-31.

[41] Santosa A, Chien P, Osherovich LZ and Weissman JS. Molecular basis of a yeast prion species barrier. *Cell* 2000; **100:** 277-88

[42] Chien P and Weissman JS. Conformational diversity in a yeast prion dictates its seeding specificity. *Nature* 2001; **410:** 223-27.

[43] Vishveshwara N and Liebman SW. Heterologous cross-seeding mimics cross-species prion conversion in a yeast model. *BCM Biol* 2009; **7:** 1-14.

[44] Osherovich LZ and Weissman JS. Multiple Gln/Asn-Rich Prion Domains Confer Susceptibility to Induction of the Yeast [*PSI*$^{+}$] Prion. *Cell* 2001; **106:** 183-94.

[45] Nelson ACG and Ross ED. Interactions between heterologous prion proteins. *Semin Cell Dev Biol* 2011; *22: 437-443.*

[46] Chen B, Newnam GP, and Chernoff YO. Prion species barrier between the closely related yeast proteins is detectable despite Coaggregation. *Proc Natl Acad Sci USA* 2007; **104:** 2791-96.

[47] Prusiner SB. Prions. *Proc Natl Acad Sci USA* 1998*;* **95:**13363–83.

[48] Chen B, Bruce KL, Newnam GP, Gyoneva S, Romanyuk AV and Chernoff YO. Genetic and epigenetic control of the efficiency and fidelity of cross-species prion transmission. *Mol Microbiol* 2010; **76:** 1483-99.

[49] Edskes HK and Wickner RB. Conservation of a portion of the S. *cerevisiae* Ure2p prion domain that interacts with the full-length protein. *Proc Natl Acad Sci USA* 2002; **99:** 16384-91.

[50] Edskes HK, McCann LM, Hebert AM and Wickner RB. Prion variants and species barriers among *Saccharomyces* Ure2 Proteins. *Genetics* 2009; **181:** 1159-67.

[51] Baudin-Baillieu A, Fernandez-Bellot E, Reine F, Coissac E and Cullin C. Conservation of the prion properties of Ure2p through evolution. *Mol Biol Cell* 2003; **14:** 3449-58

[52] Talarek N, Maillet L, Cullin C and Aigle M. The [URE3] prion is not conserved among *Saccharomyces* Species. *Genetics* 2005; **171:** 23-34.

[53] Kadnar ML, Articov G and Derkatch IL. Distinct type of transmission barrier revealed by study of multiple prion determinants of Rnq1. *PLoS Genetics* 2010; 6: 1-18.

[54] Kocisko DA, Priola SA, Raymond GJ, Chesebro B, Lansbury PT and Caughey B. Species specificity in the cell-free conversion of prion protein to protease-resistant forms: A model for the scrapie species barrier. *Proc Natl Acad Sci USA* 1995; **92:** 3923-27.

[55] Edskes HK, Gray VT and Wickner RB. The [URE3] prion is an aggregated form of Ure2p that can be cured by overexpression of Ure2p fragments. *Proc Natl Acad Sci USA* 1999; **96:** 1498-3.

[56] Schwimmer C and Masison DC. Antagonistic interactions between yeast [*PSI*$^+$] and [*URE3*] prions and curing of [*URE3*] by Hsp70 protein chaperone Ssa1p but not by Ssa2p. *Mol Cell Biol* 2002; **22:** 3590–3598.

[57] Bradley ME and Liebman SW. Destabilizing interactions amoung [*PSI*$^+$] and [*PIN*$^+$] yeast prion variants. *Genetics* 2003; **165:** 1675-1685.

[58] Allen KD, Wegrzyn RD, Chernova TA, Muller S, Newnam GP, Winslett PA, et al. Hsp70 Chaperones as Modulators of Prion Life Cycle: Novel Effects of Ssa and Ssb on the *Saccharomyces cerevisiae* prion [*PSI*$^+$]. *Genetics* 2005; **169:** 1227-42.

[59] De Pace AH, Santoso A, Hillner P, and Weissman JS. A critical role for amino-terminal glutamine/asparagine repeats in the formation and propagation of a yeast prion. *Cell* 1998; **93:** 1241–1252

[60] Scott MR, Groth D, Tatzelt J, Torchia M, Tremblay P, DeArmond SJ, *et al.* Propagation of prion strains through specific conformers of the prion protein. *J Virol* 1997; **71:** 9032–9044.

[61] Wadsworth JDF, Asante A, Desbruslais M, Linehan JM, Joiner S, Gowland I, *et al.* CJD phenotype human prion protein with valine 129 prevents expression of variant. *Science* 2004; **306:** 1793–1796.

[62] Bradley ME and Liebman SW. The Sup35 domains required for maintenance of weak, strong or undifferentiated yeast [*PSI*$^+$] prions. *Mol Microbiol* 2004; **51:** 1649–1659.

[63] Shkundina IS, Kushnirov VV, Tuite MF and Ter-Avanesyan. The role of the N-terminal oligopeptide repeats of the yeast Sup35 prion protein in propagation and transmission of prion variants. *Genetics* 2006; **172:** 827-35.

[64] Cox BS, Byrne LJ and Tuite MF. Prion stability. *Prion*. 2007; **1:** 170-178.

[65] Shewmaker F, Wickner RB and Tycko R. Amyloid of the prion domain of Sup35p has an in-register parallel ß-sheet structure. *Proc Natl Acad Sci USA* 2006; **103:** 19754-59.

[66] Wickner RB, Edskes HK, Shewmaker F, and Nakayashiki T. Prions of Fungi: Inherited Structures and Biological Roles. *Nat Rev Microbiol* 2007; **5:** 611-18.

[67] Baxa U, Keller PW, Cheng N, Wall JS, and Steven AC. In Sup35 filaments (the [*PSI*$^{+}$] prion), globular C-terminal domains are widely offset from the amyloid fibril backbone. *Mol Microbiol* 2011; **79:** 523–532.

[68] Krishnan R and Lindquist SL. Structural insights into a yeast prion illuminate nucleation and strain diversity. *Nature* 2005; **435:** 765-72.

[69] Vanik DL, Surewicz KA and Surewicz WK. Molecular basis of barriers for interspecies transmissibility of mammalian prions. *Molecular Cell* 2004; **14:** 139-45.

[70] Chang HY, Lin JY, Lee HC, Wang HL and King CY. Strain-specific sequences required for yeast [*PSI*$^{+}$] prion propagation. *Proc Natl Acad Sci USA* 2008; **105:** 13345-50.

[71] Chernoff YO. Identity determinants of infectious proteins. *Proc Natl Acad Sci U.S.A.* 2008; **105:** 13191-92.

[72] Tessier PM and Lindquist S. Prion recognition elements govern nucleation, strain specificity and species barriers. *Nature* 2007; **447:** 556-62.

[73] Tessier P and Lindquist S. Unraveling infectious structures, strain variants and species barriers for the yeast prion [*PSI*$^{+}$]. *Nal Struct Mol Biol* 2009; **16:** 598-605.

[74] Pastor MT, Esteras-Chopo A and Serrano L. Hacking the code of amyloid formation: the amyloid stretch hypothesis. *Prion* 2007; **1:** 9-14.

[75] Li J, Browning S, Mahal SP, Oelschlegel AM and Weissman C. Darwinian evolution of prions in cell culture. *Science* 2010; **327:** 869-72.

[76] Kushnirov VV, Alexandrov IM, Mitkevich OV, Shkundina IS, and Ter-Avenesyan MD. Purification and analysis of prion and amyloid aggregates. *Methods* 2006**; 39:** 50-55.

[77] Borchsenius AS, Wegrzyn RD, Newnam GP, Inge-Vechtomov SG, and Chernoff YO. Yeast prion protein derivative defective in aggregate shearing and production of new 'seeds.' *The EMBO Journal* 2001; 20: 6683-6691.

[78] Talarek N, Louis EJ, Cullin C, and Aigle M. Developing methods and strains for genetic studies in the *Saccharomyces bayanus* var. *uvarum* species. *Yeast* 2004; **21:** 1195-1203.

[79] Kaiser C, Michaelis S, and Mitchell A. “Methods in Yeast Genetics” Cold Spring Harbor Laboratory, Cold Spring Harbor, NY. 1994.

[80] Sambrook J and Russel DW. “Molecular Cloning: A Laboratory Manual.” Cold Spring Harbor Laboratory, Cold Spring Harbor, NY. 2001.

[81] Chernoff YO, Uptain SM, Lindquist SL. Analysis of prion factors in yeast. *Methods Enzymol* 2002; **351:** 499-538.

[82] Ito H, Fukuda Y, Murata K, and Kimura A. Transformation of intact yeast cell treated with alkali cations. *J Bacteriol* 1983; **153:** 163-168.

[83] Longtine MS, McKenzie A 3rd, Demarini DJ, Shah NG, Wach A, Brachat A, Philippsen P, and Pringle JR. Additional modules for versatile and economical PCR-based gene deletion and modification in *Saccharomyces cerevisiae. Yeast* 1998; **14:** 953-61.

[84] Taxis C, and Knop M. System of centromeric, episomal, and integrative vectors based on drug resistance markers for *Saccharomyces cerevisiae*. *BioTechniques* 2006; **40:** 73-78.

[85] Chernoff YO, Amyloidogenic domains, prions and structural inheritance: rudiments of early life or recent acquisition? *Curr Opin Chem Biol* 2004; 8: 665-671.

[86] Wickner RB, Edskes HK, Ross ED, Pierce MM, Shewmaker F, Baxa U, and Brachmann A. Prions of yeast are genes made of protein: amyloids and enzymes. *Cold Spring Harb Symp Quant Biol* 2004; 69: 489-496.

[87] Chernoff YO, Derkatch IL, and Inge-Vechtomov SG. Multicopy *SUP35* Gene induces *de-novo* appearance of psi-like factors in the yeast *Saccharomyces cerevisiae*. *Current Genetics* 1993; **24:** 268-270.

[88] Chernoff YO, Lindquist SL, Ono B, Inge-Vechtomov SG, and Liebman SW. Role of the chaperone protein Hsp104 in propagation of the yeast prion-like factor [*psi*$^{+}$]. *Science* 1995; 268: 880-884.

[89] Rikhvanov EG, Romanova NV, and Chernoff YO. Chaperone effects on prion and nonprion aggregates. *Prion* 2007; 1: 217-222.

[90] Liu JJ, Sondheimer BN, and Lindquist SL. Changes in the middle region of Sup35 profoundly alter the nature of epigenetic inheritance for the yeast prion [*PSI*$^{+}$]. *Proc Natl Acad Sci USA* 2002; **99:** 16446-16453.

[91] Osherovich LZ, Cox BS, Tuite MF, and Weissman JS. Dissection and design of yeast prions. *PLoS Biol* 2004; 2: E86.

[92] Lopez de la Paz M, and Serrano L. Sequence determinants of amyloid fibril formation. *Proc Natl Acad Sci USA* 2004; **101:** 87-92.

[93] Nelson R, Sawaya MR, Balbirnie M, Madsen AO, Riekel C, Grothe R, and Eisenberg D. Structure of the cross-beta spine of amyloid-like fibrils. *Nature* 2005; 435: 773-778.

[94] Toombs JA, McCarty BR, and Ross ED. Compositional determinants of prion formation in yeast *Mol Cell Biol* 2010; **30:** 319-332.

[95] Scott MR, Peretz D, Nguyen HO, Dearmond SJ, and Prusiner SB. Transmission barriers for bovine, ovine, and human prions in transgenic mice. *J Virol* 2005; **79:** 5259-5271.

[96] Ross ED, Baxa U, and Wickner RB. Scrambled prion domains form prions and amyloid. *Mol Cell Biol* 2004; **24:** 7206-7213.

[97] Ross ED, Edskes HK, Terry MJ, and Wickner RB. Primary sequence independence for prion formation. *Proc Natl Acad Sci USA* 2005; **102:** 12825-12830.

[98] Perchiacca JM, Ladiwala AR, Bhattacharya M, and Tessier PM. Structure-based design of conformation- and sequence-specific antibodies against amyloid beta. *Proc Natl Acad Sci USA* 2012; **109:** 84-89.

[99] Ladiwala AR, Bhattacharya M, Perchiacca JM, Cao P, Raleigh DP, Abedini A, Schmidt AM, Varkey J, Langen R, and Tessier PM. Rational design of potent domain antibody inhibitor of amyloid fibril assembly. *Proc Natl Acad Sci USA* 2012; **109:** 19965-19970.

[100] Kajava AV, Baxa U, Wickner RB, Steven AC. A model for Ure2p prion filaments and other amyloids: the parallel superpleated beta-structure. *Proc Natl Acad Sci U S A* 2004; **25**:7885-90.

[101] Ahmed AB and Kajava AV. Breaking the amyloidogenicity code: methods to predict amyloids from amino acid sequence. *FEBS Lett.* 2013; **17**: 1089-95.

[102] Dialvo S, Derdowski A, Pezza JA and Serio TR. Dominant prion mutants induce curing through pathways that promote chaperone-mediated disaggregation. *Nat Struct Mol Biol*. 2011; **18:** 486-492.